Post-Transcriptional Regulation Mechanisms of sRNA rnTrpL in *S. meliloti* and *E. coli*

Dissertation

for the degree Doctor of Natural Science

(Dr. rer. nat.)

submitted by Siqi Li, M. Sc.

Institute of Microbiology and Molecular Biology

Justus Liebig University Gießen

Gießen, August, 2020

This work was accomplished from October 2016 to July 2020 under the supervision of Apl. Prof. Dr. Elena Evguenieva-Hackenberg in the Institute of Microbiology and Molecular Biology, Justus Liebig University Gießen.

This work was funded by Deutsche Forschungsgemeinschaft (DFG), grant Ev42/6-1 and China Scholarship Council [No. 2017080800082].

1st Reviewer/Gutachter: Apl. Prof. Dr. Elena Evguenieva-Hackenberg
Institute of Microbiology and Molecular Biology
Justus Liebig University Gießen

2nd Reviewer/Gutachter: Prof. Dr. Kai Thormann
Institute of Microbiology and Molecular Biology
Justus Liebig University Gießen

Summary

Ribosome-mediated transcription attenuation is a basic and widespread mechanism for posttranscriptional regulation in bacteria. The liberated attenuator RNAs arising in this process are considered nonfunctional. However, the sRNA rnTrpL, which is released by transcriptional attenuation of the tryptophan (Trp) biosynthesis genes, plays important roles in posttranscriptional regulation. In this work, the *trans*-acting roles of the sRNA rnTrpL and of the peptide peTrpL encoded by this sRNA in *S. meliloti* were studied. Additionally, it was shown for the first time, that the corresponding sRNA Ec-rnTrpL in *E. coli* has important functions in *trans*.

In *S. meliloti* 2011, rnTrpL is constitutively transcribed and its release is regulated only by attenuation of transcription of the downstream genes. To study the *S. meliloti* sRNA rnTrpL, a deletion mutant 2011*ΔtrpL* was constructed. Additionally, several other deletion mutants in 2011 and 2011*ΔtrpL* background were constructed. Using these strains and suitable plasmids, systems for IPTG-induced production of the sRNA harboring a recombinant 5′-UTR or of the native-5′-end, leaderless rnTrpL were established. Using these systems for inducible sRNA production, evidence for interaction of the sRNA with several predicted targets was presented, including *trpDC*, *rpoE1* and *rplUrpmA*. Additionally, role of RNases in the sRNA regulation was studied. Interestingly, the sRNA rnTrpL shows at least two different posttranscriptional regulation mechanisms for its mRNA targets in *S. meliloti*: an antibiotic-dependent and antibiotic-independent mechanism. The *trpDC* mRNA, the amount of which is decreased upon rnTrpL induction, is a tetracycline (Tc)-independent target. Its direct base-pairing with rnTrpL was vaildated *in vivo* using an *egfp* reporter plasmids. On the other hand, the *rplUrpmA* mRNA is a Tc-dependent target, but its downregulation additionally depends on the peTrpL peptide encoded by the sRNA. An antisense RNA (asRNA) complementary to *rplUrpmA* also seems to play a role in this regulation. Transcription induction of this asRNA upon Tc exposure was proven.

Furthermore, this work provides evidence for two sRNA-independent targets of the peTrpL peptide in *S. meliloti*, *smeR* and *phoR*. The *smeR* gene encoding a transcription regulator was investigated. Co-transcription of *smeR* with the multidrug efflux pump genes *smeAB* was proven, showing the existence of a *smeABR* operon, which needs posttranscriptional regulation. In this regulation, the peTrpL peptide seems to work with an asRNA (as-*smeR* RNA), for which antibiotic-inducible transcription was validated. Alanine scanning mutagenesis revealed that S4, T8 and W12 of the 14 aa peTrpL peptide are necessary for its downregulating effect on both *smeR* and *rplUrpmA*, pointing to similar mechnanism operating on both targets. The mRNA targets and the corresponding asRNAs were affected similarly by the alanine scanning mutagenesis.

Additionally, this work shows that in *Escherichia coli* MG1655, the Ec-rnTrpL level is higher in minimal than in rich medium, because without external tryptophan supply, its transcription is derepressed. To study the effect of Ec-rnTrpL on predicted target mRNAs, first a system for inducible sRNA transcription was established. Analysis of mRNA levels after sRNA induction suggested that Ec-rnTrpL is a *trans*-acting sRNA, which affects *dnaA*, *sanA*, *rsuAbcr* and *mcp*. Interestingly, the level of the *rsuAbcr* co-transcript mRNA was decreased by sRNA Ec-rnTrpL overproduction only under Tc exposure. The sRNA base-pairing with *rsuAbcr* mRNA was validated *in vivo*. While the physiological importance of *rsuAbcr* downregulation by Ec-rnTrpL still remains to be uncovered, its role in regulation of

dnaA, the gene encoding the master regulator of initiation of chromosome replication, is supported by the presented data. Overexpression and deletion of the Ec-rnTrpL gene decreased and increased the *dnaA* mRNA levels, respectively. Base pairing between the sRNA and *dnaA* mRNA *in vivo* was validated. Furthermore, the *oriC* level was increased in the *ΔtrpL* mutant, in line with the expected DnaA overproduction and increased initiation of chromosome replication in the absence of Ec-rnTrpL. Moreover, in minimal medium cultures, the the *oriC* level was increased upon addition of tryptophan in the wild type strain but not in the *ΔtrpL* mutant. The results suggest that Ec-rnTrpL contributes to DnaA homeostasis under conditions of different nutrient availability. They also suggest that in this RNA-based regulation, tryptophan is a signal indicating nutrient availability.

Althogether, the presented data show that rnTrpL is a conserved sRNA with own functions in *trans* in alpha- and in gamma-Proteobacteria. Moreover, the data suggest that in both proteobacterial lineages the rnTrpL sRNA has antibiotic-dependent and antibiotic-independent targets.

Content

1 Introduction

1.1 Posttranscriptional Regulation in prokaryotes

Posttranscriptional regulation in prokaryotes includes stability modulation of messenger RNA (mRNA) and proteins, and translational regulation. This introduction is only focused on regulation mechanisms determining mRNA stability and translation.

1.1.1 Mechanisms Participating in mRNA Stability

1.1.1.1 RNases Involved in mRNA Decay

Decay of mRNA is essential for maintenance of organisms' life processes such as avoiding translation of aberrant mRNAs, reusing ribonucleotides, and rebalancing for environmental alterations. Nevertheless, RNA decay is also crucial for the cell to adjust the RNA concentrations. Stability of an mRNA strongly infuences its concentration (1), while stable RNAs like rRNA and tRNA are only degraded under stress or when defectiveness is found in the RNA molecule (2). Prokaryotic mRNA half-life is usually very short compared to that of eukaryotic mRNA to quickly answer environmental variations,

A hypothesis proposed by David Apirion in 1973 that mRNA decay involves endogenous nuclease cleavages and followed by exonucleolytic degradation of the remaining fragments in *Escherichia coli* is supported by much more evidences nowadays (3), (4). The coordination between endoribonucleases (endoRNases) and exoribonucleases (exoRNases) for mRNA decay in *E. coli* starts from RNA degradosome, a large multi-protein complex, which is used for the initial RNA cleavage (4). Principally four enzymes are considered as degradosome components: RNase E, polynucleotide phosphorylase (PNPase), RNA helicase B (RhlB helicase) and the glycolytic enzyme enolase. The carboxy terminal part of RNase E was established as a scaffold interacting with specific regions of the mentioned enzymes to form the degradosome (5-7). This kind of protein complex was first identified in a different proteobacteria whereas it has somewhat varied composition in different species (4). The RNA-binding protein Hfq has been proved that it can bind to the scaffold of RNase E instead of RhlB RNA helicase (8).

Due to the involvement in the 5S rRNA processing, the essential ribonuclease RNase E was first discovered (9). It has a full length of 1,061 amino acids, but only the first 500 amino acids play a catalytic role (10). So far, it was found only in gram-negative bacteria. Moreover, in *E. coli*, a well known model organism, whose enzyme has been comprehensively studied, RNase E participates in posttranscriptional RNA metabolism completely, including the tRNA maturation (11,12), rRNA, sRNA and mRNA processing, and also the decay of sRNA and mRNA (13,14). The results of microarrays and high-density tiling arrays demonstrated that about 60 % of the mRNA decay can be contributed to RNase E cleavage in the whole transcriptome of *E. coli* (15,16). RNase E cleavage sites usually are present in single-stranded A/U rich regions (1).It efficiently interacts with mRNA with a 5′ monophosphate extremity however is blocked at the 5′ end by triphosphate residues [1]. Scanning for cutting sites in mRNA and the mRNA cutting proceed in opposite directions. Scanning is from 5′ to 3′ end

but identifying and cleaving mRNA is in a 3′ to 5′ direction (17). PNPase as exoribonuclease in the complex utilizes a reversible phosphorolytic mechanism to degrade single-strand RNA molecules in the 3′ -5′direction and release 5′ diphosphate nucleosides (18). The function of RhlB helicase in the degradosome is the unwinding of RNA duplex, but the effect of enolase is not yet very clear (4).

An additional endoribonuclease, the RNase G, also participates in the decay of a limited number of mRNAs in *E. coli*. It is an RNase E ortholog sharing 40% of homology and can weakly substitute RNase E to cut with same cleavage site specificity (19). Furthermore, another endoribonuclease, RNase III, degrades double-stranded RNA and participates in about 12 % of mRNA decay of the transcriptome in *E. coli* (20), although the involvement of it in mRNA decay was neglected earlier (21). Interestingly, RNase III might participate in mRNA decay regulated by *cis*-encoded sRNAs (22).

1.1.1.2 Untranslated Regions Controlling mRNA Stability

Untranslated regions (UTRs) flanking the mRNA coding sequences regulate mRNA stability. Except from the triphosphorylated 5′ end protection of mRNA from an attack by RNase E in bacteria such as *E. coli* as mentioned above,. Secondary structures of either 5′ or 3′ end of mRNAs and RNA-binding proteins can also strongly influence their stability. In prokaryots the coupling of transcription and translation contributes to mRNA protection by ribosomes. Massive quantity of ribosomes on strongly encoded mRNAs may competitively prevent endoRNase cleavage (23). Approximately 10 bases upstream from the start codon within the 5′ UTR of mRNA located one of the well known stabilizing elements, the ribosome binding site (RBS), which is also known as Shine–Dalgarno (SD) sequence. Via complementary base pairing of the 3′ end of 16S rRNA to the SD sequence, ribosome binds mRNA making the mRNA more stable. There are some examples supporting this, such as *ermA, ermC* and *phage82* mRNAs, which become much more stable after ribosome binding their 5′ UTR (24). Regions without ribosome such as the 5′ and 3′ UTRs are receptive to exoRNase or endoRNase attacks, resulting in unstable bacterial mRNAs (25,26).

It is worth noting that the SD sequence does not have a strong effect on mRNA stability compared to a secondary structure in 5′ UTR, as tested by Sharp and Bechhofer (27). mRNAs with a stem-loop structured 5′ terminus such as *rne* and *pnp* have unusual long half-lives in *E. coli* (28-30). This also applies for the *aprE* mRNA, the half-life of which was longer than 25 min in *Bacillus subtilis* (31).

There are two different types of 3′ end poly(A) tails existing in *E. coli* and *B. subtilis*, a short (10–40 bases) homogeneous poly(A) tail and a longer (around 100 bases) heteropolymeric tail (32-34). Whereas, adding a 3′ poly(A) tail could destabilize bacterial transcripts (32). exoRNases such as RNase R and RNase II (which are homologs), and PNPase can attack a 3′ stem-loop (2). In *E. coli*, as found by Mohanty and Kushner, much more poly(A) polymerase I (PAPI) amount will increase the poly(A) level, leading to decreased mRNA stability (32).

1.1.1.3 Genome-Wide Determination of mRNA Half-Lives

mRNA half-lives at a genome-wide level have been investigated in prokaryotes. Bernstein.is the first one who tried to study mRNA half-lives in *E. coli* by utilizing a transcriptomic method (15), and found that the half-lives for almost 80 % of the mRNAs range from 3 to 8 minutes., An average half-life of around 7 minutes was reported in another study by using microarrays (35). mRNA encodes different products with diverse functions. The genome-wide investigations mentioned above suggested that mRNA decay rates are related to the gene function. For example, house keeping genes are generally more stable than other genes, and also found that mRNA stablity was dependent on functional categories Translation Regulations

Translational regulations in prokaryotes are complex and important for the cell life history. They depend on the coordinated contribution of diverse elements, including mRNA sequence and structure features, different kinds of effectors, proteins, RNAs and metabolites.

1.1.1.4 Sequence Contributions

In limited species of bacteria, it was found that sequence features exert an effect on the efficiency of translation initiation, elongation and termination. The interaction between RBS and ribosome not only contributes to the mRNA stability as discussed above, but also is related to efficient translation initiation in *E. coli*, *B. subtilis* (36) and *Desulfovibrio vulgaris* (37). However, secondary structure negatively affects translation initiation when it blocks the RBS (38). According to *D. vulgaris* (37) and *B. subtilis* (39) investigations, the start codon plays a crucial role in translation efficiency. Interestingly, in *E. coli* proteomes showed large numbers of the low-cost amino acids in highly mass of proteins (40). Thus, the speed of translation elongation could be tied by using rare codons (39). Using a modeling approach, scientists (41) worked on a hypothesis that codon bias could effect translation rate.

1.1.1.5 Riboswitches in Translation Regulation

Riboswitches can regulate gene expression at translational level due to the utilization of specific non coding RNA (ncRNA) secondary structures. They are actived by changes in the concentration of certain types of small substrate compounds, for instance nucleobases, amino acids or sugars. Riboswitches are usually located in the 5′ UTRs of genes which are linked to the metabolism of their ligands (42). A riboswitch contains an aptamer region where a ligand binds, and an expression plattform which changes its structure upon binding to form a stem-loop structure hiding the RBS and inhibiting mRNA translation (43). In Gram-negative bacteria, riboswitches mainly work to repress translation. Differently, riboswitches always control transcription in Gram-positive bacteria (42).

1.1.1.6 sRNA Functions in Translation Regulation

Small RNAs (sRNAs) is a kind of functional RNAs regulating gene expression, which is mostly shorter than 500 nucleotides in length. The scientists classify sRNAs in three classes according to their regulation mechanisms. The first class, the *cis*-sRNAs (44), and the second class, the *trans*-sRNAs, work at the level of RNA which is not only about translation, but also about stability. They can modify mRNA secondary structures by base-pairing and form new RNases cleavage sites causing mRNA degradation. The *cis*-sRNAs (44) show a perfect

complementarity to their target mRNAs, inhibit translation or destabilize the mRNAs and often work without co-factors. The *trans*-sRNAs are transcribed from a different locus of their target mRNA transcript, show imperfect complementarity to the target mRNA and also influence translation and/or stability. Most of the *trans*-sRNAs can not work alone for regulation; most of the time co-factors such as the Hfq protein are required.

Other details about sRNA regulation mechanisms will be discuss in the later chapters.

1.1.1.7 RNA Binding Proteins in Translation Regulation

RNA binding proteins (RBPs) are important players in posttranscriptional gene regulation. Well known is the regulation by ribosomal proteins. When the amount of ribosomal proteins are much more than that of ribosomal RNA, non-assembled regulatory ribosomal proteins bind to their own mRNAs and act as translation repressors (45,46); further direct results are transcription attenuation or rapid mRNA degradation (47,48) for example by the RNA-binding protein TRAP protein in regulation of transcription attenuation in *Bacillus subtilis* (48). Another famous RBP in bacteria is the hexameric Host Factor I (HFI or Hfq). The most important function of Hfq is as a RNA chaperone protein mediating post-transcriptional regulation by *trans*-acting sRNAs in *E. coli* (49) and other bacteria. In sRNA and mRNA base-pairing model, Hfq binds at A/U-rich, single-stranded regions and promotes the interaction of a sRNA with targeting mRNA (50). For example, Hfq helps sRNA *MicA* to bind *ompA* transcript and then to inhibit its translation initiation, leading also to its destabilization in *E. coli* (51).

1.1.2 Growth Stage and Stress Impact on mRNA Degradation and Translation Efficiency

Changes in mRNA stabilitycan occur following different growth phases and changing environmental conditions. Scientists have focused on the analysis of mRNA degradation mechanisms in exponential growth phase for a long time. In exponential phase, due to nutrients sufficiency, the cell don′t suffer any type of stress. As explained above, the half-life of mRNA during exponential growth is governed by several factors such as RNA accessibility for RNases (52) and the coverage by ribosomes (53). Upon entry in stationary phase, when compared to exponential phase, three different mRNA types could be classified (54): mRNAs with increased stability such as *cat* mRNA, mRNAs with decreased stability such as *ompA* mRNA, and mRNAs with no change in stability (54). Genome-wide study analyzing the alteration of mRNA stability to the change of growth conditions in microorganisms have been published, such as for *Lactocioccus lactis* during carbon starvation (55); furthermore, stabilomes were compared between two stress conditions (56).

mRNA translational regulation is also involved in adaptation to environmental conditions and growth stages.Under conditions with low temperature mRNA tends to perform secondary structures inhibiting mRNA encoding compared to normal condition. However, RNA chaperones were found to weaken mRNA secondary structures leading to ribosome binding and translation initiation. Three of the known Cold Shock Proteins (CSPs) are RNA chaperones which are only expressed at low temperature. (57). Furthermore, sRNAs are often involved in translation regulation under stress growth (58), because the response to stress by

sRNAs is fast and effective (59). For example, *dsrA* sRNA regulates *rpoS* mRNA by base pairing to facilitate translation of *rpoS* mRNA under low temperature (58). Furthermore, thermosensing RNA structures in the 5′-UTR can affect translation in response to temperature change.

Above, two aspects of the post-transcriptional regulation in prokaryotes, mRNA decay and translation regulation, were already discussed. Since sRNAs participate in both mechanisms, their importance is highlighted into more details below.

1.2 Posttranscriptional Regulation Mechanisms mediated by sRNAs

Bacterial regulatory RNA molecules were found much earlier than the eukaryotic microRNAs and short interfering RNAs. As already mentioned, importantly, most sRNAs are induced in reponse to changing conditions to exert posttranscriptional regulation. Luckly, based on technical advances, various approaches and technologies were developed to discover and identify new regulatory RNAs in different bacteria. Among them are computational predictions, tiling microarrays and deep sequencing of RNA, which help scientists to found hundreds candidates for regulatory RNAs in bacteria (60). Bacterial RNA regulators including riboswitches, attenuators, small RNA (sRNA) and CRISPR, are heterogeneous molecules that utilize different mechanisms for adaptation to various physiological responses.

1.2.1 *Cis*-Encoded Base Pairing sRNAs

Two broad classes for sRNAs regulating gene expression by base-pairing are identified, *cis*-encoded sRNAs with perfect complementarity (Figure 1.2.1A) and *trans*-encoded sRNAs with partial complementarity to target mRNAs (Figure 1.2.1B).

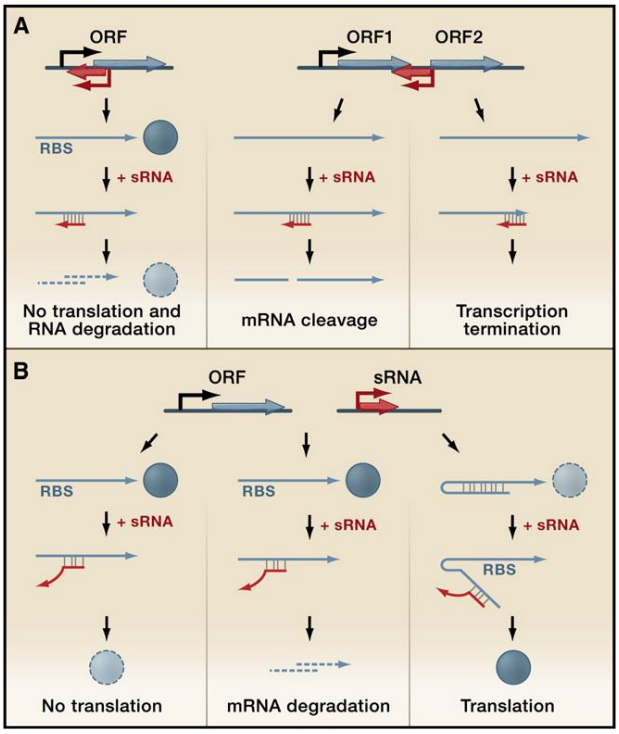

Figure 1.2.1 *Cis*-encoded (A) and *trans*-encoded (B) sRNAs base-pairing mRNA models and their outcomes (61).

Cis-encoded sRNAs originate from the opposite strand of their targets and own 75 nucleotides or more with complete complementarity to the mRNA. Thus, although sRNAs and mRNAs are transcribed from the same DNA region, they originate from opposite strands. Classical examples of *cis*-encoded antisense sRNAs include not only plasmids like ColE1 RNA I and Tn10 pOUT RNA (61), but also chromosome. For example, in *E. coli*, OhsC and IstR sRNAs are transcribed directly neigboring to genes which encoded toxic proteins and show perfect complementarity with the neigboring toxin mRNAs (61). However, many of these sRNAs are expressed from mobile elements such as plasmids. Their most prominent mechanisms are blockade of primer transcription and of translation, such as sRNA QfsR transcribed from the Ti plasmid in A*grobacterium tumefaciens* (62).

1.2.2 *Trans*-Encoded Base Pairing sRNAs

Another class of base pairing sRNAs is the *trans*-encoded sRNAs, which do not show perfect complementarity to their targeting transcripts (Figure 1.2.1B). Usually they negatively regulate translation and/or degradation of transcripts with the participation of RNases(4). Often they bind to the RBS in the 5′ UTR of mRNAs, but the *GcvB* and *RyhB* sRNAs base pair with the far upstream region of AUG for inhibiting translation (63,64).

On the other hand, some mRNAs can be positively influenced by sRNAs. In such a case, the sRNAs and mRNAs base pairing disrupts a secondary structure in the 5′-UTR to expose the RBS or protects mRNA from degradation (65-68). Interestingly, this kind of base pairing can also promote transcription termination or anti-termination reactions in the bacteria, as shown in a study of sRNA regulated transcription termination in *E. coli* (69).

Compared to the *cis*-encoded sRNAs, a majority of *trans*-encoded sRNAs are produced under particular growth conditions, such as, outer membrane stress (sigma E-induced MicA and RybB), and elevated glucose-phosphate levels (SgrR-activated SgrS), abiotic stress (AbcR2) and salt-stress (NfeR1) in *E. coli* and *S.meililoti* (70-74).

1.2.3 RNA Elements Involved in Base Pairing

It seems that sRNA looking for its targets mRNAs from thounsands of candicates is a diffcult process in the cell. Nevertheless, such sRNAs recognize their targets in a fast, high-affinity way by using several nucleotides which are exposed in single-stranded regions or in loops of stem-loop regions and therefore can base-pair with targets. Since the sRNA and mRNA base-pairing interaction often causes changes in the mRNA and sRNA secondary structures, the rest of base pairs will be formed accordingly when the first base pair interaction in the seed region happened (75). Usually, *trans*-encoded, base-pairing sRNAs have three functional domains including a 3′ end stem-loop followed by poly (U), binding site for chaperone proteins like Hfq and the region for base pairing to bind mRNAs which is frequently with high conservation (76).

We still didn′t have enough information to propose models of the seed regions of sRNAs with specific length or composition. However, some studies tried to reveal this. For example, SgrS and RybB sRNAs have been shown to have seed domain lengths of 6 or 7 nuleotides (77-79); these lengths may be suitble for a lot of sRNA-mRNA base pair models. Interestingly,

studies suggested that many seed domains were located at the 5′ ends position of sRNAs (79,80) which perhaps have functional effect. We still don′t know much about the relationship between the characteristics of targeting mRNAs and base-pairing.

1.2.4 Intimate Connections Between sRNAs and RNases

RNase E or RNase III are directly involved in the sRNAs modulation of mRNA stability (81). It was proven that after an mRNA is bound by a sRNA, they are degraded either by RNase III or E (82). For example, the sRNA *RyhB* base-pairs with its mRNA targets, and RNase E is mediated in the subsequent degradation (83). Cutting of sRNA-mRNA duplexes is always performed by RNase III (84), while RNase E works at single-stranded regions (81).

1.2.5 Functions of RNA Chaperones

The role of the RNA chaperone Hfq can not be ignored for the roles of *trans*-encoded-sRNAs in Gram-negative bacteria (85). Hfq has proved to mediate and facilitate base pairing by improving annealing rates (86-88), stabilizing sRNA-mRNA duplexes (89), or by enhancing structural changes in one of the RNA partners (90). *In vitro* experiments have proven that Hfq binding to mRNA usually occurs at A/U-rich single-stranded regions close to a secondary structure. However, we can not predict the Hfq binding sites in sRNAs because of low conservation and presence of multiple A/U-rich sites. Additionally, polyU at the 3′ end of sRNAs is combined with Hfq, probably functioning as a loading site (91,92). Nevertheless, compared to the information about Hfq binding sites on sRNAs, Hfq binding sites on mRNAs and their physiological relevance are less understood.

Studies of Hfq in posttranscriptional regulation were performed in a range of organisms. For instance, Hfq in the Gram-negative spirochaete *Borrelia burgdorferi* (93) and the Gram-positive firmicute *Listeria monocytogenes* (94), have significant differences (95). In Gram-negative species, the Sm-like protein Hfq is needed for *trans*-encoded sRNAs mediated antisense regulation , however, *trans*-encoded sRNAs regulation may happen in both Hfq-dependent and -independent conditions in Gram-positive species (94). Other bacteria like *Burkholderia cenocepacia* (96) harbor diverse Hfq-like proteins indicating possible functional complexity.

It was proposed that some other proteins could contribute to base-pairing sRNA functions. This kind of proteins could act instead of Hfq in species with non-obvious Hfq homologs. However, the second established RNA chaperon, ProQ, was found in *E. coli*, where it works in parallel to Hfq (97,98). It shows similarity in the C-terminal domain structure to Hfq (99). Another candidate is YbeY protein in *Sinorhizobium meliloti*, since the deletion of its gene has similar consequences like the deletion of *hfq* (100).

Furthermore, Hfq binds to the large C terminus of RNase E (8), indicating that RNase E is attracted to sRNA-mRNA pairs via Hfq. Recently, high-throughput studies were used to globally position Hfq connections with cellular RNAs and to uncover sRNA-mRNA interactions (98,101).

1.2.6 Regulating Protein Activity by sRNAs

The majority of sRNAs biochemical reactions are operating together with proteins *in vivo*. According to their different interactions, the connection between sRNA and protein can be separated in two groups. The first one, as mentioned above, is like chaperone protein Hfq and RNases to be involved in the sRNA-mRNA interactions to achieve mRNA destabilization. The second one is that the protein activity is regulated by sRNA.

For example, sRNAs can function as a mimic of the mRNA, regulating RNA binding proteins by competing the binding sites located in the proteins . As we know, the CsrA protein modulates mRNA translation and degradation by binding a specific sequence in the RBS. The sRNA *CsrB* harbors 18 copies of this CsrA-binding sequence and directly competes with CsrA target mRNA to interact with the CsrA protein in *E. coli* (102). More diverse CsrA- and *CsrB*-like molecules need to be invesigated to further understand the flexibility in target site recognition. *CsrB*-like sRNAs are widely present in diverse bacterial species, however, multiple CsrA-like proteins are only found in limited cases (103).

Another strategy of sRNAs binding proteins is to suppress, promote or modify the proteins enzymatic activity (Figure 1.2.6) (104-106). The classical example is 6S RNA modulating the RNA polymerase activity. 6S RNA accumulates in the stationary phase and binds RNA polymerase with the sigma 70 housekeeping factor. In this way, it contributes to the global changes in gene expression in the stationary phase (104).

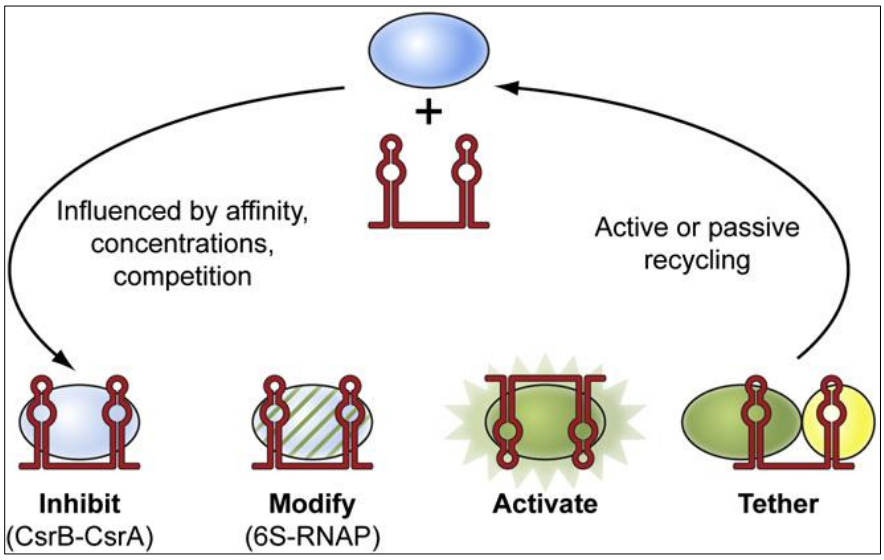

Figure 1.2.6 Modulation of Protein Activity by sRNAs (107).

1.2.7 Defining sRNA Regulons

Due to their action by imperfect complementarity, bacterial sRNAs (like miRNA in eukaryotes) can have multiple targets and own regulons. There are two basical approaches for understanding sRNAs regulons, computation and experiment. As we known now, microarrays, deep sequencing, or comparative analyses using results of experimental approaches can be used for studying gene expression which dependent on sRNAs. Furthermore, global searches, genetic screens for analysing reporter gene expression changes and/or growth phenotypes help to define sRNA regulons. Computational approaches are usually focused on predicting and

understanding the potential proteins and mRNAs which can interact with an sRNA. Experimental approaches often up- or down-regulate the sRNA gene expression to analyse whether observed effects are direct or indirect and to understand the physiological role of the sRNA. However, identification of direct effects is crucial for understanding of how sRNAs participate in regulatory networks. Some studies have already shown relationships between sRNAs regulons and physiological responses. For example, under carbon starvation, increasing *crfA* sRNA levels lead to induction of TonB-dependent receptors, thus promoting nutrient absorption in *Caulobacter crescentus* (108). In another case, low level of iron increased the level of the Fur-regulated *RyhB* sRNA, which regulates several genes to contribute to metabolic remodeling under low-iron conditions (109).

Generally, direct sRNA effects are faster than the indirect effects (110,111), but it should be considered that effects on translation and mRNA decay can have different kinetics. To validate direct effects in the sRNA-mRNA base pairing regulation model, usage of mutations in the sRNA seed region and corresponding compensatory mutations in the mRNA is still a gold standard. However, mutagenesis sometimes could not give a final result, for example if it affects the sRNA structure and thus the seed region accesisbility or if several functions are in the base-pairing region. For now to differentiate between direct and indirect modulation is still not easy (104).

In the same time we need to think that among the multiple targets regulated by an sRNA, some could be biologically more significant than others under certain conditions. Utilizing the current experimental and computational approaches, we will lose some targets which may be very important. Many researches focused on high level changes of mRNAs upon sRNAs regulation, but the low level changes are usually missed. Furthermore, sometimes sRNAs regulation do not show the biochemical reaction that mRNAs level changes, or even though mRNAs level change, this not necessarily influence the protein level. We also need to consider that a classical method to test the changes of gene expression and/or phenotypes is to overexpress the sRNA of interes to non-physiologically high level and results obtained by this method should be considered with caution.

Computation prediction is an important approach for quick, preliminary information about the potential target mRNAs of the sRNA of interest (112). However, we can not fully trust the prediction results due to high false positive rates and therefore experimenatl validation of each particular candidate is necessary.

1.2.8 Advantages of sRNA Regulators

More and more evidences have shown sRNA regulons contribute to huge regulatory networks in bacteria (107,113). Recent results implied that regulatory proteins probably modulate several sRNAs, in addition, the crosstalk between regulatory networks is much more complex than now identified.

To understand a bacterial lifestyle, the outstanding advantages between RNA-based modulation and protein-based modulation should be considered and discussed. Early reduction of metabolic energy costs and faster response were considered as benefits of RNA-

based regulation (113). Indeed, the sRNAs can produce responses in the process of coupled degradation of sRNA-mRNA pairs, which differs from the response by transcription factors (114).

1.2.9 Identification and Analysis of sRNAs

The initial standard approaches looking for sRNAs often depended on conservation or presence of promoter and terminator sequences in intergenic regions, or on the RNA size, leeading to low efficiency of sRNAs identification (60). Now advanced and mainstream approach is deep sequencing, which has ability to dig out hundreds of transcripts undetected before (115,116). The sequencing reads align to both intergenic and intragenic regions, in both sense and antisense orientations with respect to annotated known genes and correspond to transcripts of diverse sizes. So far, deep sequencing is a power tool for learning and knowing sRNAs and their interaction partners. For example, MS2-tagged sRNA can be co-purified together with its mRNA and protein binding partners (117). Furthhermore, after pull down of tagged Hfq and/or ProQ, sRNA-mRNA pairs can be identified (98). The latter approach helps us to characterize hundreds unknown sRNAs and their targets faster and easier.

Also constructing sRNAs deletion strains and suitable plasmids for induced sRNA overproduction are necessary and useful strategies, which are well establshed for *E. coli* and *Salmonella* (118-120) and must be adapted for other species such as *Sinorhizobium meliloti*. However, in many cases to relate a phenotype to changed sRNAs level in the cell is weird and subtle and only happens under specific conditions. Thus, high-throughput screens should be performed for unique strains for identifying phenotypes..

1.3 Multidrug Efflux in Gram-Negative Bacteria

Iduced efflux is an important mechanism of resistance to different toxic compounds including antibiotics, and plant-produced compounds (121). Multidrug resistance efflux systems (MDR) which are of broad existance in Gram-negative bacteria (122), are considered as the key mechanism of intrinsic and acquired multiresistance (123,124). Bacterial efflux transporters are categorized into five major superfamilies, based on accommodating multiple antimicrobials: the major facilitator superfamily (MFS); the ATP binding cassette (ABC) superfamily; the resistance-nodulation-division (RND) family; the small multidrug resistance (SMR) family; and the multi antimicrobial extrusion protein (MATE) family (125). Only the ABC superfamily members are primary transporters, the rest of families act as secondary transporters using proton or sodium gradient as a source of energy. The RND family is most commonly found in Gram negative bacteria as a part of a tripartite system (126).

Fourteen efflux systems have been discovered in plant-symbiotic *Sinorhizobium meliloti*. Among them, one RND-type pump, the SmeAB is proved to play a crucial role in the antimicrobial resistance, whereas the other two RND-type pumps, SmeCD and SmeEF, only contribute slightly. In addtion, the amount of smeAB MDR efflux pump is predicted to be modulated by SmeR (127). SmeR repressor as a transcription regulator of TetR family via binding the promoter of smeAB gene to suppress the smeAB transcription and than negatively effect translation.

1.4 DnaA Regulation

DnaA as an important protein activating initiation of DNA replication in bacteria. Importantly, the control factor for beginning the initiation phase of DNA replication is the concentration of DnaA. During growth, DnaA accumulates and sparks the initiation of replication. DNA replication starts by binding of activated ATP-DnaA to 9-mer repeats upstream of *oriC*. This leads to strands separation in a specific 13-mer repeats (128).

In *E. coli* DnaA can prevent RNA polymerase binding to the promoter of its own gene *dnaA*. The DnaA protein binding inhibits initiation of transcription of *dnaA*. That means, DnaA protein is capable to modulate its amount in the cell (129,130). Interestingly, the relative amount of DnaA is stable under different growth conditions and thus at different growth rates. It was proposed, that the DnaA homeostasis is regulated posttranscriptionally (129) , but sRNA binding to *dnaA* mRNA was not identified in *E. coli* yet.

1.5 Ribosome-dependent Transcription Attenuation

Ribosome-dependent transcription attenuation is a posttranscriptional mechanism discovered 40 years ago. It is widely distribiuted and highly conserved (131-134). Translation efficiency of a short upstream ORF (uORF) determines whether a transcription terminator stem-loop structure is formed to control the downstream genes transcription. It was supposed that the leader peptide encoded by the uORF and, in case of transcription termination, the arising attenuator sRNA do not have own functions.

Ribosome-dependent transcription attenuators are widespread in amino acid (aa) biosynthesis operons of gram-negative bacteria (133,134). In recent days, antibiotic resistance operons were also found to be modulated by attenuators in many gram-positive bacteria: upon exposure of *Bacillus* or *Listeria* to translation-inhibiting antibiotics, ribosome stalling at uORFs inhibits forming hairpin terminator structure, resulting in the inducing of the expression of downstream resistance genes (135). Moreover, as much more high synteny conservation of attenuator uORFs was identified in bacteria, the question arises whether some of their leader peptides have gained independent roles in *trans* during evolution. Indeed, more and more evidence was presented that very small proteins own important functions although their genses are not annotated (136). For example, in *Bacillus subtilis*, the basic 29-aa protein FbpC was proposed to act as an RNA chaperone (137), however, in *E. coli*, the 31-aa protein MgtS was idnetified to interact with two distinctive proteins and meidate Mg^{2+} homeostasis (138).

1.5.1 *Escherichia coli*

Escherichia coli is a Gram-negative, facultative anaerobic, rod-shaped, coliform bacterium. It′s belong to genus *Escherichia* which inhabits the lower intestine of warm-blooded organisms (139). The majority of *E. coli* strains are non-dangerous types, however several types can lead to serious disease in their hosts. The harmless strains are important bacteria in host gut that produce vitamin K2 (140) and contribute to stop of gut colonisation by pathogenic bacteria (141,142). *E. coli* enter into the enviroment from hosts via the feces.

The bacterium can exist and grow in fresh fecses under aerobic conditions with high quantity for 3 days, but its dead phase can be continued much more longer (143).

In the last six decades, as a prokaryotic model organism, *E. coli* has been tremendouly investigated . It can be cultured easily and inexpensively, and these characterisitics were used for investigations in the fields of biotechnology and microbiology. Another important characterisitic as model organism is its short division time; under suitable conditions, it takes as short as 20 minutes to duplicate.

1.5.2 *Sinorhizobium meliloti*

Sinorhizobium meliloti is an α-proteobacterium which can build a close symbiosis with the roots of legumes belonging to the genus *Medicago*, *Melilotus* and *Trigonella* (144). *S. meliloti* as symbiotic bacteria use a complex chemical dialog for coss-recognition between bacterium and plant roots, which lead to root nodule formation. In the nodules, the differentiated bacteria fix atmospheric nitrogen in an ecologically and agricultrally important reaction (145). The genome of the sequenced S. *meliloti* includes three replicons, the "chromosome" (3.65 Mb) and two mega-plasmids, pSymA (1.35 Mb) and pSymB (1.68 Mb). pSymA as larger plasmid contributes to nodulation and nitrogen fixation biochemical reactions (146-148). As a soil-dwelling organism interacting with plans, it is an important, Gram-negative model organism.

1.5.3 *trp* Genes Transcription Attenuation in *E. coli* and *S. meliloti*

The well known model of transcription attenuation is that of the Trp biosynthesis genes *trpEDCBA* which are co-transcribed in *E. coli* (132) The 5′ mRNA leader harbors the uORF *trpL*, which contains two consecutive Trp codons (the 10. and 11. codon of the 14 aa leader peptide). Under Trp insufficiency conditions, ribosome pauses at the Trp codons in order to prevent the formation of a transcriptional terminator downstream of the uORF, thus leading to co-transcription of *trpL* with the structural *trp* genes. In contrast, if enough tryptophan is present in the cell, fast translation of the Trp codons causes transcription termination between *trpL* and *trpE*. However, transcription termination between *trpL* and *trpE* is also caused by ribosome pausing in the first half of *trpL* (149).

Like in many other bacteria, the *trp* genes of *S. meliloti* are organized in three operons: *trpE(G)*, *trpDC*, and *trpFBA*. However, only *trpE(G)* is regulated by transcription attenuation (133,150). Essentially nothing was known about the posttranscription regulation of the another two operons. Recently, the 110 nt attenuator sRNA of the *trpE(G)* operon, which was originally named RcsR1 and later renamed to rnTrpL (see below), was shown to directly regulate *sinI* mRNA, which encodes an autoinducer synthase. Additionally, several other mRNAs were predicted to base-pair with rnTrpL (151). Regulating multiple mRNAs is a typical feature of bacterial sRNAs which show imperfect complementarity to their targets(107). As menioned above, for efficient target binding sRNAs often need RNA chaperones like Hfq and ProQ (97,152). However, ProQ homolog is not encoded by the *S. meliloti* genome (146) and rnTrpL was described as an Hfq-independent sRNA (151). Thus, rnTrpL probably interacts with another, yet unknown protein(s).

An important difference between the regulation of the *trp* operon in *E. coli* and the *trpE(G)* operon in *S. meliloti* exists at the transcription level. Transcription of ther *E. coli trp* operon is repressed by a TrpR represor bound to L-Trp. Unter low Trp conditions, the repressor falls off DNA and transcription is initiated. Additional fine tuning of the *trp* operon expression is mediated by the above described transcription attenuation (133). In *S. meliloti*, however, the *trpE(G)* operon is transcribed constitutively during growth and its regulation according to the Trp availability is only at the posttranscriptional level (150).

Aim of Work

Ribosome-mediated transcription attenuation is a basic and widespread mechanism for posttranscriptional regulation in bacteria. The liberated attenuator RNAs and the leader peptides arising in this process are considered nonfunctional. However, results in our laboratory revealed that in *S. meliloti*, the attenuator sRNA rnTrpL and the peptide peTrpL encoded by this sRNA have functions in *trans.*

A major goal of this work was to characterize the role and the mechanisms of the sRNA rnTrpL and the leader peptide peTrpL in posttranscriptional regulation of putative target genes in *S. meliloti*. For this, it was planned to construct suitable *S. meliloti* deletion mutants and to establish systems for induced, ectopic production of the sRNA and peptide. These systems were planned to be used for validation of the direct interaction between rnTrpL and *trpDC* mRNA, for analysis and detection of additional rnTrpL and peTrpL targets, and for alanine scanning mutagenesis addressing the mechanisms of peTrpL. A special focus of the work was the validation of antibiotic-induced asRNAs working together with antibiotic-dependent targets of rnTrpL and/or peTrpL such as *rplUrpmA* and *smeR*.

A second, major goal of this work was to test whether Ec-rnTrpL is a *trans*-acting sRNA in *E. coli*. As a preliminaty work, targets of Ec-rnTrpL were predicted by Dr. Jens Georg (University of Freiburg). It was planned to analyze the top five predicted targets addresing the following questions: 1) Are these mRNAs affected by overexpression of the sRNA or by deletion of its gene? 2) Are there antibiotic-dependent and antibiotic-independent targets in *E. coli* as observed in *S. meliloti*? 3) Is there a direct interaction between a target mRNA and Ec-rnTrpL and what are the physiological consequences of this interaction?

2 Results

2.1 The Attenuator sRNA rnTrpL in *S. meliloti*

2.1.1 Construction of a *S. meliloti* 2011*ΔtrpL* Mutant and Its Comparison to the Parental Strain under Tc Stress

In many bacteria including the plant symbiont *Sinorhizobium meliloti*, the *trp* genes are organized in several operons, only one of which is regulated by attenuation. In *S. meliloti*, the *trp* attenuator is located upstream of *trpE(G)* (Figure 2.1.1A), which is transcribed separately from *trpDC* and *trpFBA*. For further investigations in the absence of native rnTrpL RNA being transcribed from the chromosome, a deletion mutant 2011*ΔtrpL* was constructed, in which the original TSS of *trpLE(G)* with the first two nucleotides (AT) was preserved (Figure 2.1.1B and Figure 2.1.1C).

Preliminary work in our laboratory suggested that rnTrpL is important for resistance to tetracycline (Tc). Therefore, the growth of strains 2011 and 2011*ΔtrpL* was compared at different Tc concentrations. Both strains were found to reach similar ODs in the absence of Tc, and they failed to grow in medium containing 10 µg/ml Tc, which was half of the concentration used in our selective media. However, in medium supplemented with 0.2 µg/ml Tc, the parental strain grew faster than the mutant 2011*ΔtrpL*. Additionally, in medium containing 0.5 µg/ml Tc, the parental strain 2011 reached a significantly higher OD compared to the deletion mutant (Figure 2.1.1D). These results show that the native *trpL* is important for the Tc resistance of *S. meliloti*.

A

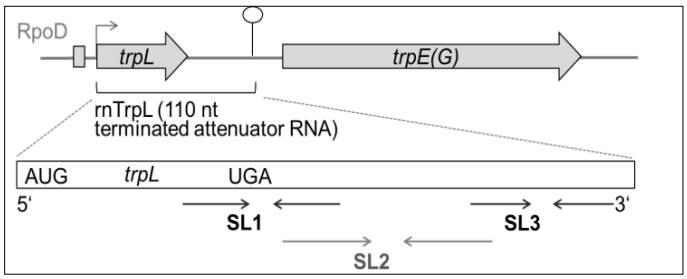

B

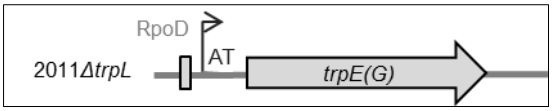

C

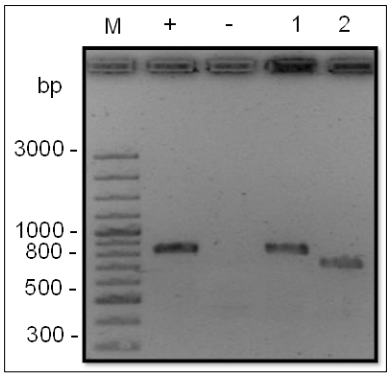

D

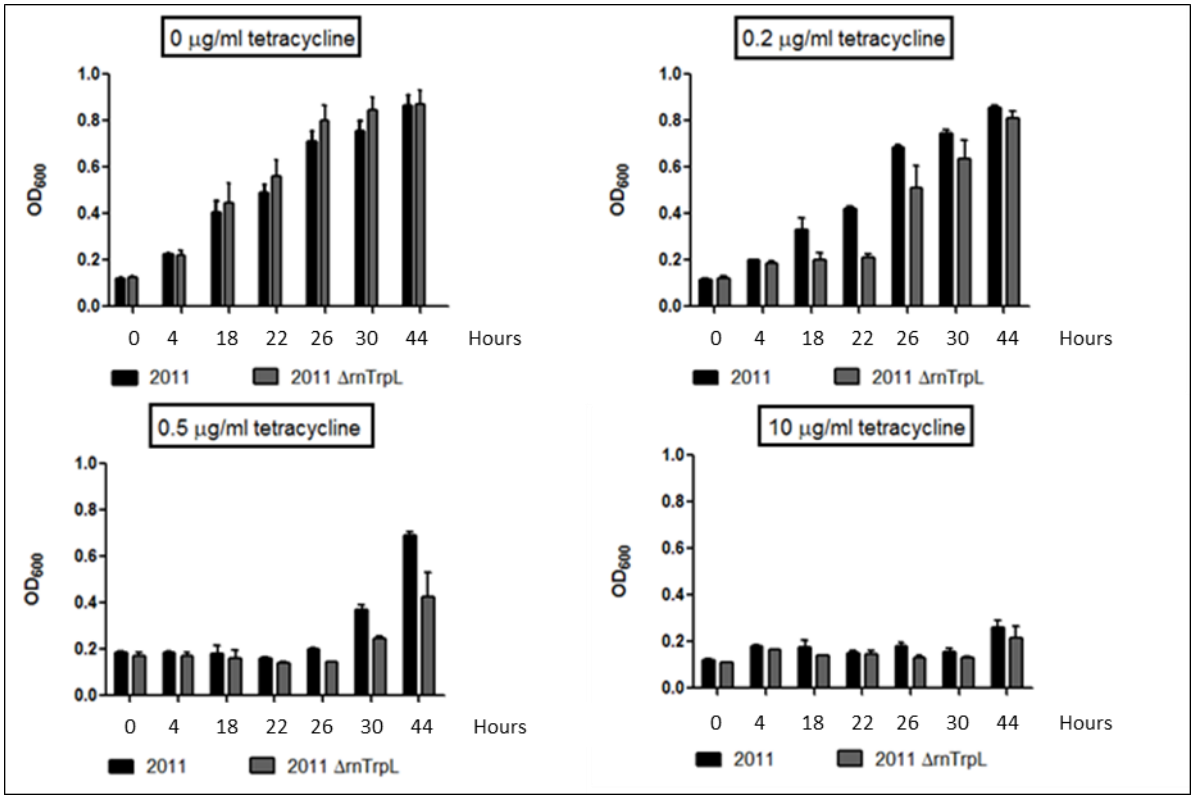

Figure 2.1.1 Construction of a *S. meliloti* 2011*ΔtrpL* Mutant and Its Comparison to the Parental Strain under Tc Stress. (**A**) Scheme of the *trpE(G)* operon and the attenuator sRNA rnTrpL of *S. meliloti*. ORFs are depicted by gray arrows, a RpoD-like promoter by a gray rectangle, transcription start sites by flexed arrows and a transcription terminator by a hairpin. The terminated attenuator sRNA rnTrpL (110 nt; synonym RcsR1) is shown as a white box with start and stop codons indicated. Below this box, regions corresponding to stem-loops (SL) 1, 2 and 3 are depicted by convergent arrows. SL2 corresponds to the antiterminator and SL3 to the terminator of transcription. SL2 is formed only in the presence of translating ribosomes that pause upon $tRNA^{Trp}$ shortage. (**B**) Scheme of the *trpE* locus in the deletion mutant 2011*ΔtrpL*. The original TSS with the first two nucleotides (AT) was preserved. (**C**) Colony PCR confirming the *ΔtrpL* deletion mutation. M is 100 bp marker, + is postive control, - is negitive control, 1 is wild type obtained after the double cross-over, 2 is sucessful *ΔtrpL* deletion after double crossover. (**D**) Strain 2011 grows better than the deletion mutant 2011*ΔtrpL* at a subinhibitory Tc concentration in microtiter plates. Strains and Tc concentrations are indicated. In this experiment, bacteria were cultured in TY medium. Data shown in the graphs were obtained from three independent experiments, each performed in technical duplicates (means and SDs are indicated).

2.1.2 Pulse-overexpression of the sRNA lacZ′-rnTrpL and Its Influence on Predicted mRNA Targets

To avoid secondary effects due to constitutive sRNA overproduction, plasmid pSRKGm-rnTrpL for IPTG-inducible transcription of recombinant rnTrpL was constructed. In this plasmid, the *trpL* ORF of rnTrpL is cloned in frame to a 38-nt *lacZ* mRNA leader harboring a ribosome-binding site (Figure 2.1.2A). Figure 2.1.2B shows the induction of this rnTrpL derivative (designated lacZ′-rnTrpL) in strain 2011*ΔtrpL* (pSRKGm-rnTrpL). Several mRNA targets were analyzed, which were predicted previously to interact with the sRNA rnTrpL (151). As expected, the levels of the candicate mRNAs *motE*, *flgA*, *phoR*, *gntR* were decreased when lacZ′-rnTrpL was induced by IPTG for 10 min. Also the level of *sinI* as positive control, which was already validated to interact with the sRNA (151), was decreased.

But *mcpU* mRNA level was not decreased upon rnTrpL induction, suggesting that *mcpU* is not targeted by lacZ'- rnTrpL (Figure 2.1.2C).

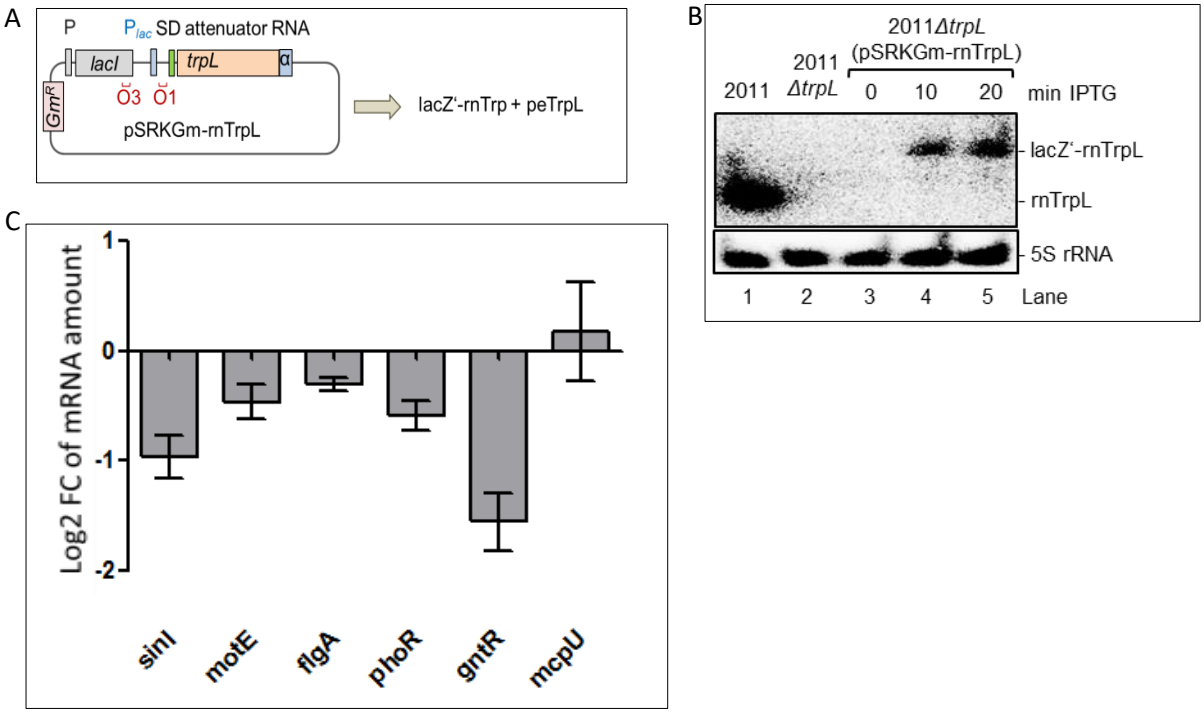

Figure. 2.1.2 Pulse-overexpression of the sRNA lacZ′ -rnTrpL and Its Influence on Predicted mRNA Targets. (**A**) Scheme of pSRKGm-rnTrpL. The pSRK-based plasmids harbor the *lac* repressor gene *lacI* with its own promoter, the *lacI-lacZ* intergenic region, the *lac*-promoter P_{lac} and the 38 nt *lacZ* leader containing the Shine-Dalgarno sequence (SD), followed by an NdeI restriction site containing ATG as the start codon for translation. Positions of the LacI-binding operators O1 and O3, the proper spacing of which ensures tight regulation at P_{lac}, are indicated. The rnTrpL corresponding sequence was cloned in frame in the NdeI site of pSRKGm. The resulting sRNA lacZ′-rnTrpL contains the 38 nt l*acZ*-leader. The scheme shows the plasmid conferring resistance to gentamycin (Gm) (pSRKGm-rnTrpL). A similar plasmid conferring resistance to tetracycline (Tc) was also constructed. (**B**) Northern blot hybridization showing IPTG-induced lacZ′-rnTrpL transcription at 10 and 20 min post induction in strain 2011*ΔtrpL* (pSRKGm-rnTrpL) (lanes 3, 4 and 5). Lanes 1 and 2 show the analysis of the indicated control strains. For the Northern Blot analysis, 5S rRNA was the reference (loading control) RNA. (**C**) qRT-PCR analysis of the levels of mRNAs predicted to interact with the sRNA rnTrpL (*sinI, motE, flgA, phoR, gntR, mcpU*). Strain 2011*ΔtrpL* (pSRKGm-rnTrpL) was used. The level of the mRNAs at the time point 10 min after 1mM IPTG addition was compared to the level before addition. In this experiment, bacteria were cultured in TY medium. For the qRT-PCR analysis, *rpoB* RNA was used as reference control RNA. Data shown in the graph were obtained from three independent experiments, each performed in technical duplicates (means and SDs are indicated).

2.1.3 Deletion of the *sinRI* Genes in Strain 2011 and Strain 2011*ΔtrpL* and Analysis of the Resulting Mutants Growth under Tc Stress

The above described sRNA induction system leads to transcription of the lacZ′-rnTrpL derivative. To use a plasmid for induction of the sRNA transcription starting with its native 5′-end, the known *sinI* promoter can be used, which needs SinR as an activator (153,154). To this end, it was necessary to delete the *sinRI* genes from the chromosome. These genes belong to the *sin* quorum sensing system of *S. meliloti*, which is inactive in the used "wild type" strain 2011. Therefore first deletion mutants were constructed, 2011*ΔtrpLΔsinRI* and

2011*ΔsinRI* (Figure 2.1.3A). Strains 2011*ΔtrpLΔsinRI* and 2011*ΔsinRI* were compared in respect to their growth under Tc stress. Both strains were found to reach similar ODs in the absence of Tc, and they failed to grow in medium containing 10 μg/ml Tc. However, in medium supplemented with 0.2 μg/ml Tc and 0.5 μg/ml Tc, strain 2011*ΔsinRI* grew faster or reached a significantly higher OD compared to the double mutant 2011*ΔtrpLΔsinRI* (Figure 2.1.3B). The results are simlar to the results obtained for strains 2011 and 2011*ΔtrpL* (Figure 2.1.1D), suggesting the lack of the *sinRI* genes in chromosome would not influcence the functions of the sRNA rnTrpL in *S. meliloti* under subinhibitory Tc exposure conditions.

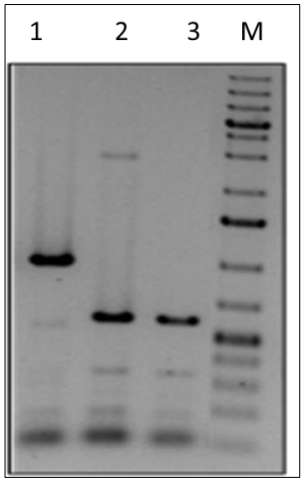

B

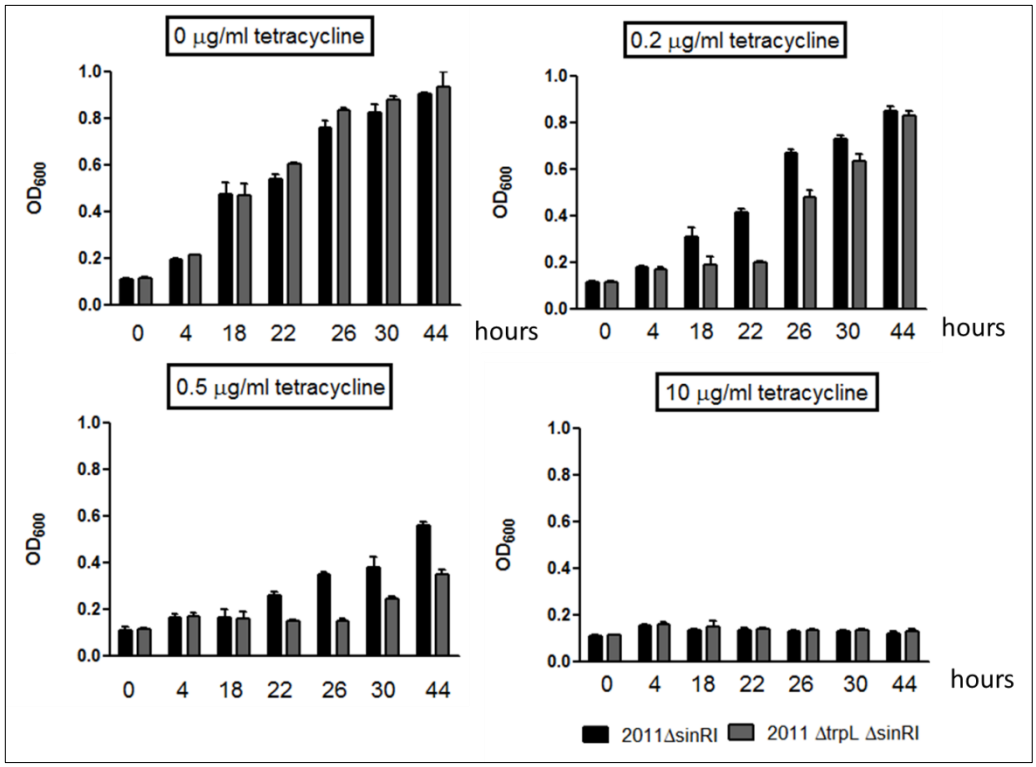

Figure 2.1.3 Deletion of the *sinRI* Genes in Strain 2011 and Strain 2011*ΔtrpL* and Analysis of the Resulting Mutants Growth under Tc Stress. (**A**) Colony PCR showing the *ΔsinRI* deletion mutations in the two genetic backgrounds. M is 1KB Plus marker, Line 1 was *S. meliloti* 2011; Line 2 was *S. meliloti* 20111 *ΔtrpL ΔsinRI*; Line 3 was *S. meliloti* 2011 *ΔsinRI*. (**B**) Strain 2011 *ΔsinRI* grows better than the double mutant 2011*ΔtrpL*

ΔsinRI at a subinhibitory Tc concentration. Strains and Tc concentrations are indicated. In this experiment, bacteria were cultured in TY medium. Data shown in the graphs were obtained from three independent experiments, each performed in technical duplicates (means and SDs are indicated).

2.1.4 Pulse-Overexpression of the sRNA rnTrpL Starting with Its Native 5′-end and its Influence on Predicted Targets

As already mentioned, the usage of pSRKGm(Tc)-rnTrpL plasmid leads to transcription of lacZ′-rnTrpL containing the 38 nt l*acZ*-leader. Since this could influence the sRNA function, a plasmid for sRNA transcription starting with the native 5′-end of the sRNA was designed. The scheme of the plasmid pSRKGm-sinRI-rnTrpL conferring resistance to gentamycin (Gm) is shown in Figure 2.1.4A. A similar plasmid conferring resistance to tetracycline (Tc) was also constructed. The plasmid harbors the IPTG-inducible *sinR* gene under the control of the *lac* promoter, the intergenic region between *sinR* and *sinI*, and the *sinI* promoter, followed by the rnTrpL sequence. To characterize this system of ectopic rnTrpL induction, first different IPTG concentrations and induction times were applied to find out the best condition for production of similar rnTrpL amount from the plasmid like from the chromosome. For short term expression, which was 10 min after IPTG addition, concentration of IPTG lower than 0.3 mM did not led to accumulation of sRNA detectable by Northern blot analysis. Further, when 0.3 mM IPTG was used, the rnTrpL level was lower than that of the chromosomally produced sRNA (Figure 2.1.4B). However, using 0.5 mM IPTG for 10 min led to a sRNA rnTrpL level comparable to that of the chromosomally transcribed sRNA (Figure 2.1.4D). In long term expression, which was 4 or 4.5 hours after IPTG induction, 0.1 mM of IPTG induced sRNA rnTrpL to a level similar to that in strain 2011*ΔsinRI* still harboring the rnTrpL gene in the chromosome (Figure 2.1.4C), and higher IPTG concentrations caused sRNA overproduction (Figure 2.1.4E).

Furthermore, a series of timepoints up to 10 min induction with 0.5 mM IPTG were tested in Northern blot hybridization analysis (Figure 2.1.4F) for sRNA accumulation and by qRT-PCR analysis for an effect of the sRNA on the predicted target *trpDC* mRNA (151) (Figure 2.1.4G). Ten min induction with 0.5 mM IPTG was considered as the best condition, since the sRNA was well detectable and *trpC* mRNA level was downregulated. Additional predicted targets (*rpmA, rpoE1, gntR, phoR, motE, mcpU and flgA*), *smeR* as a target of the peptide encoded by the sRNA (see below), and *trpE* as a negative control mRNA which is not regulated by rnTrpL or peTrpL, were analyzed by qRT-PCR before and 10 min after addition of 0.5 mM IPTG. In addition to *trpC*, all predicted target mRNAs except *rpoE1* but including *mcpU*, which was not influenced upon overproduction of lacZ'-rnTrpL(see Figure 2.1.2C above), showed reduced levels upon sRNA induction. The negative control *trpE* mRNA was no changed and postive control rnTrpL was increased as expected (Figure 2.1.4D). These results show that generally, 10 min induction of the native-5′-end-sRNA by 0.5 mM causes

similar effects like 10 min induction of the sRNA producted by the lacZ′-rnTrpL system (Figure 2.1.2C).

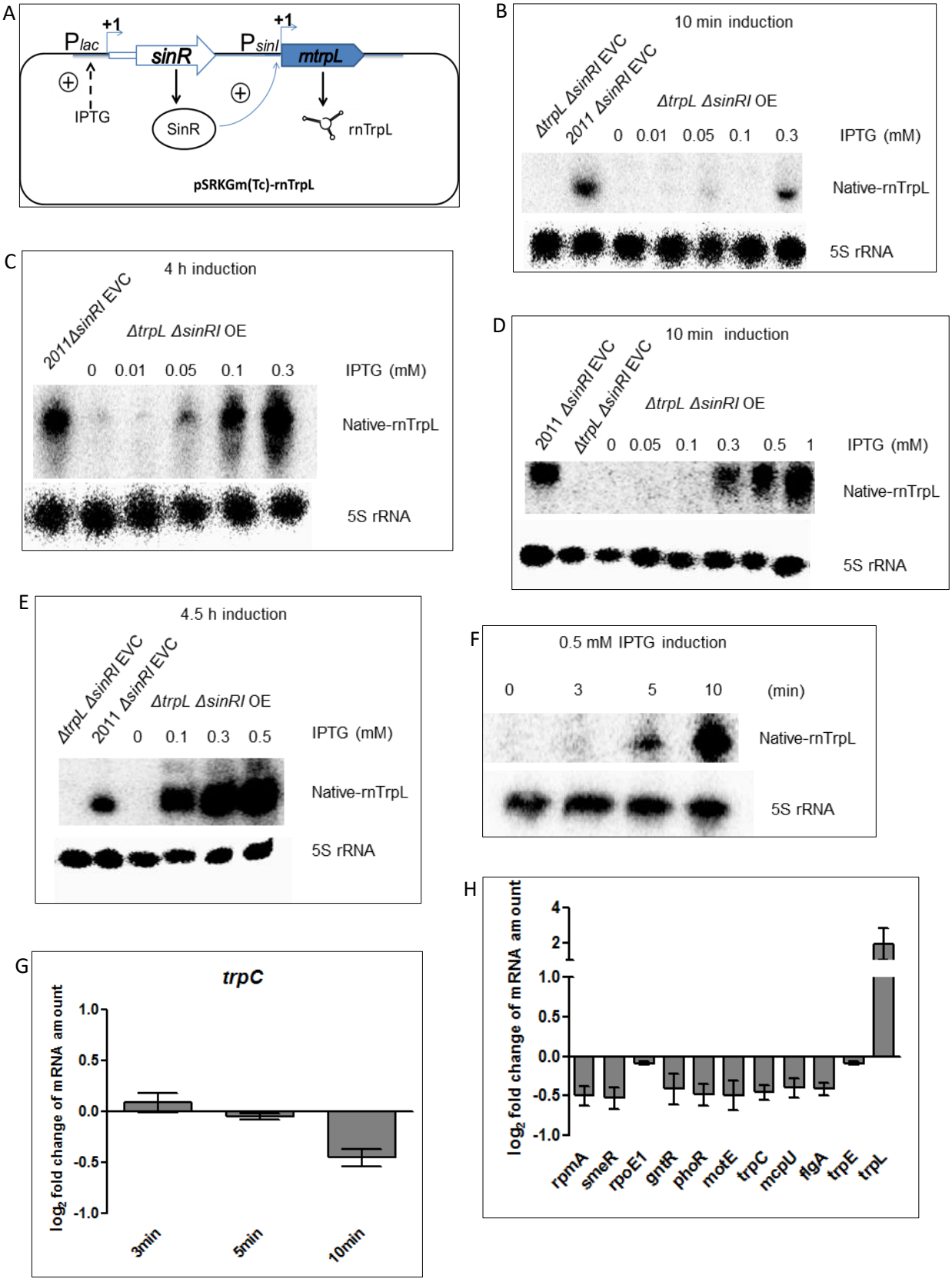

Figure 2.1.4 Pulse-Overexpression of the sRNA rnTrpL Starting with Its Native 5′ -end and its Influence on Predicted Targets. (A) Scheme of pSRKGm-sinRI-rnTrpL. This pSRK-based plasmid harbors the *lac* repressor gene *lacI* with its own promoter (not shown), the *lacI-lacZ* intergenic region, and *sinR* under the control of the *lac* promoter. In addition to *sinR*, the *sinR-sinI* intergenic region was cloned, followed by the sequence of the sRNA rnTrpL. For transcription of the sRNA starting with native 5′-end from the *sinI* promoter, *sinR* expression is necessary. Thus, indiction of *sinR* expression by IPTG activates transcription of the sRNA from the *sinI* promoter. The scheme shows the plasmid conferring resistance to gentamycin (Gm). A similar plasmid conferring resistance to tetracycline (Tc) was also constructed. **(B-E)** Northern blot hybridization showing rnTtrpL accumulation after addition of IPTG to strain *S. meliloti* 2011*ΔtrpLΔsinRI* (pSRKGm-sinRI-rnTrpL), marked as *ΔtrpLΔsinRI* OE. Used IPTG concentrations and induction times are indicated. Strains 2011*ΔtrpLΔsinRI* and 2011*ΔsinRI* were as negative and postive controls. **(F)** Northern blot hybridization showing a series of timepoints (mindicated in minutes) after addition of by 0.5 mM IPTG to strain 2011*ΔtrpLΔsinRI* (pSRKGm-sinRI-rnTrpL). Accumulation of the induced native-5′-end rnTrpL sRNA over time is shown. (**G**) qRT-PCR analysis of the *trpC* mRNA level using the RNA samples shown in panel **(**F**)** and in two additional experiments. The *trpC* mRNA levels 10 min after IPTG addition were compared to the levels before IPTG addition. (**H**) qRT-PCR analysis of changes in the levels of the indicated mRNAs 10 min after addition of 0.5mM IPTG to strain 2011*ΔtrpLΔsinRI* (pSRKGm-sinRI-rnTrpL). *trpE* was a negative control, and rnTrpL (*trpL*) was a postive control. For these experiments, bacteria were cultured in TY medium. For the Northern Blot analysis, 5S rRNA was the reference (loading control) RNA. For the qRT-PCR analysis, *rpoB* RNA was used as reference control RNA. Data shown in the graphs were obtained from three independent experiments, each performed in technical duplicates (means and SDs are indicated).

2.1.5 The sRNA rnTrpL Base-Pairs with *trpD* to Downregulate *trpDC* mRNA

Figure 2.1.4C-b above showed that overexpression of the sRNA rnTrpL leads to *trpC* mRNA decrease. The *trpC* gene is a part of the *trpDC* operon. The predicted binding of rnTrpL to a region in the *trpD* coding sequence is shown in Figure 2.1.5A. To provide conclusive evidence for these base-pairing interactions, *in vivo* assays were performed in strain 2011*ΔtrpL* using bicistronic *trpDC′::egfp* reporter constructs and lacZ′-rnTrpL derivatives. The *trpDC′::egfp* fusions (Figure 2.1.5B) were expressed from pSRKGm (conferring Gm^r) and challenged with wild type (wt) or mutated lacZ′-rnTrpL transcribed from pSRKTc (conferring Tc^r) (Figure 2.1.2A). To avoid long-term effects, fluorescence was measured 20 min after simultaneous induction of transcription of the reporter fusion construct and the sRNA.

Figure 2.1.5C shows that TrpC′-EGFP fluorescence derived from plasmid pSRKGm-trpDC′-egfp was strongly decreased if lacZ′-rnTrpL was co-expressed, supporting the idea that the sRNA binds to *trpD* and thereby induces a reduction of *trpDC′::egfp* mRNA levels. In contrast, if sRNA derivatives carrying CG40,41GC and CC46,47GG mutations, respectively, were co-expressed, no decrease in fluorescence was observed. To test whether this was due to a significantly reduced (or lack of) binding of the mutated sRNAs to *trpD* in the bicistronic reporter mRNA, appropriate mutations were introduced into the *trpD* binding site to restore the presumed base-pairing interactions (Figure 2.1.5A). Indeed, a decrease in fluorescence produced by the pSRKGm-trpD-CG985,986GC-trpC′-egfp construct was (only) observed if the corresponding base-pairing sRNA lacZ′-rnTrpL-CG40,41GC was coexpressed.

Consistent with this, the fluorescence produced by the pSRKGm-trpD-CC977,978GG-trpC′-egfp construct was (only) decreased if lacZ′-rnTrpL-GG46,47CC sRNA was co-expressed (Figure 2.1.5C). These results validate the base-pairing between rnTrpL and *trpD* and show that this interaction is responsible for the negative effect of rnTrpL on *trpDC*.

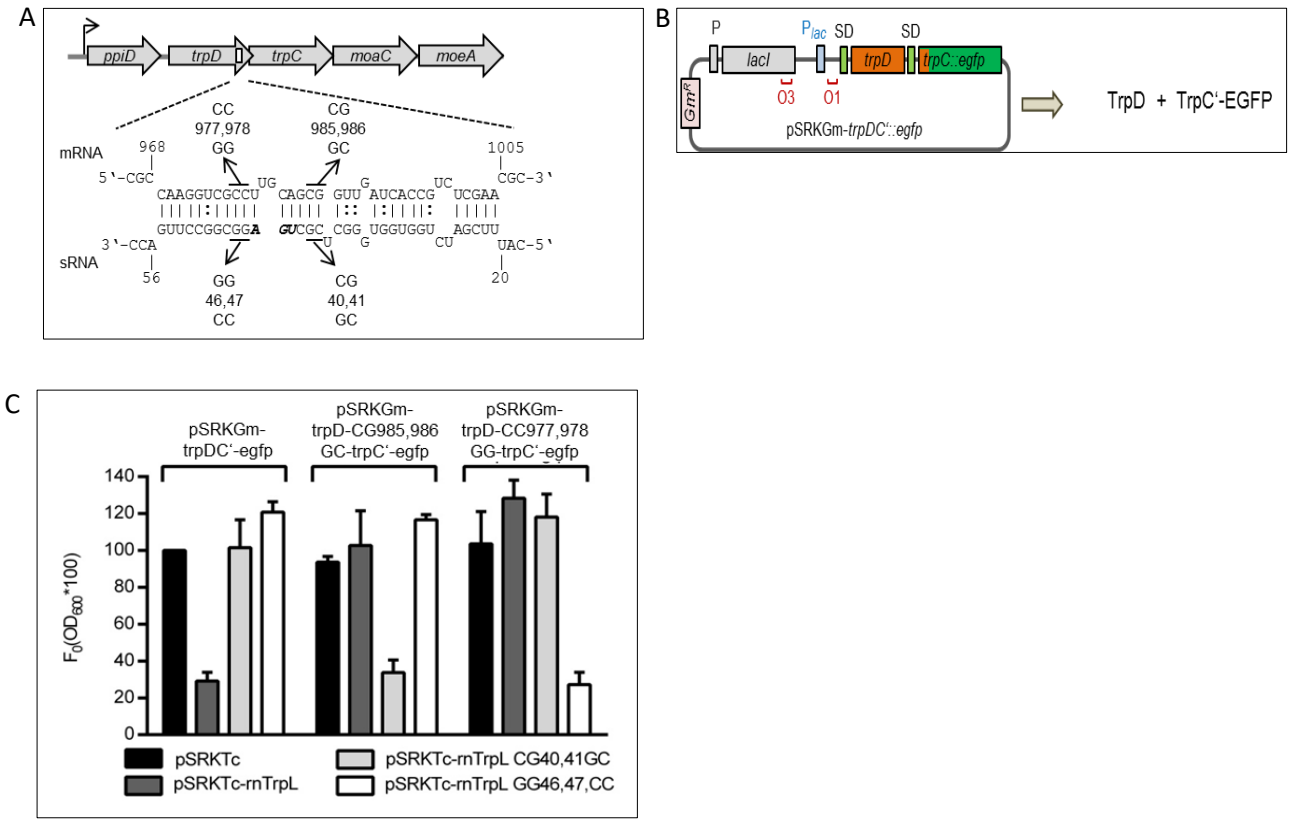

Figure 2.1.5 The sRNA rnTrpL Base-Pairs with *trpD* to Downregulate *trpDC* mRNA. (**A**) Scheme of the duplex structure predicted to be formed between *trpD* (mRNA) and rnTrpL (sRNA) (ΔG = -13.51 kcal/mol). rnTrpL mutations characterized in this experiment are given below the sRNA sequence. The *trpL* stop codon is shown in bold and italics. Compensatory *trpD* mutations used to restore base-pairing interactions are shown above the mRNA sequence. Nucleotide numbering starts at the translation start codon of both the *trpD* mRNA and the sRNA, which harbors the *trpL* sORF. (**B**) Scheme of pSRKGm-trpDC′-egfp. The *trpDC′::egfp* fusion contains the first 16 *trpC* codons fused to the third *egfp* codon. (**C**) Analysis of possible base-pairing interactions between lacZ′-rnTrpL and the fusion mRNA *trpDC′::egfp* in strain 2011*ΔtrpL*. Used plasmids are indicated. Fluorescence measurement was performed by H. Melior. Fluorescence was measured at 20 min after induction with IPTG; the fluorescence obtained for strain 2011*ΔtrpL*(pSRKGm-trpDC′-egfp, pSRKTc) was set to 100 % and used for normalization. For these experiments, bacteria were cultured in TY medium. Shown are the results from three independent experiments, each performed in duplicates (means and standard deviations are indicated).

2.1.6 Induced Production of the Peptide peTrpL Decreases the Levels of *smeR* and *phoR* mRNA

Since rnTrpL is an attenuator sRNA, it harbors the small ORF *trpL* encoding the leader peptide peTrpL (14 aa). Preliminary analyses in the laboratory suggested that peTrpL has own functions under conditions of subinhibitory Tc exposure (1 µg/ml Tc). Figure 2.1.2A shows that pSRKGm-rnTrpL will not only produce the sRNA lacZ′-rnTrpL but also the peptide

peTrpL. Therefore, a pSRKGm-based plasmid was constructed, from which only peTrpL (and not the whole sRNA) can be induced by IPTG (Figure 2.1.6A).

To test the influence of peTrpL induction on the mRNA levels, strain 2011*ΔtrpLΔsinRI* (pSRKGm-peTrpL) was used. To cultures grown in the presence of Gm, overproduction of the peptide peTrpL was induced with IPTG, and simultaneously, 1 µg/ml Tc was added. Of all the candicate mRNAs which have proved to be downregulated upon the sRNA rnTrpL (and peTrpL) induction (Figure 2.1.2C, Figure 2.1.4D), only *smeR* and *phoR* mRNA were downregulated when peTrpL production was induced in the absence of the sRNA (Figure 2.1.6B). Thus, these two mRNAs are good candidates for peptide targets, while the posttranscriptional regulation of the other mRNAs could be exerted by rnTrpL only or rnTrpL and peTrpL together. Indeed, Hendrik Melior have shown that *rpmA* is downregulated by both peTrpL and rnTrpL.

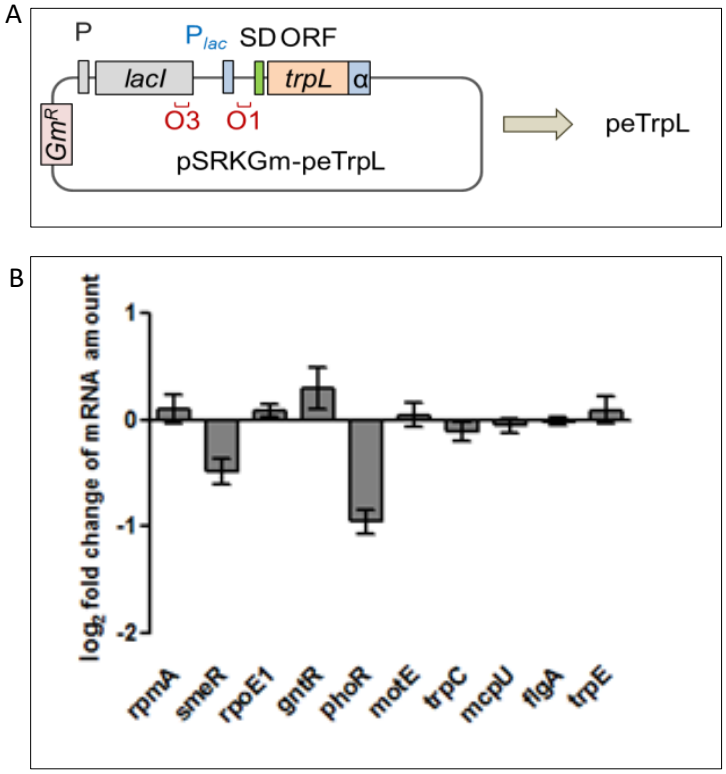

Figure 2.1.6 Induced Production of the Peptide peTrpL Decreases the Levels of *smeR* and *phoR* mRNA. (**A**) Scheme of pSRKGm-peTrpL. The pSRK-based plasmid harbors the *lac* repressor gene *lacI* with its own promoter, the *lacI-lacZ* intergenic region, the *lac*-promoter P_{lac} and the 38 nt *lacZ* leader containing the Shine-Dalgarno sequence (SD), followed by an NdeI restriction site containing ATG as the start codon for translation, which was the start codon of the cloned *trpL* ORF, which also harbored its own stop codon. Positions of the LacI-binding operators O1 and O3, the proper spacing of which ensures tight regulation at P_{lac}, are indicated. (**B**) qRT-PCR analysis of the effect of the induced peTrpL production on the levels of the indicated mRNAs, most of which are predicted targets of the sRNA rnTrpL (*sinI, motE, flgA, phoR, gntR, mcpU*). Cultures of 2011*ΔtrpLΔsinRI* (pSRKGm-peTrpL) were used, to which 1 µg/ml Tc was added along with 1 mM IPTG. The level of mRNAs 10 min after addition of Tc and IPTG was compared to the level before addition. In this experiment, bacteria were cultured in TY medium. The *rpoB* RNA was used as reference control RNA. Data

shown in the graphs were obtained from three independent experiments, each performed in technical duplicates (means and SDs are indicated).

2.1.7 Prediction of the peTrpL Structure

To deeply understand the mechanism of peTrpL, basical information of peTrpL is needed. Figure 2.1.7A shows the amino acid sequence of peTrpL, and Figure 2.1.7B presents the prediction of the 3D stucture of peTrpL which suggests only one alpha helix at the C-terminal end of peptide (pink region).

A

M	A	N	T	Q	N	I	S	I	W	W	W	A	R	
Met	Ala	Asn	Thr	Gln	Asn	Ile	Ser	Ile	Trp	Trp	Trp	Ala	Arg	END
ATG	GCA	AAC	ACG	CAG	AAC	ATT	TCG	ATC	TGG	TGG	TGG	GCT	CGC	TGA

B

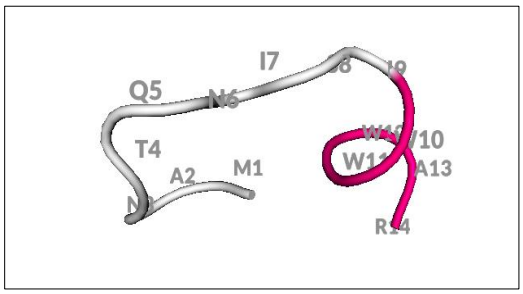

Figure 2.1.7 Prediction of the peTrpL Structure. (A) Scheme of peTrpL, Line 1, 2 and 3 are sort ascending, abbreviation and codon of amino acids of the peTrpL peptide. **(B)** Prediction of the 3D stucture of peTrpL made by PEP-FOLD(http://bioserv.rpbs.univ-paris-diderot.fr/PEP-FOLD**).**

2.1.8 Alanine Scanning Mutagenesis of Peptide peTrpL

According to the results of CoIP (155), *smeR*, *rplUrpmA* and their antisense RNAs (asRNAs) interact with peTrpL. To determine the amino acid (aa) residues in peTrpL, which are important for regulation of *rplUrpmA* and *smeR* in *S. meliloti*, alanine scanning mutagenesis was performed and functionality of the mutagenized peptides was tested in strain 2011. The strongest differences in comparison to the wild type peTrpL were caused by the exchange of Thr4, Ser8 and Trp12. Induced production of these mutated peptides led to an increase in the levels of sense (se)-*rpmA* (Figure 2.1.8B), *as-rpmA* (Figure 2.1.8C), se-*smeR* (Figure 2.1.8E), and as-*smeR* (Figure 8F), instead of a decrease, which was observed after induction of the wild type peptide.

A

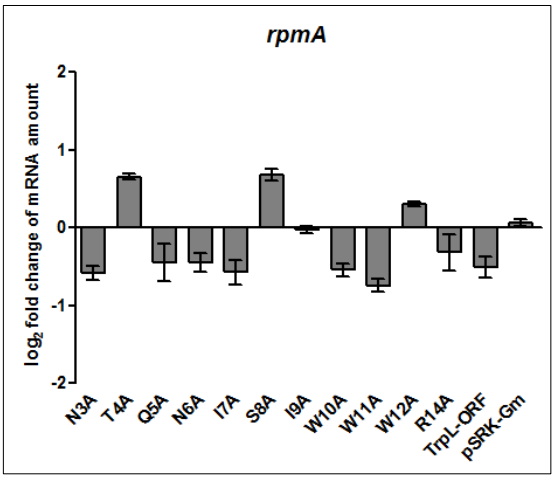

B

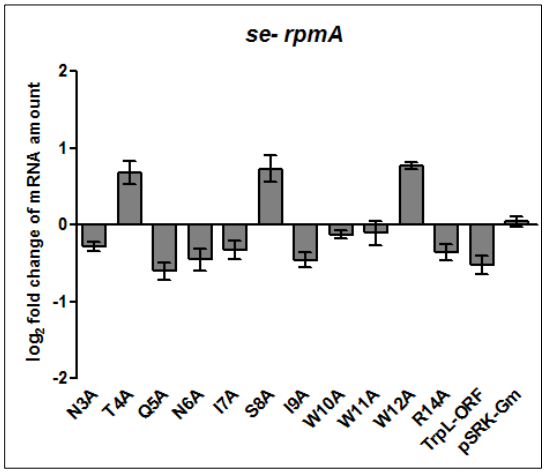

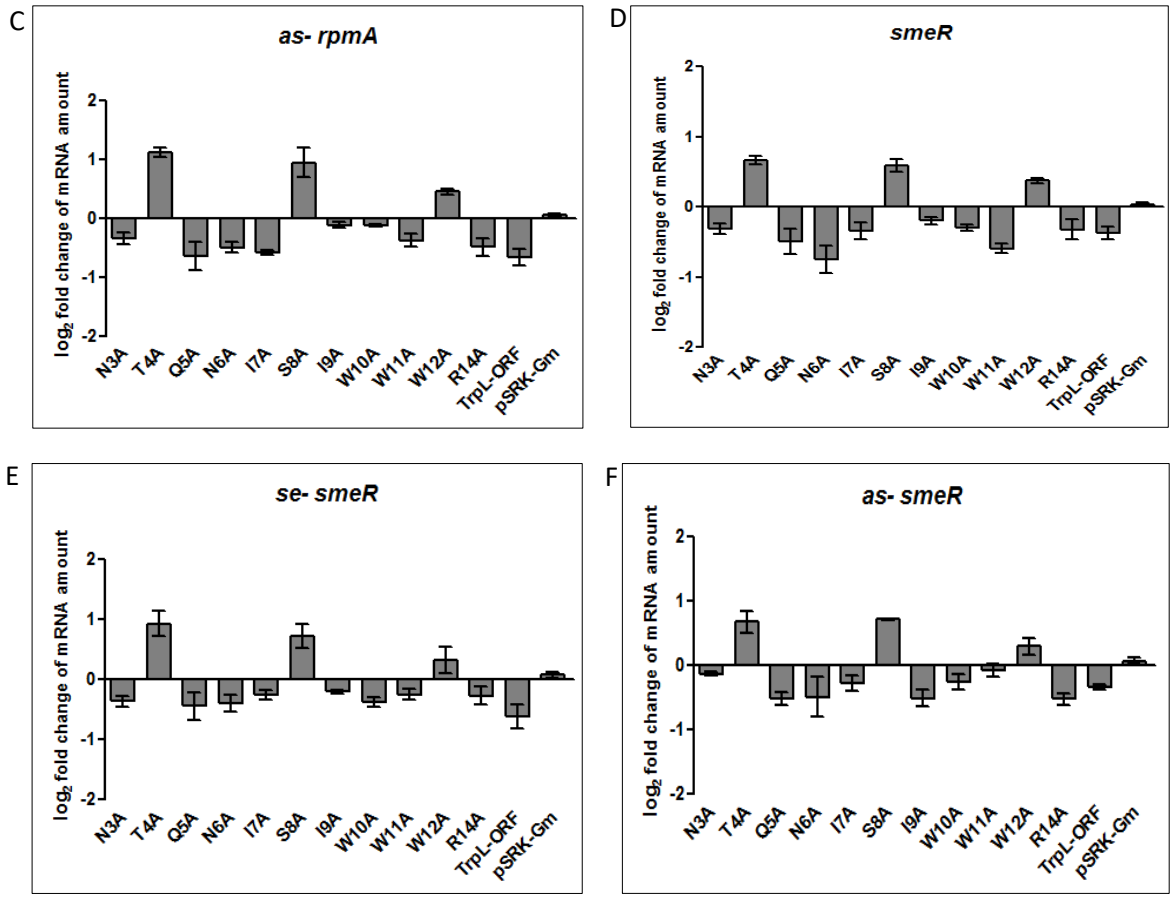

Figure 2.1.8 Alanine Scanning Mutagenesis of Peptide peTrpL. (A and **D).** Changes in the levels of *rpmA* and *smeR* were determined by one-step qRT-PCR 10 min after addition of IPTG to induce the overproduction of peTrpL variants with the indicated aa exchanges in strain 2011. The EVC contained pSRKGm and pRK4352, while the strains overproducing wt peTrpL (TrpL-ORF) or its variants with aa exchanges contained pSRKGm-peTrpL (see Figure 2.1.6A) or its mutated derivatives in addition to pRK4352. pRK4352 was present in all strains to ensure bacterial growth in the presence of Tc, which is needed for the peTrpL function. Thus, all cultures were grown with Gm and Tc. The one-step qRT-PCR analyzes sense and antisense RNAs simultaneously. **(B** and **C)** Changes in the levels of sense and anti-sense *rpmA* RNA were determined by strand specific qRT-PCR. **(E** and **F)** Changes in the levels of sense and anti-sense *smeR* RNA were determined by strand specific qRT-PCR. For these experiments, bacteria were cultured in TY medium. For the qRT-PCR analysis, *rpoB* RNA was used as reference control RNA. Data shown in the graphs were obtained from three independent experiments, each performed in technical duplicates (means and SDs are indicated).

2.1.9 Analysis of The *smeABR* Operon and of Antisense RNAs Related to peTrpL Function

The *smeR* gene is located downstream of *smeAB* (Figure 2.1.9A). To better understand the role of peTrpL in the regulation of *smeAB* and *smeR*, RT-PCR was applied to test tested whether *smeR* is cotranscribed with *smeAB*. The results showed that *smeB* and *smeR* are cotranscribed (Figure 2.1.9B). This implies that upon exposure of S. *meliloti* to Tc, a condition under which *smeAB* upregulation, but *smeR* downregulation would be favorable, the *smeABR* genes are cotranscribed. Thus, the posttranscriptional downregulation of *smeR* by

peTrpL probably serves to achieve differential expression of *smeAB* and *smeR* despite their cotranscription.

Coimmunoprecipitation with FLAG-tagged peTrpL revealed antisense RNAs in complex with the target mRNAs *smeR* and *rplUrpmA* (153). Thus, asRNAs are probably involved in the *smeR* and *rplUrpmA* regulation by peTrpL. To test whether a Tc-inducible and/or peTrpL-inducible antisense promoters P_{as} are present downstream of *smeR* and *rplUrpmA*, plasmids pSUP-PasRegfp and pSUP-PasrpmAegfp harboring transcriptional fusions of *egfp* to the putative P_{as} promoters (Figure 2.1.9C) were used. Each plasmid was integrated into the non-functional *expR* gene in the chromosome.

Firstly, the P_{as} promoter downstream of *smeR* was studied. The fluorescence of the reporter eGFP was analyzed in strain 2011expR:: pSUP-PasRegfp (pSRKGm-peTrpL). The integrated pSUP-PasRegfp harbors a Tc resistance gene. However, it was necessary to test the effect of Tc addition to the cultures. Therefore, cultures were incubated with only Gm overnight, and reinoculated in Gm-containing medium (without Tc) in the morning. The integrated plasmid was not lost during the incubation without Tc, as shown by qPCR using plasmid-specific primers (Figure 2.1.9D). After growth to the exponential phase, Tc, IPTG or both was added. Tc was added to test whether the P_{as} promoter is induced by Tc. IPTG was added to see whether peTrpL is needed for this induction. The results show increase in fluorescence 20 min, 2 h and 15 h after Tc addition. At the time points 20 min and 2h, there was not significant difference if IPTG was applied in addition to Tc, and 15 h after Tc addition a small difference was observed (Figure 2.1.9E).

To detect faster effects caused by transcription initiation at P_{as} downstream of *smeR*, in the next experiments changes in the level of the reporter *egfp* mRNA were analyzed by qRT-PCR 10 min after Tc and/or IPTG addition. The level of the reporter mRNA *egfp* was strongly increased after addition of Tc and Tc with IPTG, with no difference between these treatments (Figure 2.1.9F). Furthermore, other known SmeR-effectors: the plant flavonoid genistein (Gs) and the antibiotics chloramphenicol (Cl), erythromycin (Em) and rifampicin (Rf) induced transcription from the P_{as} promoter (Figure 2.1.9G). In contrast, Kanamycin (Km) and the flavonoid luteolin (Lt), which are not SmeR effectors (127), did not induce transcription from this promoter. Thus, transcription of the as-*smeR* RNA was induced by the same antimicrobial compounds which induce the *smeABR* transcription. This suggests that the as-*smeR* RNA could be involved in downregulation of *smeR* and may even work together with peTrpL.

To find how fast is the induction of transcription from the P_{as} promoter, the level of the reporter mRNA *egfp* was analyzed by qRT-PCR at different time points after antibiotic addition to the cultures. Figure 2.1.9H shows that the *egfp* mRNA level was very high 10 min after Tc addition and then decreased. Analysis of the *egfp* mRNA level after P_{as} induction by the antibiotics Em and Cm suggested an increase from 3 min to 5 min after antibiotic addition, and after 5 min the mRNA level decreased (Figure 2.1.9I). As expected, Km addition did not cause a significant increase. The results suggest that very soon (3 to 5 min) after exposure to SmeR- effectors, transcription from P_{as} is induced (Figure 2.1.9I).

According to Figure 2.1.8C, another antisense-RNA, as-*rplUrpmA*, probably has the similar regulation as *as-smeR* RNA. Figure 2.1.9J shows that the *egfp* mRNA level was very high 10 min after Tc addition to cultures of strain *S. meliloti* 2011 *expR*::pSUP-PasrpmAegfp.

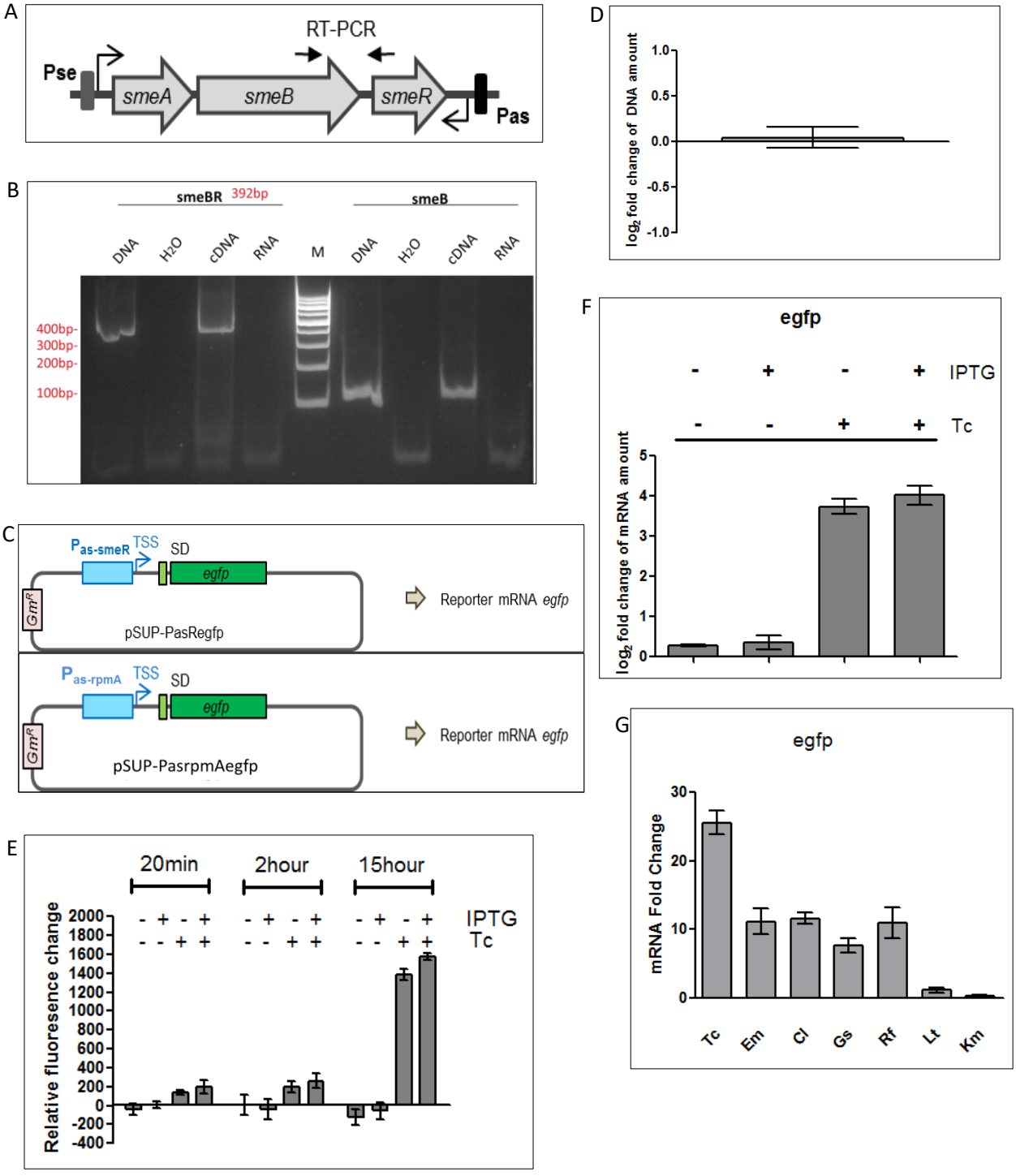

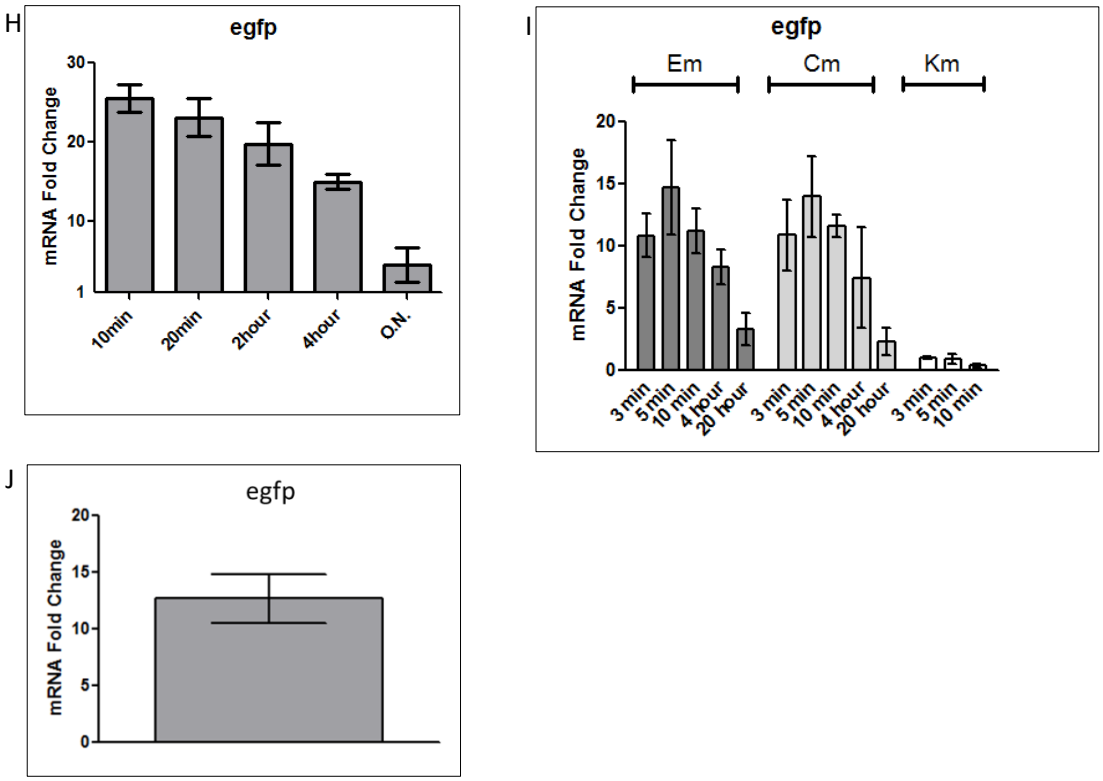

Figure. 2.1.9 Analysis of The *smeABR* Operon and of Antisense RNAs Related to peTrpL Function. (A) Current model of the *smeABR* operon. Exposure to SmeR-effectors relieves the *smeABR* repression by SmeR at the P_{se} promoter and leads to induction of asRNA transcription at the P_{as} promoter. **(B)** Co-transcription of *smeB* and *smeR* revealed by RT-PCR analysis of strain 2011*ΔtrpL*, 10 min after addition of 20 µg/ml Tc. Template input for the PCR reaction is indicated above the panel. **(C)** In pSUP-PasRegfp, the genomic region containing the promoter of the asRNA as-*smeR* and the putative two first nucleotides of the asRNA were fused to a sequence containing a standard Shine-Dalgarno ribosome binding site, followed by the *egfp* gene, P, promoter, SD, Shine-Dalgarno sequence (upper panel). The structure of pSUP-PasrpmAegfp is similar to that of pSUP-PasRegfp, but a putative promoter of as-*rpmA* RNA was used (bottom panel). **(D)** qPCR test with pSUP-specific primers. The level of the plasmid in a culture incubated overnight without Tc was compared to the level of the plasmid in the culture used for inoculation, which was incubated in Tc-containing medium. **(E)** Fluorescencee values of the eGFP reporter protein produced from plasmid pSUP-PasRegfp. The eGFP fluorescence was measured 20 min, 2 hours, and 15 hours after addition of Tc (20 µg/ml) or/and IPTG (1 mM/ml) to cultures of strain *S. meliloti* 2011 expR::pSUP-PasRegfp (pSRKGm-peTrpL). A culture without Tc and IPTG addition was used as negative control. **(F)** qRT-PCR analysis of the reporter *egfp* mRNA, transcribed from plasmid pSUP-PasRegfp in the strain metioned in the previous panel. The *egfp* mRNA level at 10 min after addition of Tc (20 µg/ml) or/and IPTG (1 mM/ml) was compared to the level before addition. A culture without Tc and IPTG addition was used as negative control. **(G)** qRT-PCR analysis of the reporter *egfp* mRNA, transcribed from plasmid pSUP-PasRegfp. The *egfp* mRNA level 10 min after addition of Tc (20 µg/ml) or one of the indicated antimicrobial substances (added at subinhibitory concentrations) was compared to the level before addition. **(H)** qRT-PCR analysis of the reporter *egfp* mRNA, transcribed from plasmid pSUP-PasRegfp. The *egfp* mRNA level at 10 min, 20 min, 2 hours, 4 hours and overnight after addition of Tc (20 µg/ml) was compared to the level before addition. **(I)** qRT-PCR analysis of the reporter *egfp* mRNA, transcribed from plasmid pSUP-PasRegfp. The *egfp* mRNA level at the indicated time points after addition of Em, Cap and Km was compared to the level before addition. Km as negative control was only tested at the time points 3 min, 5 min and 10 min. **(J)** qRT-PCR analysis of the reporter *egfp* mRNA, transcribed from plasmid pSUP-PasrpmAegfp in strain *S. meliloti* 2011. The *egfp* mRNA level at 10 min after addition of Tc (20 µg/ml) was compared to the level befor Tc addition. In these experiments, bacteria were cultured in TY medium. For qRT-PCR analysis, *rpoB* RNA was used as reference control RNA. All subinhibitory antibiotic concentrations corresponded to the 90% MIC (127). Data shown in

the graphs were obtained from three independent experiments, each performed in technical duplicates (means and SDs are indicated).

2.1.10 Construction of *smeR* Gene Deletion Mutants

For further understanding the interaction relationship between peptide peTrpL and sense and antisense-*smeR* mRNA, it was necessary to introduce a *ΔsmeR* mutation in *S. meliloti* 2011 and 2011 *ΔtrpL* genetic backgrounds. Figure 2.1.10A shows the results of colony PCR confirming the deletion mutation in strains 2011 *ΔsmeR* and 2011 *ΔtrpLΔsmeR*. Since *smeR* is the repressor of the major multidrug efflux pump genes *smeAB*, it is expected that the efflux genes are derepressed in the *ΔsmeR* mutants. A comparison of the growth of strains 2011 *ΔsmeR* and 2011 in microtiter plates, in media with increasing Tc concentrations, revealed that the strain 2011 *ΔsmeR* grew under 2 µg/ml Tc concentration condition, but the strain 2011 only tolerated 0.5 µg/ml Tc concentration under these conditions (Figure 2.1.10B).

Furthermore, the *smeB* mRNA levels were compared between the strains 2011 *ΔsmeR* and 2011 under short term Tc exposure. Figure 2.1.10C suggests that the level of *smeB* mRNA in the strain 2011 *ΔsmeR* was about 4 fold higher than that in the strain 2011. These results are in line with ther repressor function of SmeR. In future, among others, the *ΔsmeR* mutants can be used to test whether the P_{as} promoter of the antisense RNA is repressed by SmeR.

A

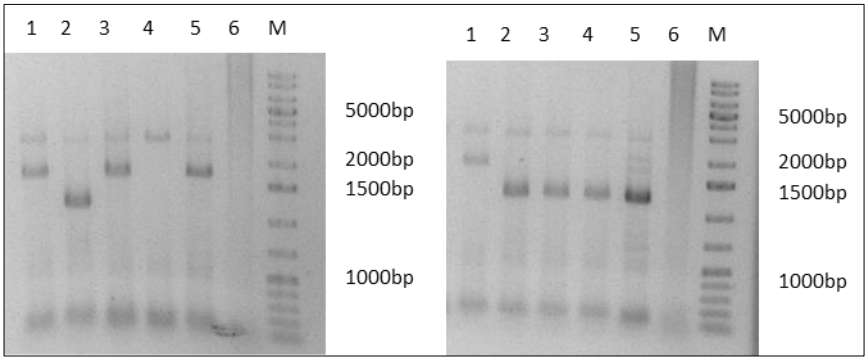

B

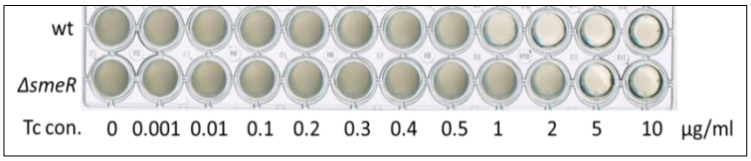

C

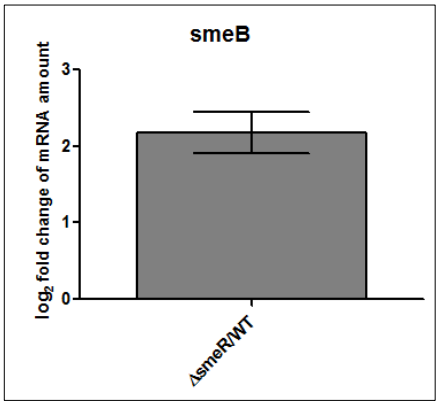

Figure 2.1.10 Construction of *smeR* Gene Deletion Mutants. (**A**) Results of colony PCR validating the deletion mutation *ΔsmeR* in wildtype (**left**) and *ΔtrpL* (**right**). M was 1KB Plus marker. Left gel for validation of 2011 *ΔsmeR:* Lane 1 was *S. meliloti* 2011, lane 2 was *S. meliloti* 2011 *ΔsmeR*, lanes 3 and 5 corespond to wild type clones after double cross-over, lane 4 did not provide expected signal, lane 6 was a negative control - DNA free water was used instead of cell suspension. Right gel for validation of 2011 *ΔtrpLΔsmeR:* Lane 1 was *S.meliloti* 2011, lanes 2-5 were *S.meliloti* 2011*ΔtrpLΔsmeR*, lane 6 was a negative control. (**B**) Deletion mutant 2011 *ΔsmeR* grows at higher Tc concentration than the strain 2011 in TY medium. Strains and Tc concentrations are indicated. (**C**) qRT-PCR analysis of the *smeB* mRNA level difference between deletion mutant 2011 *ΔsmeR* and strain 2011. In this experiment, bacteria were cultured in TY medium. For qRT-PCR analysis, *rpoB* RNA was used as reference control RNA. Data shown in the graph were obtained from three independent experiments, each performed in technical duplicates (means and SDs are indicated)**.**

2.1.11 Role of RNases in Regulation by the sRNA rnTrpL

Another very important aspect in regulation of mRNA levels by an sRNA is the involvement of RNases. To learn which RNase participates in regulation by the sRNA rnTrpL and/or peptide peTrpL, available RNase mutant strains were used to compare targets mRNA levels before and after induction of the sRNA rnTrpL. Figure 2.1.11A shows that induced overproduction of rnTrpL in RNase E and RNase III mutant strains leads to increase of the levels of *rpmA* and *trpC* mRNAs instead of decrease as in the parental strain 2011. However, only in the RNase E strain *smeR* and *sinI* mRNAs levels were increased instead to be decreased upon rnTrpL induction, while the lack of RNase III had no such influence on these mRNAs. Furthermore, presence of YbeY was found to be crucial for the regulation of *smeR* and *sinI* by peTrpL and rnTrpL, respectively .

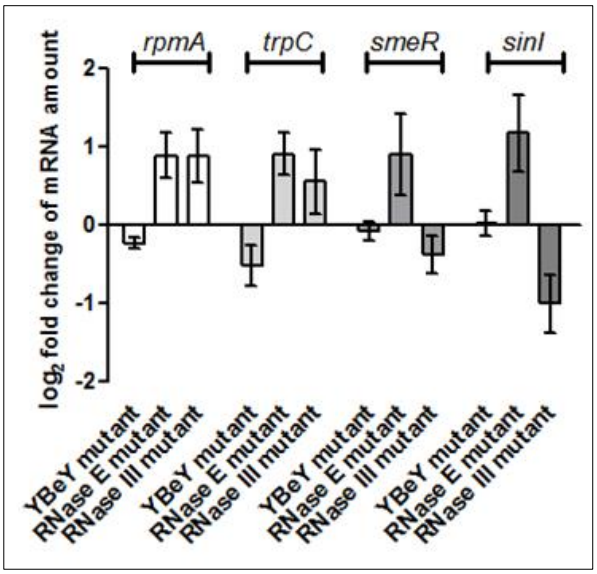

Figrue 2.1.11 Role of RNases in Regulation by the sRNA rnTrpL. qRT-PCR analysis of the mRNAs *rpmA*, *trpC*, *smeR* and *sinI* in the indicated RNase mutants (*YBeY*, *RNase E*, and *RNase III* mutants). Each mutant contained pSRKTc-rnTrpL. The mRNA levels 10 min after addition of 1mM IPTG were compared to the levels before IPTG addition. In this experiment, bacteria were cultured in TY medium. For qRT-PCR analysis, *rpoB* RNA was used as reference control RNA. Data shown in the graph were obtained from three independent experiments, each performed in technical duplicates (means and SDs are indicated).

2.1.12 Analysis of the Predicted *rpoE1* mRNA Target of rnTrpL

Since the sRNA rnTrpL is derived from the transcription attenuator of the *trpE(G)* operon (Figure 2.1.1A), it probably regulates its targets in response to Trp availability. To address posttranscriptonal regulation in *trans* by rnTrpL at different concentrations of Trp in *S. meliloti* cells, it was necessary to construct a Trp auxotrophic mutant. For this, deletion in the *trpC* gene in the chromosomes of strains 2011 and 2011 *ΔtrpL* was performed, so that the cells can not product Trp by themselves and rely only on the Trp added to the minimal growth medium. Figure 2.1.12A shows the results of colony PCR that validated the two mutant strains 2011 *ΔtrpC* and 2011 *ΔtrpLΔtrpC*. These mutants were useful for showing that rnTrpL regulates the *trpDC* operon in *trans* according to the Trp concentration (156).

Here, the mRNA of the sigma factor gene *rpoE1* was analyzed, which was predicted to base-pair with rnTrpL (Figure 2.1.12B). This gene is co-transcribed with the gene of the anti-sigma factor anti-RpoE1. Figure 2.1.12C shows the Northern Blot results of strain 2011 *ΔtrpLΔtrpC* (pSRKGm-rnTrpL) at low and high Trp concentrations, before and after induction of the sRNA lacZ′-rnTrpL. Before induction, the sRNA was not detectable. The lacZ′-rnTrpL amount which accumulated 10 min and 20 min after IPTG addition at low (2 µg/ml) Trp concentration (Low Trp) was much less than that at high (20 µg/ml) Trp concentration (High Trp). This is in agreement with less termination of the sRNA transcription under conditions of Trp insufficiency.

Next, changes in the levels of *rpoE1* and *anti-σE1* mRNAs were determined 10 min after IPTG addition to cultures grown under Low and High Trp conditions (Figure 2.1.12D). When the sRNA was induced in the Low Trp cultures of strain 2011 *ΔtrpLΔtrpC* (pSRKGm-rnTrpL), the levels of the *rpoE1* and *anti-σE1* mRNAs were decreased. The level of the control mRNA *rpmA* was also slightly decreased, although this was not expected, since Tc was not added to the culture. Furthermore, the level of the control mRNA *trpD* was not decreased, probably because of the lacking *trpC* part in the corresponding polycistronuc transcript. However, when the sRNA was induced in the High Trp cultures, the levels of the the *rpoE1* and *anti-σE1* mRNAs were not changed. The *rpmA* level was also not changed, and unexpectedly, the *trpD* level was increased. These results suggest that Trp may influence gene expression by mechanisms including changes in the target prioritization of rnTrpL under different conditions and/or mechanisms beyond the regulation by rnTrpL. These questions can be addressed in future.

Another experiment was conducted for analysis of the native rnTrpL, which was transcribed from chromosome in strain 2011*ΔtrpC*, and of *rpoE1* and *anti-σE1* mRNAs levels under different Trp conditions (Figure 2.1.12E and Figure 2.1.12F). Cells grown in minimal medium with 20 µg/ml Trp (High Trp) from OD_{600} 0.2 to OD_{600} 0.4, and then they were washed in medium without Trp and incubated in medium with 2 µg/ml Trp (Low Trp) for 4 h. Samples for RNA isolation were withdrawn under both conditions. Then Trp was added again to a final concentration of 20 µg/ml, and 10 min later, RNA was isolated. Changes in the levels of the mRNAs *rpoE1* and *anti-σE1*, and of the control mRNA *trpD*, after changing the Trp conditions, were analyzed by qRT-PCR.

As expected, when the Trp concentration was decreased, the level of the native sRNA rnTrpL was also decreased (due to less transcription termination; Figure 2.1.12E), and the level of *trpD* mRNA was increased (Figure 2.1.12F). The levels of *rpoE1* and *anti-σE1* were also increased, in line with the proposed regulation by rnTrpL. Furthermore, when Trp was added to the Low Trp cultures, as expected, the level of the native sRNA rnTrpL was increased (Figure 2.1.12E) and the level of *trpD* mRNA was decreased (Figure 2.1.12F). Similar decrease was observed for the levels of *rpoE1* and *anti-σE1* mRNAs, suggesting that they are also regulated by rnTrpL in response to Trp availability.

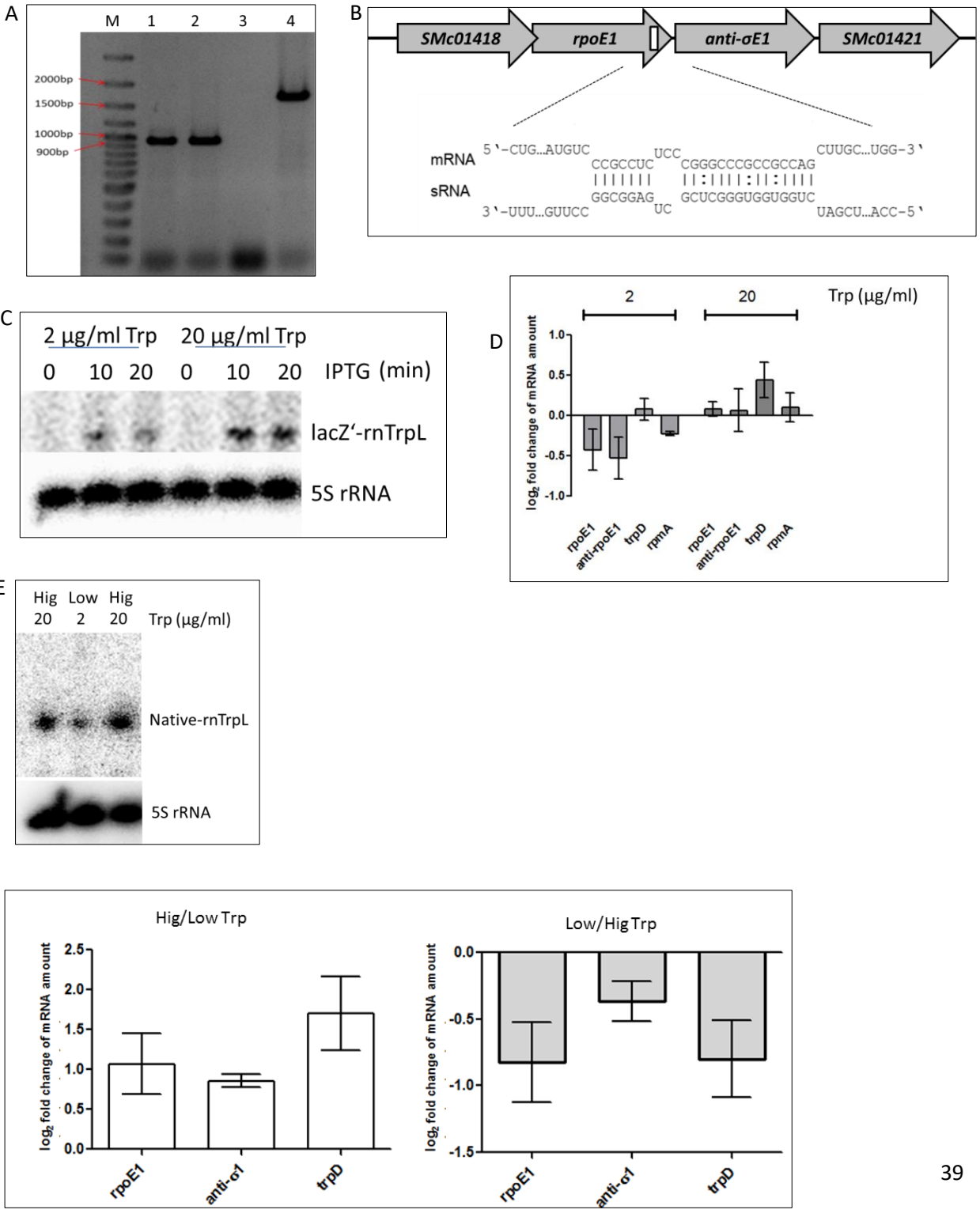

Figure. 2.1.12 Analysis of the Predicted *rpoE1* mRNA Target of rnTrpL. (A) Colony PCR validating the deletion mutation *ΔtrpC* in two genetic backgrounds. M is 100 bp plus marker; Line 1 was *S.meliloti* 2011-*ΔtrpC*; Line 2 was *S.meliloti* 2011-*ΔtrpLΔtrpC*; Line 3 was DNA free water as negative control; Line 4 was *S.meliloti* 2011 as negative control. **(B)** Scheme of the duplex structure predicted to be formed between *rpoE1* (mRNA) and rnTrpL (sRNA). **(C)** Northern blot analysis of the level of sRNA lacZ′-rnTrpL in *S. meliloti* 2011*ΔtrpL ΔtrpC* (pSRKGm-rnTrpL) cultures grown in minimal medium with 2 µg/ml and 20 µg/ml Trp. Samples were collected 0 min, 10 min and 20 min after addition of IPTG to induce the lacZ′-rnTrpL sRNA transcription. **(D)** qRT-PCR analysis of the mRNA level of *rpoE1, anti-rpoE1, trpD* and *rpmA* in the RNA samples described in panel C). **(E)** Northern blot analysis of the level of sRNA rnTrpL under different Trp conditions in the *S. meliloti* 2011 *ΔtrpC* strain. Changes in the level of rnTrpL were detected when the cells were transferred from High Trp (20 µg/ml Trp) to Low Trp (2 µg/ml) condtions, and after restoring High Trp conditions. Trp concentration (in µg/ml) is indicated. **(F** left panel**)** qRT-PCR analysis of changes in the mRNA levels of *rpoE1, anti-rpoE, trpD* and *rpmA* in response to Trp availablity. The initial High Trp RNA samples were compared to the corresponding Low Trp RNA samples descibed in panel E. **(F** right panel**)** qRT-PCR analysis of changes in the mRNA levels of *rpoE1, anti-rpoE1, trpD* and *rpmA* in response to Trp availablity. The Low Trp RNA samples were compared to the High Trp RNA samples obtained after adding Trp to the Low Trp cultures as descibed in panel E. In these experiments, bacteria were cultured in GMX minimal medium. For Northern blot analysis, 5S rRNA was used as a loading control RNA. For qRT-PCR analysis, *rpoB* RNA was used as reference control RNA. Data shown in the graphs were obtained from three independent experiments, each performed in technical duplicates (means and SDs are indicated).

2.2 Attenuator sRNA rnTrpL Regulation in *E. coli*

2.2.1 Construction of Pulse-Overexpression System for Ec-rnTrpL and Analysis of Putative Target mRNAs

The best understood model of ribosome-dependent transcription attenuation is that of the Trp biosynthesis genes *trpEDCBA* which are co-transcribed in *E. coli* (132). The 5′ mRNA leader harbors the uORF *trpL*, which contains two consecutive Trp codons (the 10. and 11. codon of the 14 aa leader peptide) (Figure 2.2.1A). Upon transcription attenuation, a sRNA is released, which was named Ec-rnTrpL to distinguish it from rnTrpL in *S. meliloti*. To address the question whether Ec-rnTrpL plays a role in *trans*, plasmids pSRKTc(Gm)-Ec-rnTrpL for induced transcription of the sRNA were constructed (Figure 2.2.1B). As described above for *S. meliloti*, here a sRNA lacZ′-Ec-rnTrpL and peptide Ec-peTrpL are produced after induction with IPTG. In this case, the native 5′-region of Ec-rnTrpL was replaced by the 5′-UTR of *lacZ*.

Figure 2.2.1C presents Northern Blot results of the sRNA lacZ′-Ec-rnTrpL level after addition of 0.3 mM, 0.5 mM and 1mM IPTG for 0, 3, 5 and 10 min to cultures of strain *E. coli* MG1655 (pSRKTc-Ec-rnTrpL) grown in LB medium. It was clearly seen that the sRNA lacZ′-rnTrpL amount was increased with the induction time. Also, increasing concentration of IPTG caused increased accumulation of lacZ′-Ec-rnTrpL. However, there was no native-Ec-rnTrpL signal in the *E. coli* EVC and in the sample of the overexpressing (OE) strain before IPTG addition (0 min). This could be explained by repressed transcription of *trpL* and the *trp* operon in *E. coli* in LB medium, which is a rich Trp source.

A fast and effective way to identify candicate target mRNAs of base-pairing sRNAs is prediction by computer science. The prediction of Ec-rnTrpL candidates was performed by Dr. Jens Georg (University of Freiburg). The top ten predicted tagets are shown in Table 2.2.1.

Here, five of the top 10 mRNAs, which were predicted to interact with the sRNA Ec-rnTrpL (Table 2.2.1), were analyzed. The levels of *rsuA*, *dnaA* and *sanA* mRNAs were decreased when Ec-rnTrpL was induced by IPTG for 5 min, while *trpE* as a negative control was not downregulated (Figure 2.2.1D). Furthermore, the level of *ycaO* mRNA was not changed, suggesting that this gene is not regulated by the sRNA. Finally, the level of *mhpC* mRNA was increased, indicating that this gene could be positively regulated by Ec-rnTrpL.

A

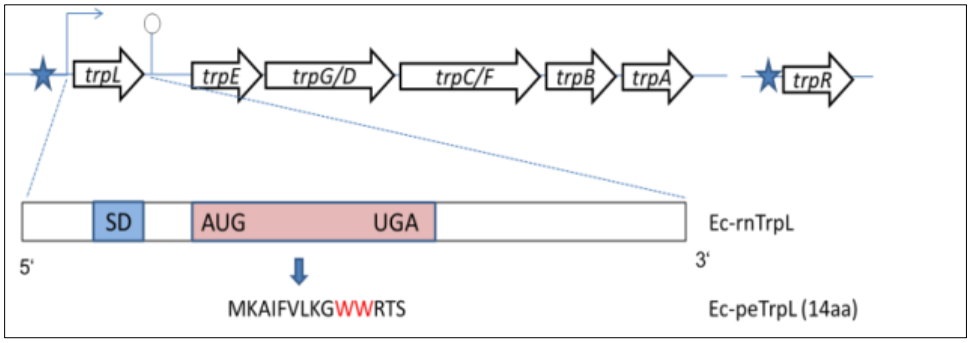

B

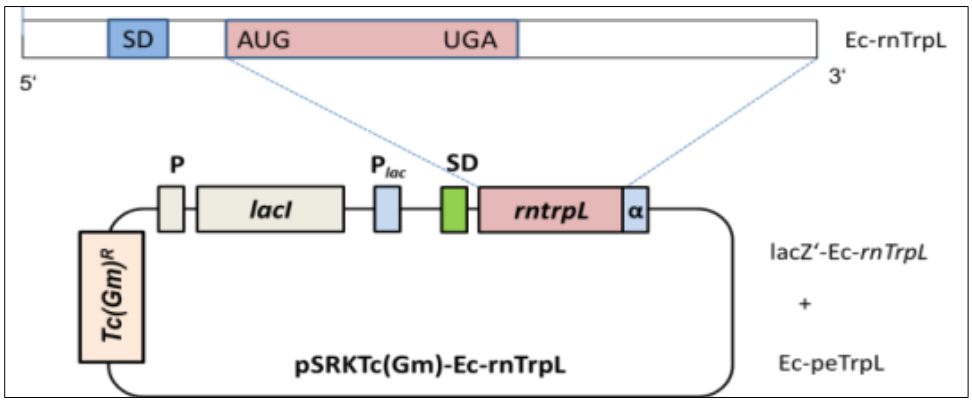

C

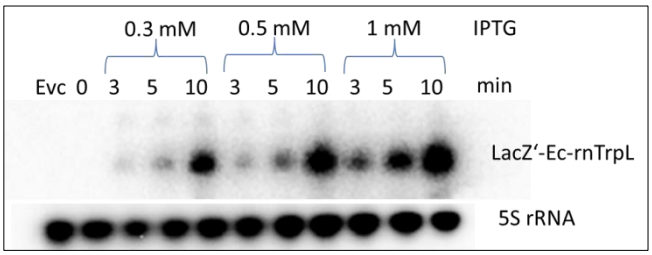

D

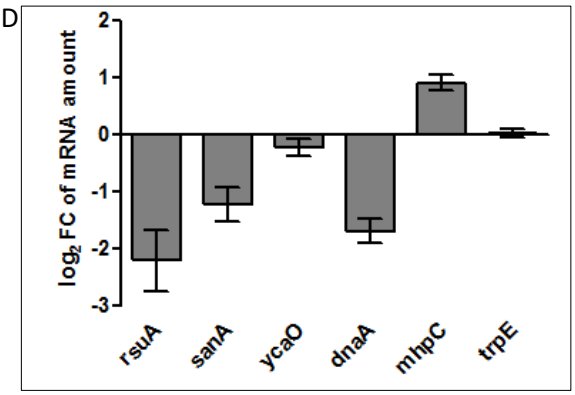

Figure. 2.2.1 Construction of Pulse-Overexpression System for Ec-rnTrpL and Analysis of Putative Target mRNAs. (A) Scheme of the *trp* operon, transcription repressor (blue asterisk) and the attenuator RNA Ec-rnTrpL of *E. coli*. ORFs are depicted by white arrows, the transcription start site by a flexed arrow and the transcription terminator by a hairpin. The terminated attenuator sRNA Ec-rnTrpL (141 nt) is shown as a white box with a Shine-Dalgarno sequence (SD), and start and stop codons of the *trpL* ORF indicated. Below this box, the amino acid sequence of the leader peptide Ec-peTrpL (14 aa) is shown. **(B)** Scheme of pSRKTc-rnTrpL. The pSRK-based plasmids harbor the *lac* repressor gene *lacI* with its own promoter, the *lacI-lacZ* intergenic region, the *lac*-promoter P_{lac} and the 38 nt *lacZ* leader containing the Shine-Dalgarno sequence (SD), followed by ATG. In pSRKTc-rnTrpL plasmid, the ATG is the start codon for translation of the Ec-*trpL* ORF, which is followed by the 3′-UTR including the transcription terminator. The resulting sRNA lac*Z*′-Ec-rnTrpL contains the 38 nt l*acZ*-leader instead of its native 5′-UTR. The scheme shows the plasmid conferring resistance to tetracycline (Tc) (pSRKTc-rnTrpL). A similar plasmid conferring resistance to gentamycin (Gm) was also constructed. **(C)** Northern blot hybridization showing Ec-rnTrpL in strain *E. coli* MG1655 (pSRKTc-rnTrpL) after addition of IPTG. Used IPTG concentrations and induction times are indicated. EVC was used as a negative control. **(D)** qRT-PCR analysis of the indicated mRNAs in strain *E.coli* MG1655 (pSRKTc-Ec-rnTrpL). The level of mRNAs 5 min after 1mM IPTG addition was compared to the level before IPTG addition. In this experiment, bacteria were cultured in LB medium. For Northern blot analysis, 5S rRNA was used as a loading control RNA. For qRT-PCR analysis, *rpoB* RNA was as reference control RNA. Data shown in the graph were obtained from three independent experiments, each performed in technical duplicates (means and SDs are indicated).

Table 2.2.1: Top 10 predicted targets of Ec-rnTrpL, based on the CopraRNA p-value.

p-value	Locustag	Gene	Interaction site coordinates	Experimentally tested	Regulation	Annotation
6,55E-09	b3702	*dnaA*	+12 to + 87	yes	negative	chromosomal replication initiator protein DnaA
2,58E-05	b0905	*ycaO*	+70 to +89	yes	no effect	ribosomal protein S12 methylthiotransferase accessory factor YcaO
5,32E-05	b2145	*yeiS*	-180 to -142	yes	negative	DUF2542 domain-containing protein YeiS
7,95E-05	b0349	*mhpC*	-200 to -177	yes	positive	2-hydroxy-6-ketonona-2 4-dienedioate hydrolase
0,000186	b2182	*bcr*	-74 to -20	no	negative	multidrug efflux pump Bcr
0,000189	b0661	*miaB*	-200 to -185	no	NA	isopentenyl-adenosine A37 tRNA methylthiolase
0,000368	b3052	*rfaE*	-95 to -87	no	NA	fused heptose 7-phosphate kinase/heptose 1-phosphate adenyltransferase
0,000433	b2465	*tktB*	-178 to -169	no	NA	transketolase 2
0,000488	b1888	*cheA*	-1 to +6	no	NA	chemotaxis protein CheA
0,000766	b2808	*gcvA*	-142 to -118	no	NA	DNA-binding transcriptional dual regulator GcvA

2.2.2 Analysis of the Half-Life of the Native Ec-rnTrpL with and without Tc Exposure

According to the well known model for regulation of the Trp biosynthesis operon *trpEDCBA* in *E. coli*, if enough Trp is present in the cell (for example during growth in LB medium), operon transcription is repressed. In line with this, native Ec-rnTrpL was not detected by Northern blot hybridization of RNA from cultures grown in LB (see Figure 2.2.2.A, left panel). In minimal medium, however, Trp must be synthesized by the cells and transcription of the *trp* operon takes place. Under these conditions, transcription attenuation ensures fine tuning of the *trp* genes expression: when enough Trp is produced, transcription is terminated between *trpL* and the structural genes, and the sRNA Ec-rnTrpL is released. Indeed, Ec-rnTrpL was detected by Northern blot hybridization of RNA from cultures grown in M9 medium (see the first lane in Figure 2.2.2.A, right panel). Furthermore, since abolished *trpL* translation leads to hyperattenuation (157), it could be expected that during growth in M9 medium, upon exposure to translation inhibiting antibiotics such as Tc, the level of Ec-

rnTrpL will increase. However, Figure 2.2.2.A (right panel) shows that native sRNA Ec-rnTrpL was only detected without Tc exposure condition. In contrast, signal corresponding to the native sRNA Ec-rnTrpL was missing after 3 min and 5 min Tc exposure (1 µg/ml Tc). This could be explained by strong Ec-rnTrpL destabilization under Tc stress, for example if Ec-rnTrpL has Tc-dependent target(s) and is codegraded with those traget(s) upon Tc exposure.

To test this, the half-life of Ec-rnTrpL was determined in exponentially growing M9 cultures with and without Tc exposure. Very short (40 s) after addition of 10 µl Tc to achieve a final concentration of 1 µg/ml, rifampicin (Rif) was added to stop cellular transcription and decay of Ec-rnTrpL in time was determined by Northern blot hybridization (Figure 2.2.2B). To negative control cultures, 10 µl of the solvent was added (70 % ethanol; 2.2.2C). Excitingly, the amount of native sRNA Ec-rnTrpL under the 1 µg/ml Tc exposure treatment was obviously lost each minute since Rif addition (Figure 2.2.2B), while sRNA was much more stable in the control cultures (Figure 2.2.2C). The half –life of native sRNA Ec-rnTrpL under Tc exposure was 2 min 20 s ± 20 s, and that without Tc exposure was 6 min 40 s ± 20 s (Figure 2.2.2D). So the conclusion is that native sRNA Ec-rnTrpL under Tc stress was much more qucikly degraded.

A

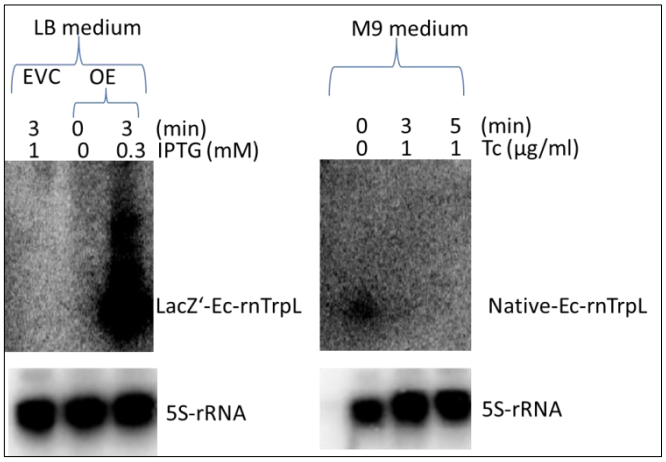

B

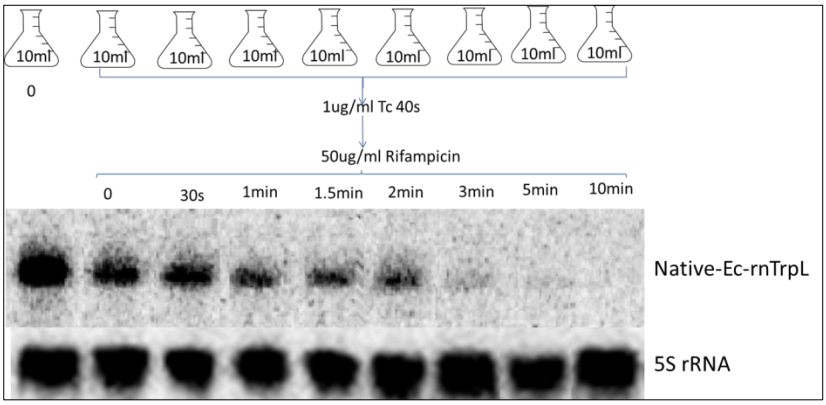

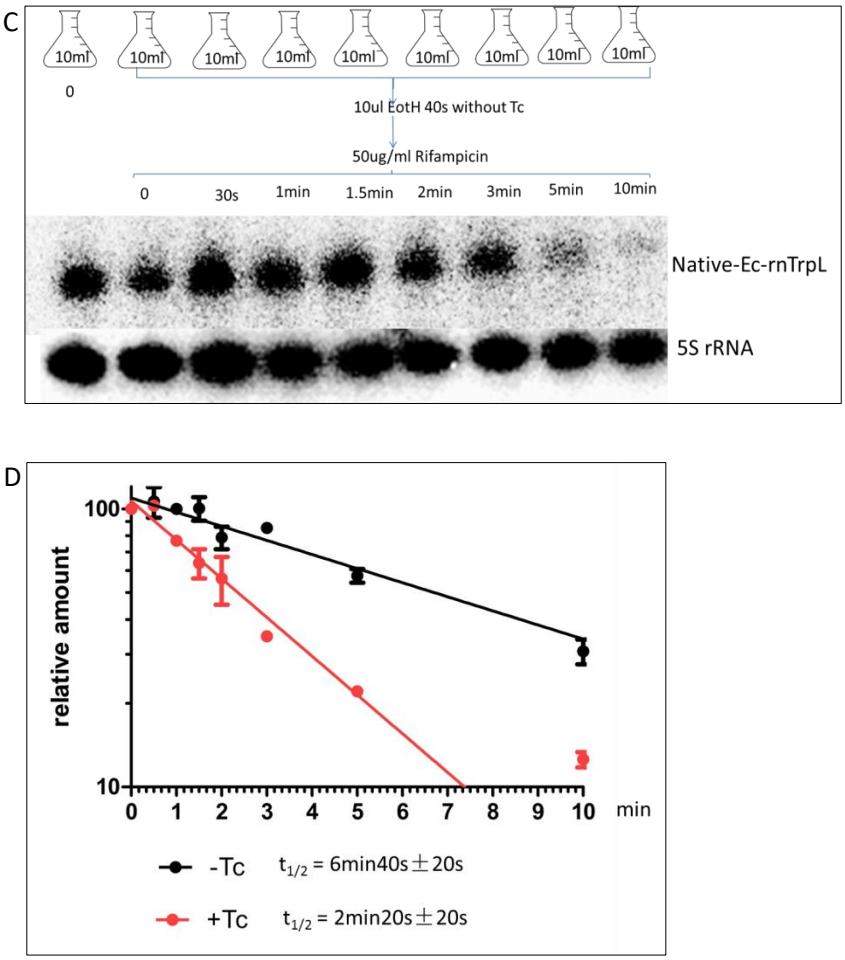

Figure 2.2.2 Analysis of the Half-Life of the Native Ec-rnTrpL with and without Tc Exposure. (A) Northern blot hybridization showing lacZ′-Ec-rnTrpL accumulation after IPTG addition to LB cultures (left) and native rnTrpL in M9 cultures with and without Tc addition (right). Used strains, concentrations and induction/exposure times are indicated. **(B)** Northern blot hybridization analysis of the half-life of the native-Ec-rnTrpL sRNA in *E. coli* MG1655 after 40s exposure to Tc. 50 µg/ml rifampcin was used for inhibition of RNA synthesis. The time points after rifampicin addition are indicated. In the first lane, sample before Tc addition was used as postive control for the whole experiment. 5S rRNA was used as reference control RNA. The bacteria were cultured in M9 minimal medium. **(C)** Northern blot hybridization analysis of the half-life of the native-Ec-rnTrpL in cultures, to which 10 µl 70% EtOH was added instead of 10 µl Tc solution. For other descriptions, see panel (B). **(D)** Linear-log graphs were used for half-life calculation. The relative Ec-rnTrpL amount was plotted against the time after rifampicin addition. Shown are data from two independent experiments. The results were very similar, and therefore the standard deviations for some of the time points are smaller than the graph symbols.

2.2.3 Activity of P_{trp} at Diferent Trp or Tc Exposure Conditions

Based on the Figure 2.2.2 results, there will be three available explanations why native sRNA Ec-rnTrpL was disappeared 3 min after Tc addition. The first one was already mentioned in Figure 2.2.2B and C, Tc could accelerate Ec-rnTrpL degradation. The second

one is that Tc as inhibitor could stop/decrease the *trp* promoter (P_{trp}) activity. The third one is that the promoter is inhibited and the sRNA is destabilized at the same time. So it is very important to use transcription fusion reporter to analyze P_{trp} activity in the presence and absence of Tc. Furthermore, it is important to test the influence of Tc on transcription attenuation. Therefore, it was necessary to construct and use reporter fusion plasmids containing the *trp* promoter and the promoter and attenuator, respectively.

To this end, three *egfp*-containing plasmids were constructed: the promoterless pRS1-sSD-egfp (EVC), pRS1- P_{trp}sSD-egfp (for analysis of the P_{trp} activity), and pRS1-P_{trp}rnTpL-sSD-egfp (for analysis of the readthrough, which reflects transcription attenuation and its relieve) (Figure 2.2.3A). To detect promoter activity and readthrough, eGFP fluorescence was measured. Firstly, fluorescence of overnight cultures grown in minmal medium was measured. Fluorescence value of strain *E. coli* MG1655 (pRS1- P_{trp} sSD-egfp) was measured above 10 000, while fluorescence value of strain *E. coli* MG1655 (pRS1- P_{trp}rnTrpLsSD-egfp) was measured somewhat lower than 4 000, but it was still higher than the fluorescence of the EVC (Figure 2.2.3B). Thus, as expected, transcription from the *trp* promoter is derepressed in minimal medium, when the cells should synthsize Trp. Additionally, as expected, in order to save energy, the transcription attenuator decreases the expression of downstream genes whenever the cells produced enough Trp.

Next, the promoter and attenuator activities were analyzed at different Trp concentrations. Fluorescence of overnight cultures was measured. In line with the above results, in minimal medium without Trp, the fluorescence value of strain *E. coli* MG1655 (pRS1- P_{trp}sSD-egfp) was measured above 8 000, and fluorescence value of strain *E. coli* MG1655 (pRS1- P_{trp} rnTrpLsSD-egfp) was measured around 4 000. Furthermore, when tryptophan was added to the medium, the fluorescence value of strain *E.coli* MG1655 (pRS1- P_{trp}sSD-egfp) was measured around 1 000, and fluorescence value in strain *E. coli* (MG1655 pRS1-P_{trp}rnTrpLsSD-egfp) was measured around 200. Thus, fluorescence was decreased when tryptophan was present in the medium, for both constructs. But *E.coli* MG1655 (pRS1-P_{trp}sSD-egfp) present stronger effect than the effect of *E. coli* MG1655 (pRS1- P_{trp} rnTrpLsSD-egfp), because of the role of the attenuator. In addition, fluorescence value in both strains was gradually decreased when tryptophan concentration was gradually increased (Figure 2.2.3C). These results are in line with transcription repression and transcription attenuation in the presence of Trp.

Finally, Tc as potential effector was tested by a short term treatment. Fluorescence was measured at 3 time points, including -30 min, 0 min (time point of addition of Tc to a final concentration of 1 μg/ml), and +30 min. The fluorescence continuously increased in time in cultures of strain *E. coli* MG1655 (pRS1- P_{trp}sSD-egfp), in line with a continuous eGFP production during growth. However, in strain *E. coli* MG1655 (pRS1- P_{trp}rnTrpLsSD-egfp) cultures, increase of fluorescence was slowed after Tc addition (Figure 2.2.3D). These results suggest that Tc does not negatively affect the P_{trp} activity, but modulated the readthrough. Thus, transcription attenuation seems to be increased in the presence of Tc.

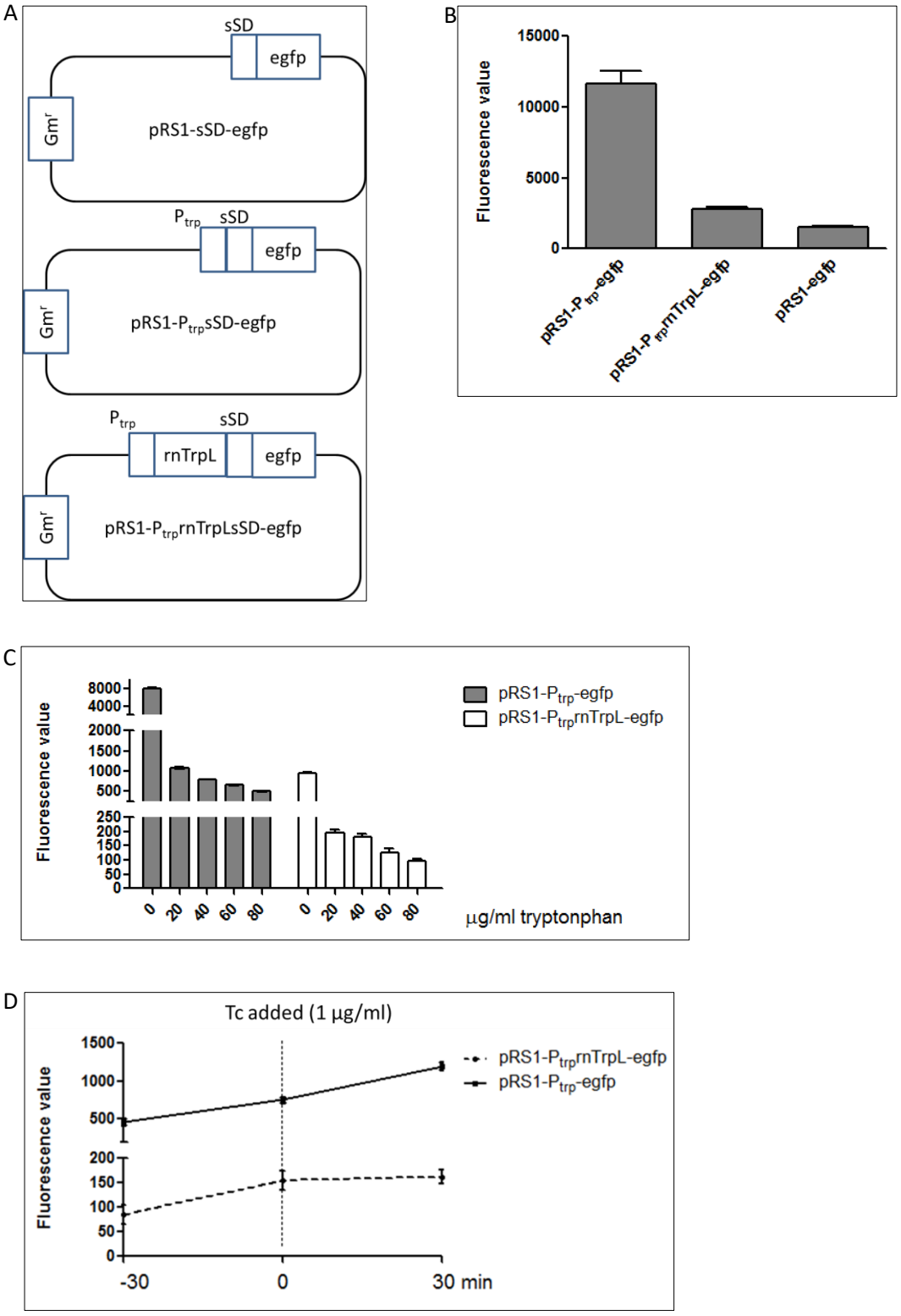

Figure 2.2.3 Activity of Ptrp at Diferent Trp or Tc Exposure Conditions. (A) Scheme of pRS1-egfp, pRS1-P_{trp}-egfp and pRS1-P_{trp}rnTrpL-egfp. P_{trp}, genomic region containing the promoter of the *trp* operon. rnTrpL, the *trp* attenuator sequence corresponding to rnTrpL. sSD, standard Shine-Dalgarno sequence, Shine-Dalgarno sequence from plasmid pQE30 (Qiagen). egfp, *egfp* gene. **(B)** Analysis of promoter activity and transcription

attenuation in M9 minimal medium without tryptophan. Fluorescence was measured after cells were cultured overnight. **(C)** Analysis of promoter activity and transcription attenuation in M9 minimal medium containing the indicated tryptophan concentrations. Fluorescence was measured after cells were cultured overnight and values were normalized to the EVC containing pRS1-sSD-egfp. **(D)** Analysis of promoter and attenuator activity in M9 minimal medium . At the time point – 30 min, the cultures had an OD_{600} of 0.5. At the time point 0 min, Tc was added. The values were normalized to the EVC containing pRS1-sSD-egfp. All graphs shown results from three independent experiments, each performed in duplicates (means and standard deviations are indicated).

2.2.4 The sRNA Ec-rnTrpL Base-Pairs with *dnaA* mRNA to Decrease Its Level in a Tc-Independent Manner

As a target of Ec-rnTrpL showing top p-value for base-pairing possibility, *dnaA* was predicted, which encodes the regulator of induction of chromosome replication. Figure 2.2.4A shows the predicted base-pairing of the sRNA Ec-rnTrpL with *dnaA* mRNA. As recently shown in our laboratory for the sRNA rnTrpL in *S. meliloti*, rnTrpL can have Tc-dependent and Tc-independent targets. Therefore, for understanding the mode of action of the sRNA Ec-rnTrpL in *E. coli*, changes in the level of the target mRNA *dnaA* were examined upon induced Ec-rnTrpL overproduction in the presence or absence of Tc. For this, plasmids based on pSRKTc and pSRKGm were used. As Figure 2.2.4B shows, the *dnaA* mRNA level was decreased about 2 fold when the sRNA Ec-rnTrpL transcription was induced by addition of 1 mM IPTG for 5 min. However, this decrease was independent of and was not influenced by Tc. And as negative control, there was almost no change of *dnaA* mRNA level in EVC strains. In addtion, *trpE* mRNA used as negative control, which should be not affected by ectopic induction of Ec-rnTrpL, showed no changes (Figure 2.2.4C). This suggests that the sRNA Ec-rnTrpL may specifically regulate *dnaA*.

Next, it was necessary to provide evidence for direct interaction (base-pairing) between Ec-rnTrpL and *dnaA* mRNA. Thus, plasmids were constructed for induced production of mutated lacZ′-Ec-rnTrpL sRNA versions. Two sRNA mutations were introduced: mutation-1 (UGG/ACC) and mutation-2 (GGA/CUU) (Figure 2.2.4A). Then the effect on the *dnaA* mRNA level of sRNA lacZ′-Ec-rnTrpL and the two mutated sRNAs after induction with IPTG were compared. Interestingly, the result for the sRNA with mutation-1 result was like the EVC result, showing that mutation-1 abolished the effect of the sRNA on *dnaA* mRNA. In contrast, the result for the sRNA with mutation-2 result was like that for the wildtype sRNA, showing that this mutated sRNA can still downregulate *dnaA* (Figure 2.2.4D).

To finally validate the base-pairing between *dnaA* mRNA and Ec-rnTrpL, *in vivo* assays were performed in strain *E. coli* MG1655 using *dnaA′::egfp* reporter constructs and lacZ′-Ec-rnTrpL derivatives. The *dnaA′::egfp* fusions (Figure 2.2.4E) were expressed from pSRKGm (conferring Gm^r) and challenged with wt or mutated lacZ′-rnTrpL transcribed from pSRKTc (conferring Tc^r) (Figure 2.2.1B). Although this strategy worked well in *S. meliloti*, where fluorescence was measured 20 min after IPTG addition, it was not possible to measure fluorescence in *E. coli* using the described constructs. Therefore, and to avoid long-term effects, the mRNA level of the report gene *egfp* was measured 3 min after simultaneous induction of transcription of the reporter fusion construct and the sRNA.

(Figure 2.2.4F left panel) shows that the level of *dnaA-egfp* mRNA derived from plasmid pSRKGm-dnaA′-egfp was strongly decreased if lacZ′-Ec-rnTrpL or its derivative with mutation-2 was co-induced, supporting the idea that the sRNA binds to *dnaA* mRNA and thereby induces a reduction of *dnaA′::egfp* mRNA levels. In contrast, if the sRNA derivative carrying mutation-1 was co-induced with the reporter construct, the *dnaA′::egfp* mRNA level remained like in the EVC, in which only the reporter mRNA was induced. To prove that the observed effects are due to base pairing with *dnaA* mRNA or its abolishment, compensatory mutation was introduced into the *dnaA* binding site (dnaAMUT) to restore the presumed base-pairing interactions with the sRNA carrying mutation-1 (see Figure.2.2.4A). Indeed, a stromg decrease in fluorescence produced by the pSRKGm-dnaAMut(CCA/GGU)–egfp construct was only observed if the corresponding base-pairing sRNA lacZ′-rnTrpL-mutation-1 was coexpressed (Figure 2.2.4F right panel). These results validate the base-pairing between Ec-rnTrpL and *dnaA* in the regions of mutation-1 and dnaAMUT and show that this interaction is responsible for the negative effect of Ec-rnTrpL on *dnaA*.

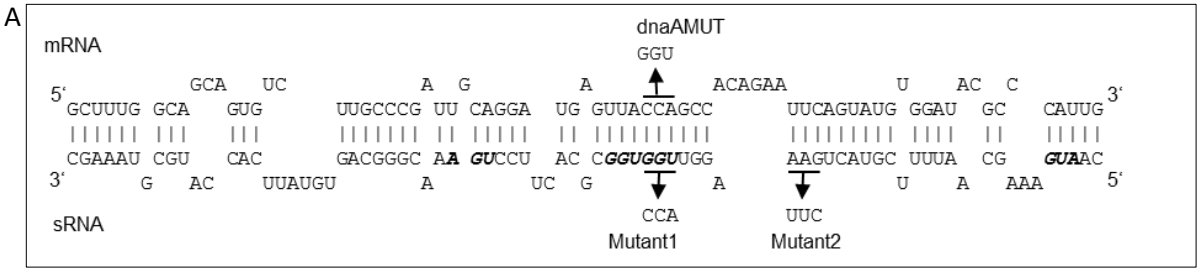

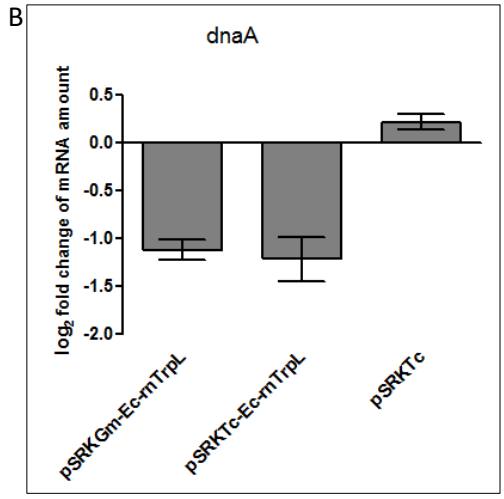

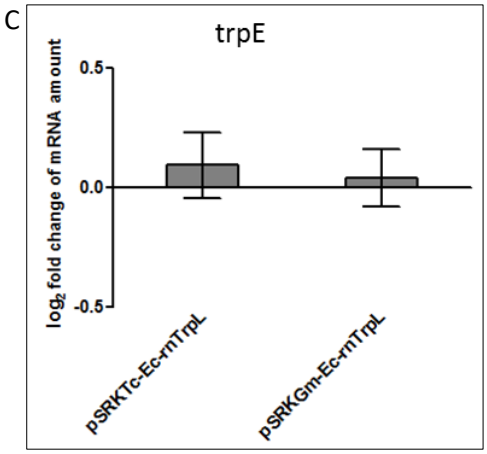

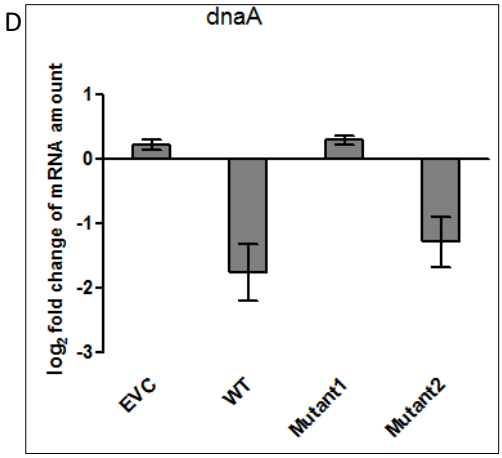

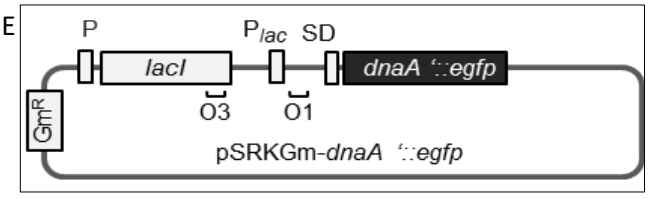

F

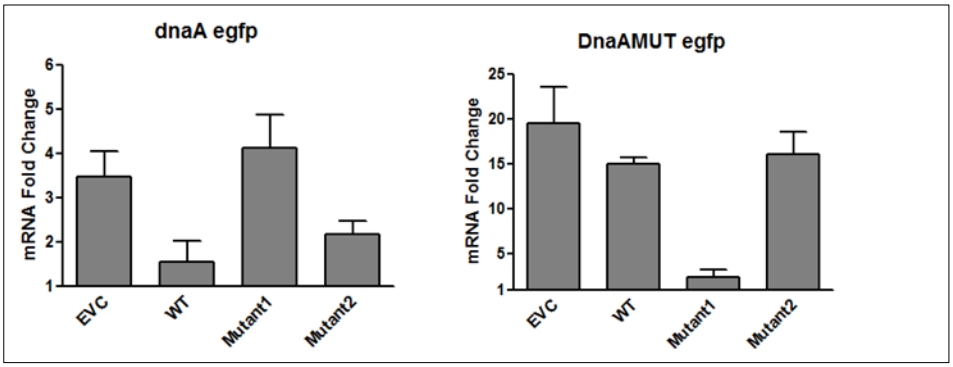

Figure 2.2.4 The sRNA Ec-rnTrpL Base-Pairs with *dnaA* mRNA to Decrease Its Level in a Tc-Independent Manner. (A) Scheme of the duplex structure predicted to be formed between *dnaA* (mRNA) and Ec- rnTrpL (sRNA). Ec-rnTrpL mutations (mutant1, mutant2) characterized in this experiment are given below the sRNA sequence. The *trpL* start, stop and Trp codons are shown in italics and bold. Compensatory *dnaA* mutations used to restore base-pairing interactions (dnaAMut) are shown above the mRNA sequence. **(B)** qRT-PCR analysis of changes in the *dnaA* mRNA level after induction of the sRNA lacZ′-Ec-rnTrpL transcription for 5 min with 1 mM IPTG in strains *E. coli* MG1655 (pSRKTc-Ec-rnTrpL) and *E. coli* MG1655 (pSRKGm-Ec-rnTrpL). The empty vector control (EVC) strain *E. coli* MG1655 (pSRKTc) was used as negative control. **(C)** qRT-PCR analysis of changes in the *trpE* mRNA level after induction of the sRNA lacZ′-Ec-rnTrpL. For other descriptions see panel B. **(D)** qRT-PCR analysis of changes in the *dnaA* mRNA level after induction of the sRNA lacZ′-Ec-rnTrpL or its derivatives harboring mutation-1 and mutation-2 (indicated). For other descriptions see panel B. **(E)** Scheme of pSRKGm-dnaA′-egfp. The *dnaA′::egfp* fusion contains the *dnaA* region predicted to base-pair with Ec-rnTrpL codons fused to the third *egfp* codon. **(F)** Analysis of possible base-pairing interactions between lacZ′-Ec-rnTrpL and the fusion mRNA *dnaA′::egfp* in strain *E. coli* MG1655. EVC, pSRKTc was used; WT, plasmid pSRKTc-Ec-rnTrpL was used; Mutant 1, plasmid pSRKTc-Ec-rnTrpL-Mutant-1 was used; Mutant 2, plasmid pSRKTc-Ec-rnTrpL-Mutant-2 was used. All strains contained plasmid pSRKGm-dnaA′-egfp. The graph shows the results of qRT-PCR analysis of the reporter *egfp* mRNA. The *egfp* mRNA level 3 min after addition of IPTG (0.5 mM) was compared to the level before addition. For other descriptions see panel B. In these experiments, bacteria were cultured in LB medium. For qRT-PCR analysis, *rpoB* RNA was used as reference control RNA. Data shown in the graph were obtained from three independent experiments, each performed in technical duplicates (means and SDs are indicated).

2.2.5 The sRNA Ec-rnTrpL Base-Pairs with *rsuA* mRNA to Decrease Its Level in a Tc-Dependent Manner

After analyzing the top target *dnaA*,the further analysis focused on *rsuA* encoding the pseudouridine synthase RsuA which serves to produce the pseudouridylation of 16S rRNA at position 516 (158,159). Figure 2.2.5A shows the predicted base-pairing between the sRNA Ec-rnTrpL and mRNA *rsuA*. As described above for mRNA *dnaA*, it was firstly tested whether the effect of the sRNA Ec-rnTrpL on mRNA *rsuA* was Tc dependent or not. As Figure 2.2.5B shows, upon overexpression of the sRNA Ec-rnTrpL, the *rsuA* mRNA level was decreased more than 2 fold, and this change in the level only happened in the presence of Tc (e.g., when pSRKTc-based plasmid was used and therefore Tc was present in the growth medium). In the absence of Tc (e.g., when pSRKGm-based plasmid was used), the result after IPTG addition was similar to the result for the EVC. This suggests that the effect of the sRNA on *rsuA* may depend on Tc.

To further analyze the effect of Tc on the interaction between the sRNA and *rsuA* mRNA in the absence of a Tc-resistance plasmid, it was necessary to find suitable subinhibitory Tc concentration for *E. coli*. Figure 2.2.5C results show the growth of strain *E. coli* MG1655 (pSRKGm-Ec-rnTrpL) at different Tc concentrations. At Tc concentration of 2 µg/ml or higher cells did not grow. So 0, 0.5, 1, and 1.5 µg/ml Tc was used to test relationship between Tc and the effect of the sRNA Ec-rnTrpL on *rsuA* mRNA. In the next experiment, IPTG was added together with Tc and 3 min thereafter, samples were withdrown for RNA isolation. Changes in the level of *rsuA* mRNA were analyzed by qRT-PCR. Interestingly, with increased Tc concentrations, the decrease in the level of *rsuA* mRNA was stronger (Figure 2.2.5D). These results strongly indicated that Tc is a factor participating in the negative regulation of *rsuA* by the sRNA Ec-rnTrpL.

To validate by *in vivo* experiment the predicted base-pairing between Ec-rnTrpL and *rsuA* mRNA, the sRNA derivatives with mutation-1 and mutation-2 were used (Figure 2.2.5A). After overexpression of the sRNA with mutation-1, the level of *rsuA* mRNA was decreased to a lesser extend than after overexpression of the wildtype sRNA lacZ′-Ec-rnTrpL. Furthermore, there was no change in the *rsuA* mRNA level after overexpression of the mutation-2 sRNA or in the EVC (Figure 2.2.5E). Thus, in contrast to the interaction of the sRNA with *dnaA*, mutation-1 sRNA region seem to be involved in the interaction with *rsuA* mRNA, but the region of mutation-2 seems to be crucial.

Since the predicted interaction site is located at the end of the *rsuA* gene and overlaps with the intergenic region between *rsuA* and *bcr*, it was necessary to construct a bicistronic *rsuAbcr'::egfp* fusion in order to test *in vivo* the predicted base pairing. The *in vivo* assays were performed in strain *E. coli* MG1655 using the bicistronic *rsuAbcr'::egfp* reporter construct, its derivative harboring a mutation rsuAMUT restoring complementarity with mutation-2 of the sRNA, and lacZ′-Ec-rnTrpL as well the mutated derivatives of the sRNA. The *rsuAbcr'::egfp* fusions (Figure 2.2.5F) were expressed from pSRKGm (conferring Gm^r) and challenged with wildtype or mutated lacZ′-rnTrpL transcribed from pSRKTc (conferring Tc^r) (see Figure 2.2.1B above). The mRNA level of the reporter construct was analyzed by qRT-PCR using *egfp* specific primers. Changes in the mRNA level were measured 3 min after simultaneous induction of transcription of the reporter fusion construct and the sRNA.

Figure 2.2.5G (left panel) shows that the level of *rsuAbcr'-egfp* mRNA derived from plasmid pSRKGm-rsuAbcr′-egfp was strongly decreased if lacZ′-Ec-rnTrpL and lacZ′-Ec-rnTrpL with mutation-1 was co-expressed, although a statistically significant difference was observed. In contrast, if the sRNA derivative carrying mutation-2 was co-expressed, no decrease in fluorescence was observed (the result was similar to the EVC). To test whether this was due to a significantly reduced (or lack of) binding of the sRNA with mutation-2 to *rsuAbcr* in the bicistronic reporter mRNA, appropriate mutation UUC/AAG (rsuAMUT) was introduced into the *rsuA* binding site to restore the presumed base-pairing interactions (Figure 2.2.5A). Indeed, using the mutated reporter construct, a decrease in fluorescence was only observed if the corresponding base-pairing sRNA lacZ′-rnTrpL-mutation-2 was coexpressed (Figure 2.2.5G right panel). These results validate the base-pairing between Ec-rnTrpL and

rsuAbcr and show that this interaction is responsible for the negative effect of Ec-rnTrpL on *rsuA*.

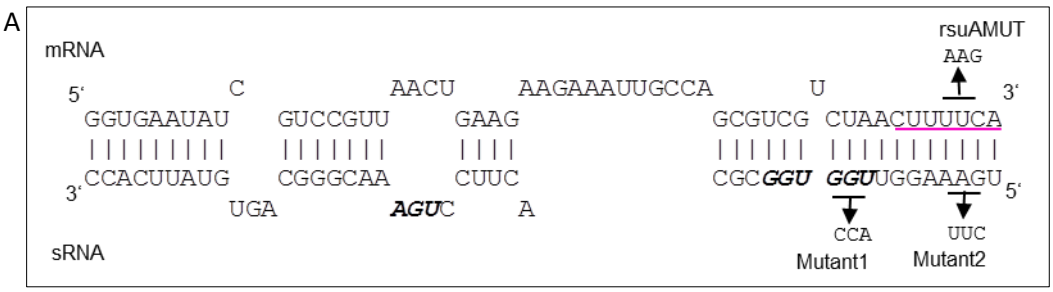

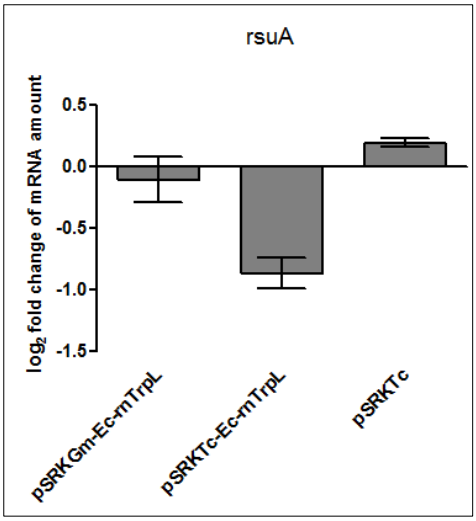

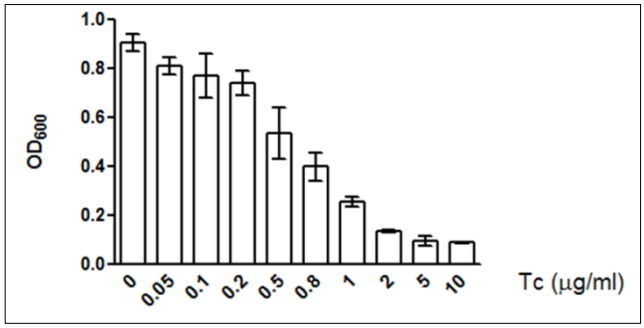

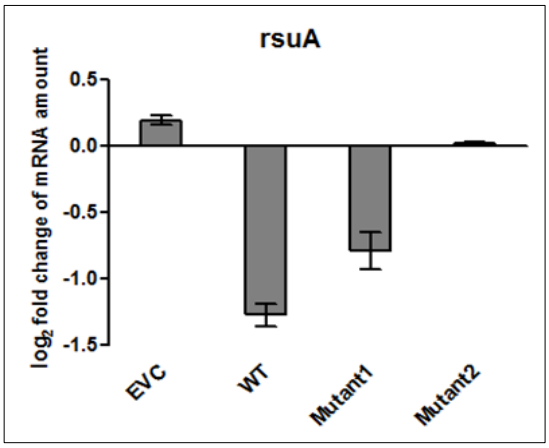

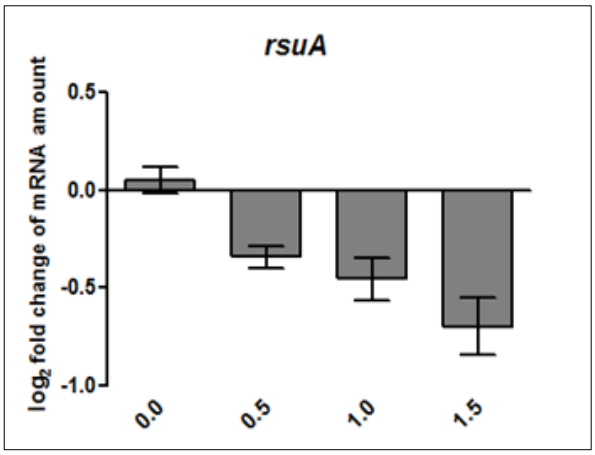

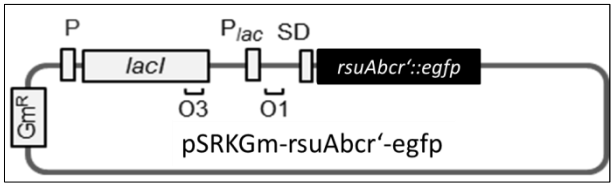

G

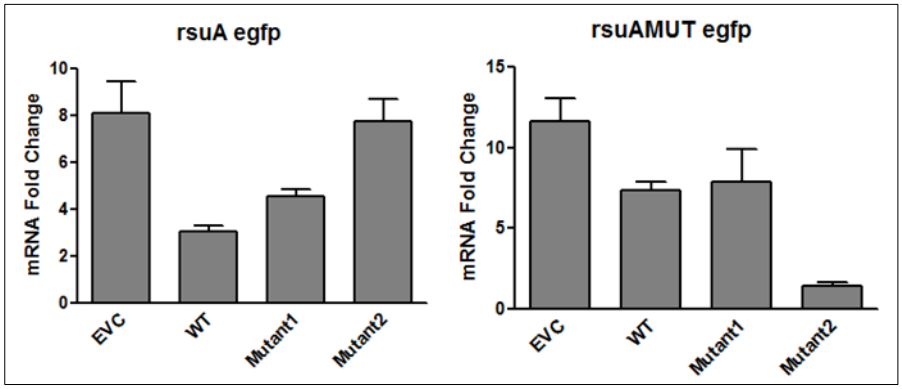

Figure. 2.2.5 The sRNA Ec-rnTrpL Base-Pairs with *rsuA* mRNA to Decrease Its Level in a Tc-Dependent Manner. (**A**) Scheme of the duplex structure predicted to be formed between *rsuAbcr* (mRNA) and Ec- rnTrpL (sRNA). Ec-rnTrpL mutations (mutant1, mutant2) characterized in this experiment are given below the sRNA sequence. The *trpL* stop codon and the Trp codons are shown in italics and bold. Underlinded in purple is a part of the intergenic sequence between *rsuA* and *bcr*, which is located immediately downstream of the *rsuA* stop codon. Compensatory *rsuA* mutations used to restore base-pairing interactions (rsuAMut) are shown above the mRNA sequence. (**B**) qRT-PCR analysis of changes in the *rsuA* mRNA level 5 min after addition of 1 mM IPTG to induce transcription of the sRNA lacZ′-Ec-rnTrpL in strains *E. coli* MG1655 (pSRKTc-rnTrpL) and *E. coli* MG1655 (pSRKGm-rnTrpL). Strain *E. coli* MG1655 (pSRKTc) was the empty vector control (EVC) used was as negative control. (**C**) Growth of strain *E. coli* MG1655 at different Tc concentrations (indicated). The initial OD_{600} after inoculating was OD_{600} 0.2, and the cells were growth overnight. (**D**) qRT-PCR analysis of changes in the *rsuA* mRNA level 5 min after addition of 1 mM IPTG to induce transcription of the sRNA lacZ′-Ec-rnTrpL under a series of subinhibitory Tc concentrations (indicated below the panel in μg/ml). (**E**) qRT-PCR analysis of changes in the *rsuA* mRNA level 5 min after addition of 1 mM IPTG to induce transcription of the sRNA lacZ′-Ec-rnTrpL or its derivatives with the indicated mutations. For other details, see panel (B). (**F**) Scheme of pSRKGm-rsuAbcr′-egfp. The *rsuA′bcr::egfp* fusion contains the mRNA region predicted to base-pair with the sRNA Ec-rnTrpL. **(G)** Left panel: Analysis of possible base-pairing interactions between the fusion mRNA *rsuAbcr′::egfp* and lacZ′-Ec-rnTrpL or its derivatives with the indicated mutations. Shown are results of a qRT-PCR analysis with *egfp* specific primers. Changes in mRNA level were analyzed 3 min after addition of IPTG (0.5 mM/ml). Right Panel: Analysis of possible base-pairing interactions between the fusion mRNA *rsuA-MUTbcr′::egfp* and lacZ′-Ec-rnTrpL or its derivatives with the indicated mutations. For further details, see (G right panel). For the qRT-PCR analysis, *rpoB* RNA was used as reference control RNA. In these experiments, bacteria were cultured in LB medium. Data shown in the graphs were obtained from three independent experiments, each performed in technical duplicates (means and SDs are indicated).

2.2.6 Genes *rsuA* and *bcr* are Cotranscribed and the sRNA Ec-rnTrpL Decreases the Level of *bcr* mRNA in a Tc-Dependent Manner

The *bcr* gene is located downstream of *rsuA* (Figure 2.2.6A) and there was no predicted promoter of the *bcr* gene, so probably *bcr* and *rsuA* genes are cotranscribed. RT-PCR was applied to test whether *bcr* is cotranscribed with *rsuA*. The results show that the two genes are cotranscribed in *rsuAbcr* mRNA in strain *E. coli* MG1655 (Figure 2.2.6B). Thus, both genes are probably coregulated by the sRNA Ec-rnTrpL. To test whether the influence of the sRNA on *rsuA* and *bcr* is similar, qRT-PCR analysis with *bcr* specific primers was conducted as described above for *rsuA*. Indeed, the *bcr* mRNA level was decreased after indiuction of Ec-rnTrpL transcription, and this was observed only in the presence of Tc (Figure 2.2.6C).

Furthermore, addition of increasing Tc concentrations led to an increased effect of the sRNA induction on the mRNA (Figure 2.2.6D). Moreover, Ec-rnTrpL harboring mutation-2 was ineffective for downregulation of *bcr* mRNA. These results were very similar to the results obtained for *rsuA* mRNA. (Figure 2.2.6E). Together, these results suggest that due to the co-transcription of *rsuA* and *bcr*, both genes are negatively co-regulated by the sRNA Ec-rnTrpL in a Tc-dependent manner.

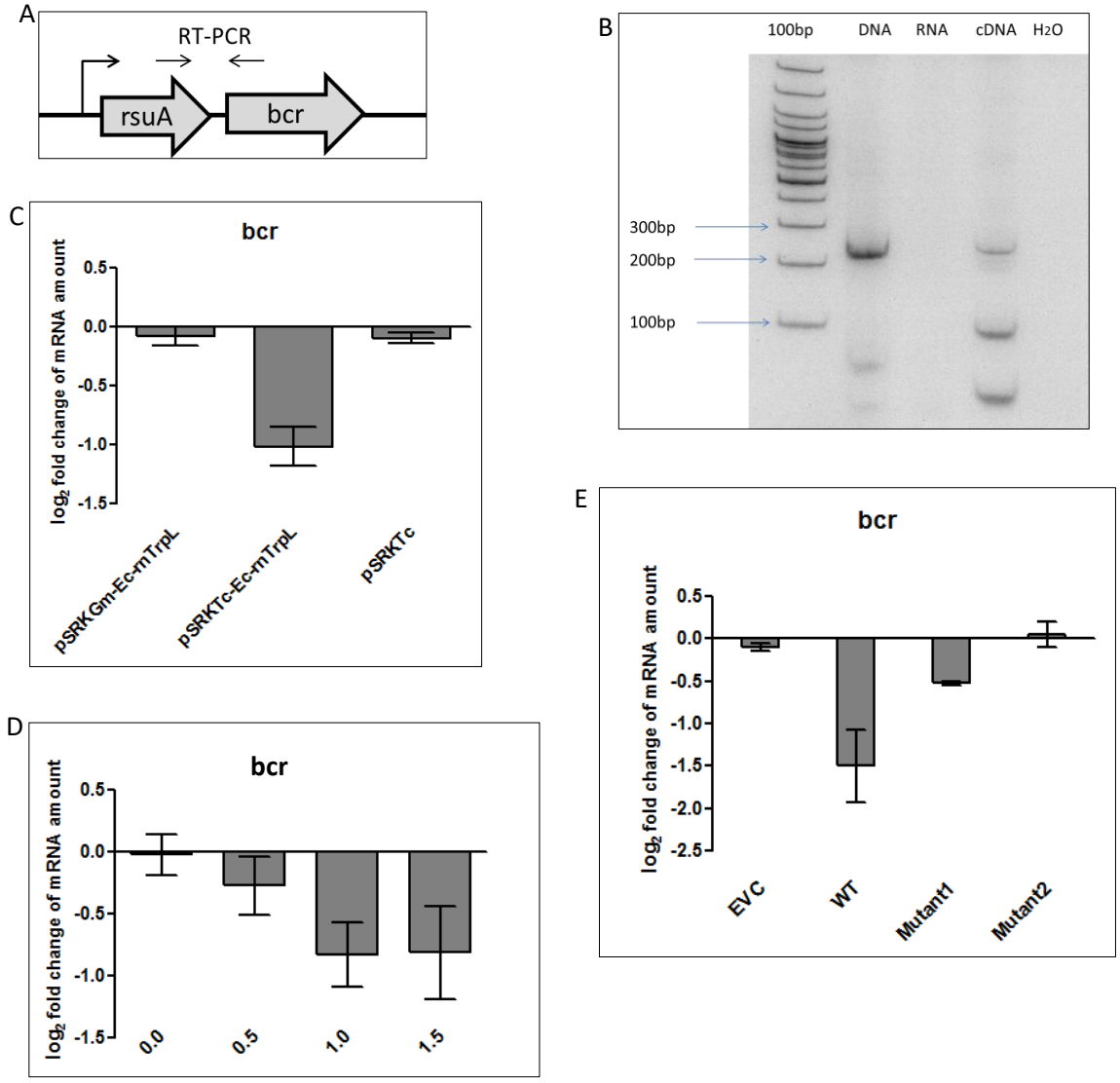

Figure 2.2.6 Genes *rsuA* and *bcr* are Cotranscribed and the sRNA Ec-rnTrpL Decreases the Level of *bcr* mRNA in a Tc-Dependent Manner. (**A**) Scheme of *rsuA* and *bcr* genes locus in *E. coli* chromosome. (**B**) Co-transcription of *rsuA* and *bcr* revealed by RT-PCR analysis of strain *E. coli* MG1655. The template input is specified above the panel. (**C**) qRT-PCR analysis of changes in the *bcr* mRNA level 5 min after addition of 1 mM IPTG to induce transcription of the sRNA lacZ′-Ec-rnTrpL in strains *E. coli* MG1655 (pSRKTc-rnTrpL) and *E. coli* MG1655 (pSRKGm-rnTrpL). Strain *E. coli* MG1655 (pSRKTc) was the empty vector control (EVC) used was as negative control. (**D**) qRT-PCR analysis of changes in the *bcr* mRNA level 5 min after addition of 1 mM IPTG to induce transcription of the sRNA lacZ′-Ec-rnTrpL under a series of subinhibitory Tc concentrations (indicated). (**E**) qRT-PCR analysis of changes in the *bcr* mRNA level 5 min after addition of 1 mM IPTG to induce transcription of the sRNA lacZ′-Ec-rnTrpL or its derivatives with the indicated mutations. For other

details, see panel (C). In these experiments, bacteria were culturedd in LB medium. For qRT-PCR analysis, *rpoB* RNA was used as reference control RNA. Data shown in the graphs were obtained from three independent experiments, each performed in technical duplicates (means and SDs are indicated).

2.2.7 Analysis of The Role of Peptide Ec-peTrpL

Figure 2.2.1A shows that pSRKGm-Ec-rnTrpL will not only produce sRNA lacZ′-Ec-rnTrpL but also peptide Ec-peTrpL. To test whether the peptide Ec-peTrpL plays a role in the above mentioned posttranscription regulation mechanisms, a plasmid was constructed for induced production of this peptide independently of the sRNA. The peptide production plasmid was based on pBAD-bgaB2 (Figure 2.2.7A), which allows for induction by arabinose. Based on similar experiments with *S. meliloti*, it was expected that upon addition of arabinose, the level of *dnaA* mRMA could be decreased, if the peptide is a limiting factor and works together with the native sRNA Ec-rnTrpL transcribed from the chromosome. Similarly, it was expected that upon addition of arabinose and Tc, the level of *rsuAbcr* mRNA will be decreased, if the peptide works together with the native sRNA.

In this experiment, either arabinose, or Tc or both Tc and arabinose were added to strain *E. coli* MG1655 (pBAD-bgaB2-Ec-peTrpL) and changes in the levels of the mRNAs *dnaA*, *rsuA* and *bcr* were analyzed by qRT-PCR. The *trpE* mRNA was also analyzed as negative control. Figure 2.2.5B shows that while the level of *trpE* mRNA was not significantly changed, and increase in the levels of the targets of the sRNA Ec-rnTrpL was detected under all tested conditions (arabinose to induce peptide production; Tc; Tc and arabinose). Thus, induction of the peptide does not lead to a decrease in the level of the targets of its cognate sRNA.

A

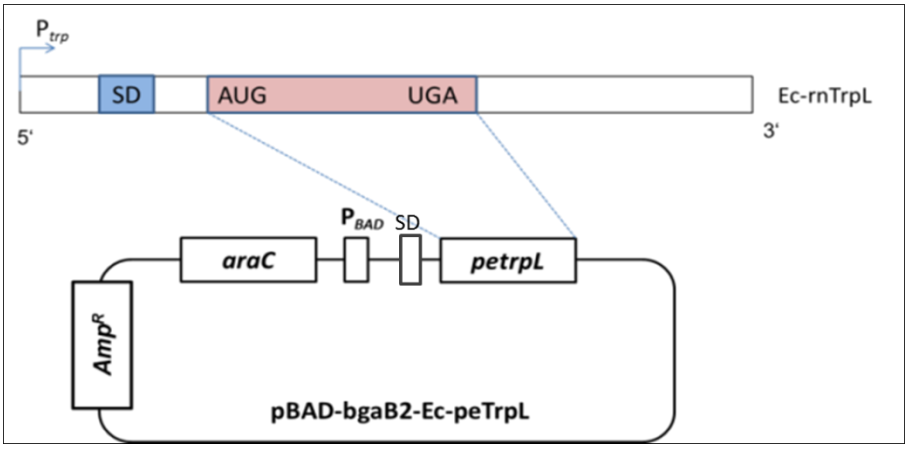

B

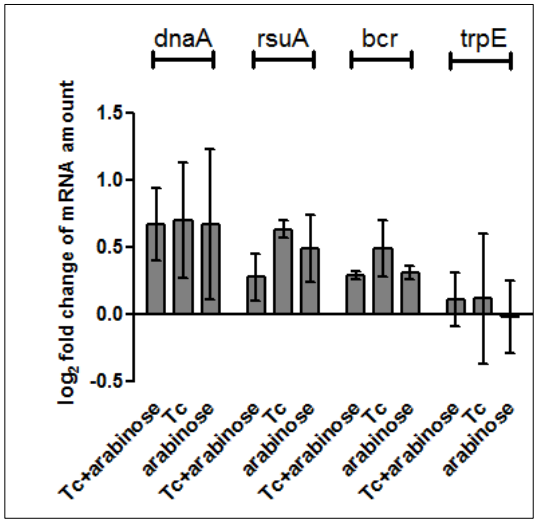

Figure 2.2.7 Analysis of The Role of Peptide Ec-peTrpL. (**A**) Scheme of pBAD-bgaB2-Ec-peTrpL. The pBAD-bgaB2-based plasmid harbor the *ara* repressor gene *araC* with its own promoter, the promoter P_{BAD} and contains a Shine-Dalgarno sequence (SD), followed ATG as the start codon for translation. (**B**) qRT-PCR analysis of changes in the levels of the indicated mRNAs 5 min after addition of arabinose, Tc or both (indicated) to cultures of strain *E. coli* MG1655 (pBAD-bgaB2-Ec-peTrpL). 0.2% arabinose and/or 1 µg/ml Tc was used. In this experiment, bacteria were cultured in LB medium. For qRT-PCR analysis, spike in RNA was used as reference control RNA. Data shown in the graphs were obtained from three independent experiments, each performed in technical duplicates (means and SDs are indicated).

2.2.8 Comparison of Target mRNA Levels between *E. coli* MG1655 and *E. coli* MG1655 *ΔtrpL*

Above changes in mRNA levels were analyzed after overproduction of the sRNA Ec-rnTrpL. This is a fast and easy way to touch the mechanism; however, sRNA overproduction may lead to artifacts (mRNAs could be affected due to unnaturally high sRNA levels). Also another problem is that the sRNA Ec-rnTrpL transcribed from pSRK-plasmids was lacZ′-Ec-rnTrpL, not the native one. To provide additional evidence for the role of Ec-rnTrpL in posttranscriptional regulation, it was necessary to construct a deletion mutant and to compare it to the wild type strain.

A deletion mutant named *E. coli* MG1655 *ΔtrpL* was constructed, which lacks the Ec-rnTrpL sequence (from the ATG start condon of *trpL* to the end of the terminator; Figure 2.2.8A, Figure 2.2.8B). Due to the used method, the short sRNA sequence was replaced by a slightly longer *scar* sequence, which has no function (Figure 2.2.8B).

In the deletion mutant and the wild type, the levels of the following mRNAs were compared by qRT-PCR: *dnaA, rsuA, bcr, ycaO, sanA, mphC, trpE,* and *rpoB*. Since it can be expected that in the deletion mutant, due to the lack of transcription attenuation, the level of *trpE* mRNA will be increased, *trpE* could not be used as a negative control in this experiment. Therefore, *rpoB* mRNA was used as a negative control (a Ec-rnTrpL independent sRNA), and a *spike in* control RNA was used as reference.

Bacteria were cultivated to the exponential growth phase in M9 minimal medium, in which the Ec-rnTrpL is naturally present in the wild type MG1655 due to the *trp* promoter derepression. In M9 medium without Tc, the *dnaA* mRNA level was two-fold higher in the deletion mutant *E. coli* MG1655 *ΔtrpL* than in *E. coli* MG1655 wildtype, while the levels of *rsuA* and *bcr* mRNAs in both strains were similar (Figure 2.2.8C). Furthermore, Figure 2.2.8C shows that from the analyzed target candidates, *sanA* is possibly a Tc-independent target of the sRNA Ec-rnTrpL. As expected, due to the lack of transcription attenuation in the deletion mutant, the level of *trpE* mRNA level was increased. Importantly, the level of *rpoB* used as a negative control was similar in both strains.

When Tc (used at subinhibitory concentration) was present in the M9 medium, the levels of *dnaA, rsuA,* and *bcr* mRNA were lower in the wild type strain than in the *ΔtrpL* deletion

mutant (Figure 2.2.8D). This result is in line with the decrease of these mRNAs upon induced lacZ′-Ec-rnTrpL overproduction, which was described above. Of note, this result supports the view that *rsuAbcr* is a Tc-dependent target of Ec-rnTrpL. Furthermore, as expected, the *trpE* mRNA level was lower in the wild type due to transcription attenuation.

However, the difference in the *trpE* mRNA level between the wild type and the deletion mutant was higher in the presence of Tc (2-fold) than in its absence (approximately 1.3 fold). This could be explained by increased transcription attenuation in the presence of Tc. Indeed, it is known that when no translation takes place, hyperattenuation happens (157).

Next, the question was addressed whether in the deletion mutant, the lack of posttranscriptional regulation of *dnaA* by Ec-rnTrpL influences the initiation of chromosome replication. It is known that *dnaA* overexpression leads to increased initiation of chromosome replication, which can be measured as an increase in the copy number of chromosomal origins (*oriC*) in the cell (160). For this experiment, cultures of strains MG1655 and MG1655 *ΔtrpL* were grown in M9 medium at an $OD_{600\ nm}$ = 0.2. DNA was purified and using qPCR, the ratio of the *oriC* (origin of chromosome replication) level to the *terC* (site of termination of chromosome replication) level in the the mutant was compared to that in wild type. Increased level of *oriC* was detected in the mutant (Figure 2.2.8E), in line with increased initiation of chromosome replication due to higher *dnaA* expression in the absence of the sRNA Ec-rnTrpL.

The above result suggests that Trp could be a signal for upregulation of *dnaA* and thus for increased initiation of chromosome replication under conditions of nutrient availability. To test whether the chromosome initiation increases upon addition of Trp in a *trpL*-dependent manner, wild type and *ΔtrpL* strains were grown in M9 medium at an $OD_{600\ nm}$ = 0.2. Then Trp was added (20 µg/ml) and 1 h later, the *oriC/terC* ratio was measured by qPCR. Indeed, the *oriC* level was increased upon Trp addition, but only in the wild type (Figure 2.2.8F).

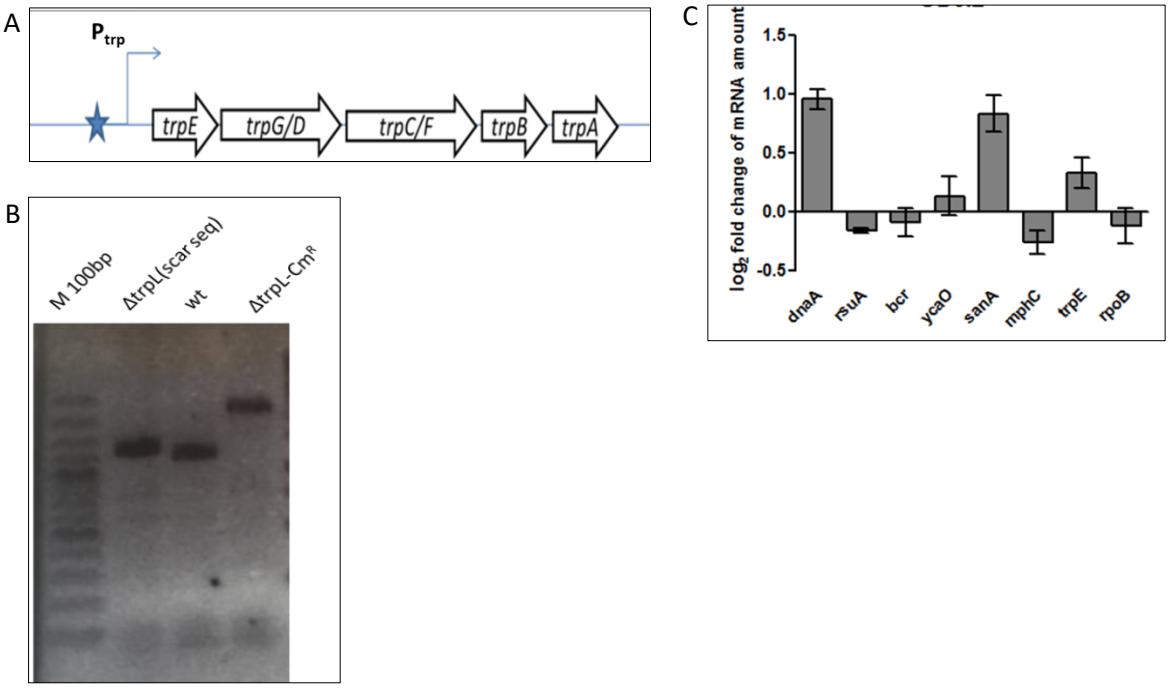

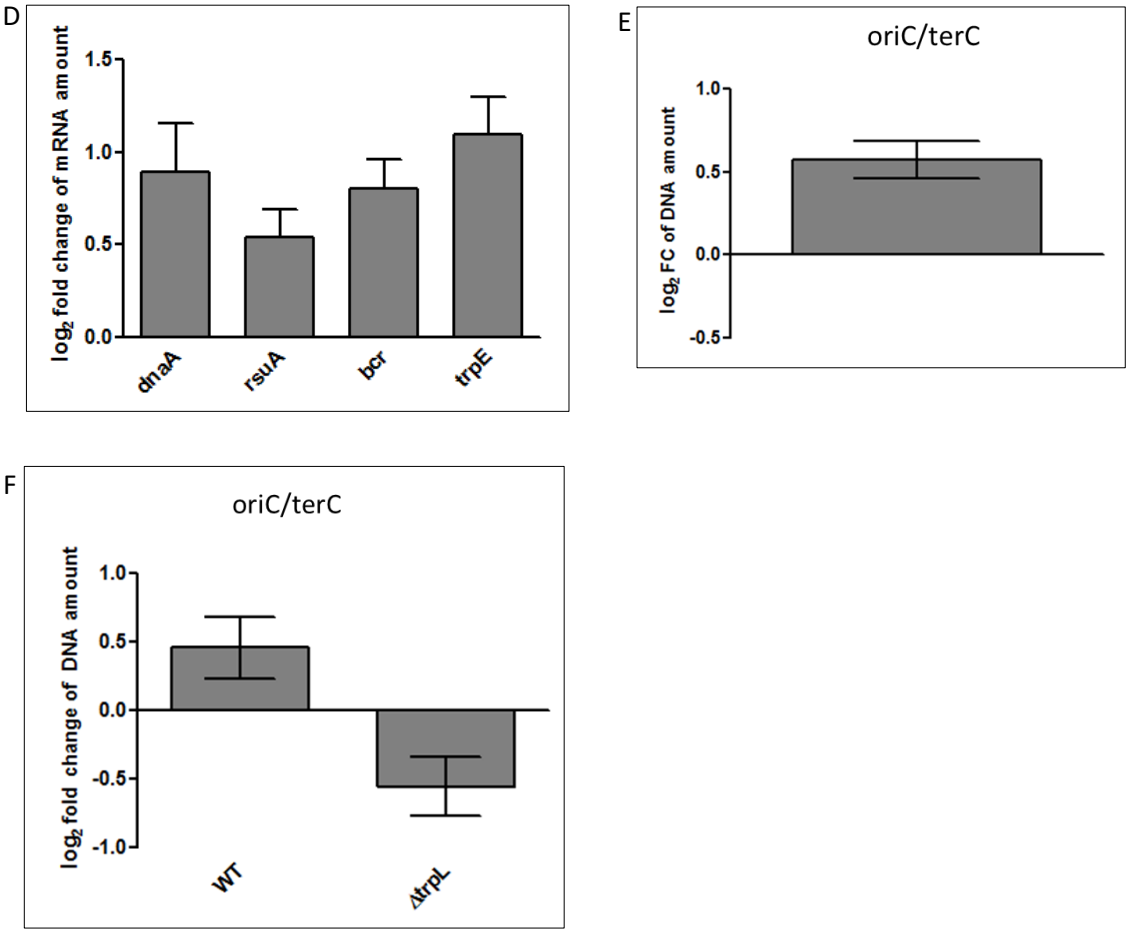

Figure 2.2.8 Comparison of Target mRNA Levels between *E. coli* MG1655 and *E. coli* MG1655 *ΔtrpL*. (A) Scheme of the *trp* operon locus in the deletion mutant *E. coli* MG1655 *ΔtrpL*. The Ec-rnTrpL was deleted from ATG start codon. The original P_{trp} was preserved. **(B)** Colony PCR verifying the replacement of the Ec-rnTrpL sequence by the *scar* sequence in *E. coli* MG1655 *ΔtrpL*. M is 100 bp plus marker; Lane 1 was *ΔtrpL*-Cm^R, the Ec-rnTrpL sequence was replaced by the selection marker Cm^R; *ΔtrpL* (*scar seq*), in the deletion mutant, the selection marker Cm^R was replaced by the non-functional *scar* sequence; wt, wildtype. **(C)** qRT-PCR analysis of the levels of the indicated mRNAs in the exponential phase at OD_{600} of 0.2. Shown is the difference between *E. coli* MG1655 *ΔtrpL* and *E. coli* MG1655 wildtype. **(D)** qRT-PCR analysis of the levels of the indicated mRNAs in the exponential phase at OD_{600} of 0.3, three minutes after addition of Tc (1 µg/ml). For other descriptions see panel (C). *Spike in* RNA was used as a reference control RNA in panels C) and D). **(E)** qPCR analysis of the level of DNA near *oriC* and *terC* in the exponential phase at OD_{600} of 0.2. Difference is shown between *E. coli* MG1655 *ΔtrpL* and *E. coli* MG1655. Shown is the difference between the *oriC/terC* ratio in *E. coli* MG1655 wildtype and *E. coli* MG1655 *ΔtrpL*. (**F**) qPCR analysis of the change in the *oriC* amount after addition of Trp to cultures grown in M9 medium. The cells for qPCR were harvested before and 60 min after 20 µg/m) Trp was added. The analysis was performed in cultures of strains *E. coli* MG1655 (WT) and *E. coli* MG1655 *ΔtrpL* (ΔtrpL). *terC* was used for normalization (internal control gene). Used strains are indicated. Data shown in the graphs were obtained from three independent experiments, each performed in technical duplicates (means and SDs are indicated).

2.2.9 Ec-rnTrpL is a *hfq*-Dependent sRNA, Which Downregulates *dnaA* with the Help of Ribonuclease E

Finally, *hfq*, *rnc* and *rne* mutants were used to test whether Ec-rnTrpL works with Hfq, RNase III and RNase E, respectively. Figure 2.2.9A shows that in the absence of Hfq, the levels of *dnaA* and *rsuA* mRNA are not decreased upon Ec-rnTrpL overproduction, showing that the action of Ec-rnTrpL depends on the RNA chaperone Hfq. Furthermore, according to Figure 2.2.9B and Figure 2.2.9C, RNase E but not RNase III is necessary for downregulation *dnaA* by Ec-rnTrpL. Surprisingly, neither RNase E nor RNase III were found to be necessary for downregulation of *rsuA* mRNA by Ec-rnTrpL, suggesting that a novel mechanism operates in this antibiotic-dependent regulation.

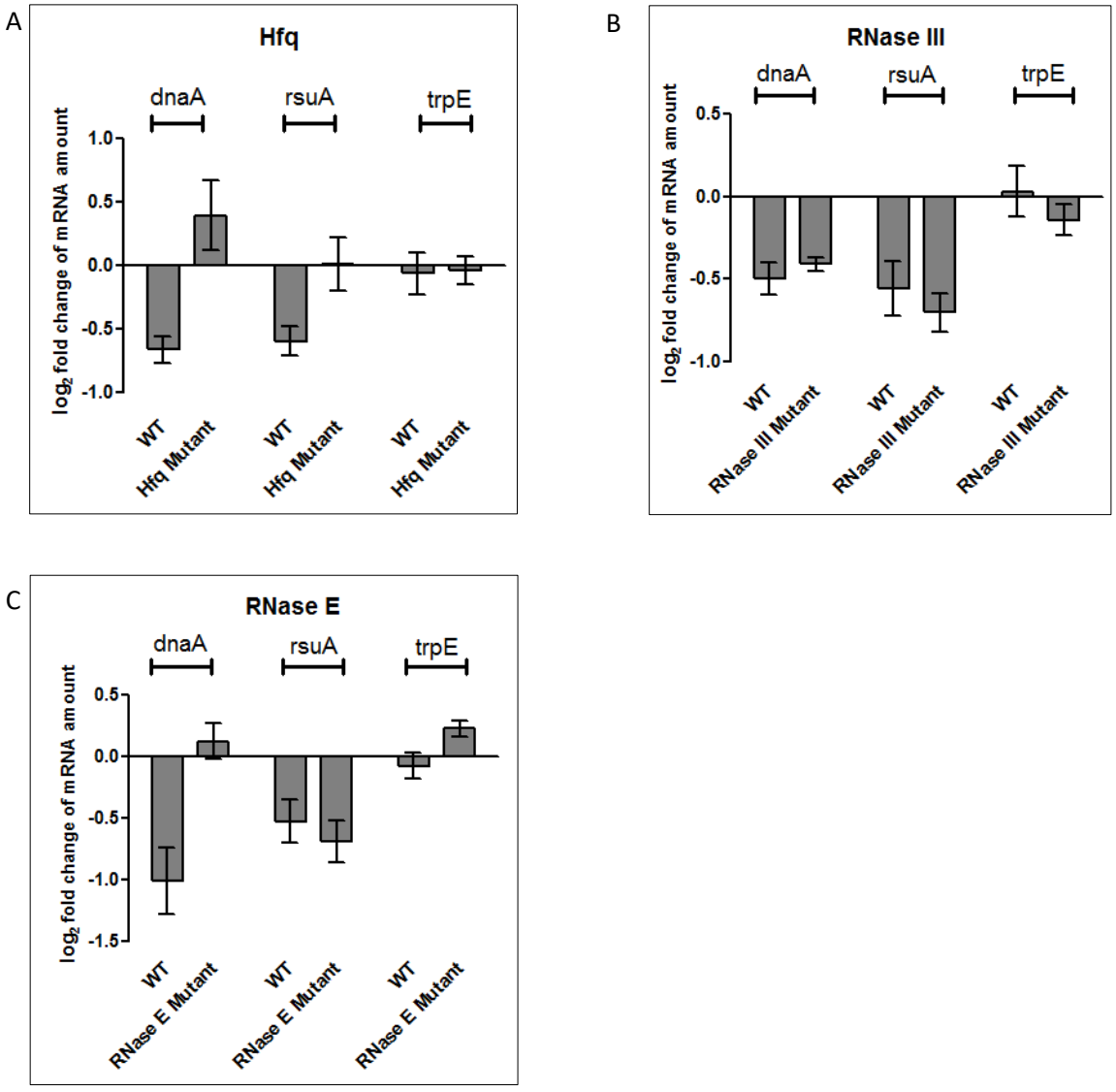

Figure 2.2.9 Ec-rnTrpL is a *hfq*-Dependent sRNA, Which Downregulates *dnaA* with the Help of Ribonuclease E. (A) qRT-PCR analysis of changes in the levels of *dnaA*, *rsuA* and *trpE* mRNAs 3 min after addition of IPTG to induce the sRNA overproduction at exponential phase (OD_{600} of 0.3). Shown is analysis of *E. coli* MG1655 (pSRKTc-rnTrpL) (WT) and *E. coli* MG1655 *Δhfq* (pSRKTc-rnTrpL) (Hfq Mutant) strains. **(B)**

qRT-PCR analysis of *E. coli* BL322 (pSRKTc-rnTrpL) (WT) and *E. coli* BL321 *rnc* (pSRKTc-rnTrpL) (RNase III Mutant). For other descriptions, see panel (A). **(C)** qRT-PCR analysis of *E. coli* N3433 (pSRKTc-rnTrpL) (WT) and *E. coli* N3431 (pSRKTc-rnTrpL) (RNase E Mutant). For other descriptions, see panel (A). Since the RNase E mutant is not a deletion mutant, but a thermosensitive mutant, the cells were firstly cultured from OD_{600} of 0.02 to exponential phase at OD_{600} of 0.3 at 37 °C, and then cells were shifted to 42℃ for 10 min, before IPTG was added. At the time points 0 min and 3 min after IPTG addition, RNA for qRT-PCR was isolated. For qRT-PCR analysis, *spike in* RNA was used as reference control RNA. Data shown in the graphs were obtained from three independent experiments, each performed in technical duplicates (means and SDs are indicated).

3 Discussion

3.1 sRNA rnTrpL of *S. meliloti*

In this study, the sRNA rnTrpL and the leader peptide peTrpL translated from this sRNA were characterized. Previous bioinformatic prediction showed that the sRNA rnTrpL has the capacity to base pair with multiple mRNAs (151). To characterize the sRNA into more detail, it was necessary to construct suitable deletion mutants. In this work, construction of deletion mutants of *S. meliloti* was established in our laboratory. Furthemore, suitable systems for induced expression of the sRNA and/ or the leader peptide were established.

According to Figure 2.1.2B, the level of the pulse-overexpressed sRNA dervative lacZ′-rnTrpL was lower than the level of the native sRNA transcribed from the chromosome. Despite this, the ectopically produced sRNA lacZ′-rnTrpL was able to decrease the levels of several predicted targets and to base-pair with *trpDC* mRNA. It is not clear whether the *lacZ* 5′-UTR, which makes this sRNA derivative to be longer than the native, leaderless sRNA, and which most probably increases the translation of the *trpL* ORF, has influence on the base-pairimg function of the sRNA, for example by changing target prioritization. These questions can be addressed in a future study by using the SinR-P_{sinI} system for induced rnTrpL production, which was established in this study. In this system, production of the SinR protein is induced by IPTG, and SinR then activates promoter *sinI* (153), which controls the transcription of rnTrpL starting with its native 5′-end (starting with ATG of the *trpL* ORF). According to the data (Figure 2.1.4G, Figure 2.1.4H), the levels of several predicted target mRNAs, including the validated target *trpC* mRNA, were decreased 10 min after induction of sRNA production by this system. However, in most of the experiments in this work the lacZ′-rnTrpL system was used.

As we know, there are three *trp* operons participating in Trp synthesis in *S. meliloti*: *trpE(G)*, *trpDC* and *trpFBA*. The initial step of Trp biosynthesis is performed by the protein encoded by gene *trpE(G)*, while the enzymes of the next two steps are translated from *trpDC* mRNA. The *trpFBA* operon encodes the residual enzymes of the pathway, phosphoribosyl anthranilate isomerase and Trp synthase. This work shows that the sRNA rnTrpL can base-pair with *trpD* and the reporter gene assay shows that complementarity between rnTrpL and *trpD* is necessary for down-regulation of *trpDC* (Figure 2.1.4G and Figure 2.1.5C). This downregulation is based on mRNA destabilization (156). However, overexpression of rnTrpL does not affect *trpFBA* and the regulation of this operon according to trp availability is not clear (156).

In Gram-negative bacteria, to understand the mechanism of sRNA-mediated mRNA destabilization, analysis the role of an endoribonucleolytic RNases such as RNase III or RNase E is necessary. In a previous work, it was demonstrated that RNase E specifically cleaves in the 5′-UTR of *sinI* mRNA, which base-pairs with rnTrpL in an Hfq-independent manner (61,151). Based on the data in Figure 2.1.11, RNase E participates in degradation of *trpDC*, *rplUrpmA* and *smeR* mRNAs. However, according to Figure 2.1.11, RNase III also exerts a significant role in downregulation of *trpDC* and *rplUrpmA*, while this RNase is not

needed for *smeR* mRNA downregulation. One possible explanation of these results is that both RNases are needed for the function of rnTrpL on its targets but not for the rnTrpL-independent function of the peptide. Indeed, *trpDC* and *rplUrpmA* mRNA base-pair with the rnTrpL sRNA, while *smeR* mRNA is not targeted by rnTrpL but only by the peTrpL peptide (see discussion below). Indeed, *smeR* mRNA was discovered as a peTrpL target by CoIP (155). RNase III specifically cleaves double-stranded RNA. Since the antisense RNA as-*smeR* seems to participate in the peTrpL-dependent downregulation of *smeR*, it is difficult to understand while RNase E but not RNase III participate in this regulation. According to the data in Figure 2.1.5, sRNA rnTrpL binds to target mRNAs by imperfect complementarity like shown for *trpD*(161). This suggests that an RNA chaperone such as Hfq (61,107) or ProQ (162) should mediate rnTrpL interaction with mRNA targets. However, *S. meliloti* does not own a ProQ homolog and rnTrpL is an Hfq-independent sRNA (151,163). While the peTrpL peptide and antibiotic such as Tc may exert a role replacing a chaperone, which serves to mediate the interaction between *rplUrpmA* and rnTrpL, it is not clear whether the interaction between *trpDC* mRNA and rnTrpL needs a chaperone.

As mentioned above, the *trp* genes of *S. meliloti* are organized in three operons *trpE(G)*, *trpDC*, and *trpFBA*. However, only *trpE(G*) operons is regulated by attenuation in the 5′-UTR (133,150). Based on the *trp* genes organization, several bacterial groups are known. The one operon model is present in *Escherichia*, *Salmonella*, *Vibrio* and most members of *Bacillales* and *Lactobacillales*, while Alpha- Beta- Gamma-, Delta- and Epsilon-Proteobacteria, *Spirochaeta* and most *Actinobacteriadae* harbor serveral operons (133). The several *trp* operons in bacteria are considered that allow for more flexibility and a complex strategy in regulation of expression, because precursors or products of different *trp* operons are used in different metabolic pathways (133). For now, transcription attenuation in *cis* was found only upstream of one operon, normally that starting with *trpE* (133). This work highlights the mechanism of a novel stategy for regulation of another *trp* operon (*trpDC*) by a sRNA which originates from the *trpE(G)* transcription attentuation and acts by base-pairing in *trans*. Thus, the rnTrpL RNA sequence acts by two different mechanisms, as a transcription attenuator to regulate *trpE(G)* in *cis* and as a sRNA to destabilize *trpDC* in *trans*.

CoIP data showed that the *smeR* and *rplUrpmA* mRNA directly interact with the peptide peTrpL (155). While *rplUrpmA* mRNA was predicted to base-pair with the sRNA rnTrpL, *smeR* mRNA was not. Here, a decrease in the level of *rplUrpmA* mRNA was shown when sRNA rnTrpL and peptide peTrpL were overproduced for 10 min in the presence of Tc (Figure 2.1.4H). However, no significant decrease was observed when only peptide peTrpL was produced in a *ΔtrpL* background (Figure 2.1.6B), in line with the finding that both the sRNA and the peptide are needed for *rplUrpmA* downregulation. In contrast, *smeR* is targeted by the peptide only. Indeed, Figure 2.1.6B shows that upon overexpression of the peptide peTrpL in *ΔtrpL* background, *smeR* mRNA amount in the cell is decreased under Tc stress. SmeR is the repressor of SmeAB MDR efflux pump genes which is important to *S. meliloti* resistance agianst Tc and other antibiotics.

For *rplUrpmA* downregulation by rnTrpL, peTrpL and an antibiotic such as Tc is needed. A new posttranscriptional strategy may be indicated by the antibiotic mediated

downregulation of *rplUrpmA* which is used to modulate the production and/or function(s) of the protein biosynthesis machinery. The *rplUrpmA* mRNA level change in the cell may affect the level of L21 and L27 proteins an may lead to biogenesis of ribosmes with alternative composition. Even though we don′t know the role of L21, *E. coli* L27-deficient mutants were identified to have downregulated peptidyl transferase activities (164). Interestingly, in *Pseudomonas aeruginosa*, an upreuglated expression of multidrug efflux pump genes and enhanced resistance to aminoglycosides is caused finally by decreasing *rplUrpmA* mRNA level. This was explained by attenuation of transcription termination, due to pausing of L21- and L27-less ribosomes (165). It is reasonable to propose that destabilization of *rplUrpmA* mRNA by rnTrpL may serve similar adaptation mediated by specific changes in translation.

peTrpL is known to be the leader peptide of the Trp biosynthesis gene *trpE(G)*. Similar to the *leu* operon in *Salmonella typhimurium*, and different from the *trp* operon in *E. coli* and *Salmonella*, the *trpE(G)* expression in *S. meliloti* during growth is exclusively regulated by transcription attenuation (132,133,156,166). When sufficient Trp is supplied, termination of transcription between *trpL* and *trpE(G)* occur (133,150,156), but further peTrpL production is potentialy guaranteed by the *trpL* ORF–harboring sRNA rnTrpL. Probably, the Trp-independent transcription of rnTrpL enabled the development of Trp-unrelated functions of the peptide peTrpL. Indeed, its functions in *trans* are linked to mechanisms working in response antibiotics.

The results shown in Figure 2.1.6B, Figure 2.1.8D-F, and Figure 2.1.9A-I suggest that the mechanism of *smeR* mRNA degradation is based on its base-pairing with the anti-sense *smeR* mRNA, which is induced by Tc or other substrates that are pumped out by the SmeAB MDR efflux pump. This degradation is mediated by peTrpL and the respective antibiotic by a novel mechnanism (155,156). This work shows that *smeR*, which encodes the repressor of *smeAB* (127), is cotranscribed with *smeB*. Thus, upon antibiotic exposure, the *smeABR* genes are cotranscribed. However, uncoupling of *smeAB* and *smeR* expression after exposure to antibiotics is obviously needed. Downregulation of *smeR* at the posttranscriptional level supports *smeAB* expression, antibiotic efflux and thus antibiotic resistance. The downregulation probably depends on the asRNA induced by the same antibiotics. Interestingly, the increase in the level of as-*smeR* RNA upon antibiotic exposure was hard to test (155), but was easily detected when a transcription reporter mRNA was used (this work). The asRNA induction was transient (Figure 2.1.9G, Figure 2.1.9H, Figure 2.1.9I). Furthermore, parallel decrease and increase of the mRNA and the asRNA were observed upon overproduction of wild type and mutated peptides (Figure 2.1.8D-F), suggesting co-degradation of both RNAs. Probably, this differential, posttranscriptional regulation of *smeABR* is aiming to suppress the SmeR synthesis by concomitant SmeAB production. The results suggest a model of peTrpL-dependent *smeABR* regulation: exposure to SmeAB substrates can successfully induce the transcription of *smeABR* and as-*smeR* RNA. In the tricistronic *smeABR* mRNA, the as-*smeR* RNA forms a duplex with the *smeR* transcript and the duplex is degraded with the help of the peptide peTrpL and Tc or another SmeAB substrate (127,155).

Interestingly, in rich medium (under Trp-rich conditions; Figure 2.1.4H) sRNA rnTrpL does not control *rpoE1* mRNA, which is a predicted target of rnTrpL. However, regulation occurred in minimal GMX medium (Figure 2.1.12D, Figure 2.1.12F). The *rpoE1* gene encodes an extracytoplasmic function (ECF) sigma factor. The role of ECF factors is to control gene expression for responding to physical, chemical or biological stress conditions (167). Most ECF sigma factors have their own specific anti-sigma factor to control their activity. Bacteria with a strong ability to deal with different kinds of environmental stressors harbor genes for many ECF sigma factors (168,169).

While RpoE2 was described as the major ECF sigma factor in *S. meliloti* which is activated by various stresses, including heat, salt and stationary phase (170-172), little is known about the function of RpoE1. This work figured out that the level of *rpoE1* mRNA decreases when the cells are transferred from high-Trp conditions to low-Trp conditions (Figure 2.1.12F left panel). And in contrast, *rpoE1* mRNA level increses when the conditions are changed from low-Trp to high-Trp (Figure 2.1.12F right panel). The observation that the *rpoE1* mRNA level was decreased upon overproduction of the sRNA rnTrpL under low-Trp conditions, while under high-Trp conditions no change was observed, it puzzling. One possible explanation is that *rpoE1* mRNA is regulated by the sRNA only under low-Trp condtions (Figure 2.1.12D). However, under these conditions *trpLE(G)* are cotranscribed and almost no sRNA is present in the cell. Most probably, the physiological conditions under which *rpoE1* mRNA is regulated by rnTrpL still remain to be uncovered. The observation that the results of Figure 2.1.12F do not fit to the results of Figure 2.1.12D suggests that lacZ'-rnTrpL, which was used in Figure 2.1.12D, is not well suited for this analysis. Thus, in future, the *ΔtrpC* mutation should be introduced in *ΔsinRI* background, and the effect of native 5'-end sRNA on *rpoE1*should be tested.

3.2 sRNA rnTrpL of *E.coli*

As mentioned above, *S. meliloti* has three *trp* operons, only *trpE(G)* is regulated by transcription attenuation, and the arising sRNA rnTrpL has antibiotic-independent and antibiotic-dependent targets. Thus the question arises whether in *E. coli* having one *trp* operon, the homologous sRNA is functional in a similar manner.

This work provides evidence for functions in *trans* of the sRNA Ec-rnTrpL, which arises by transcription attenuation of the *E. coli trp* operon. The bioinformatic prediction showed that this sRNA has the capacity to base pair with multiple mRNAs, and Figure 2.2.1D shows that the levels of several predicted targets was changed after sRNA oberproduction. The results from the validation experiments strongly suggested that *dnaA* mRNA is a direct, Tc-independent target of this sRNA: the *dnaA* mRNA level was decreased upon sRNA overproduction independently of the Tc presence and was increased in the *ΔtrpL* deletion mutant (Figure 2.2.4 and Figure 2.2.8C). Interestingly, the results of this work suggest that *rsuA* mRNA, which is co-transcribed with *bcr*, is directly regulated by the sRNA Ec-rnTrpL, and this regulation is Tc-dependent. Indeed, only under Tc exposure, the levels of *rsuAbcr* mRNA were increased in the *ΔtrpL* deletion mutant (compare Figure 2.2.8.C and Figure 2.2.8.D). Base-pairing *in vivo* was demonstrated by using *egfp* reporter fusion constructs showing that sRNA Ec-rnTrpL negatively affects the expression of both *dnaA* and *rsuAbcr*

(Figure 2.2.4 and Figure 2.2.5). Furthermore, the observation that the levels of *sanA* and *mhpC* mRNA were inversely affected in the overproducing and deletion mutant strains (Figure 2.2.1. and Figure 2.2.8) suggests that Ec-rnTrpL binds to the predicted interaction regions in *sanA* and *mhpB* mRNA and regulates the expression of the corresponding genes and operons in a negative and a positive way, respectively. In future, it will be interesting to test additional predicted targets and investigate whether they directly bind to Ec-rnTrpL.

It should be noted that the predicted base pairing of the sRNA with each of the five top predicted targets overlaps with the *trpL* ORF. The functionally important Trp codons UGGUGG of the *trpL* ORF are predicted to be involved in the base pairing of Ec-rnTrpL with *dnaA* and *rsuA* mRNAs (Figure 2.2.4A, Figure 2.2.5A), which were affected to a similar extent in the deletion mutant (Figure 2.2.8C Figure 2.2.8D). Moreover, the crucial importance of the first tryptophan codon for the *in vivo* interaction between Ec-rnTrpL and *dnaA* mRNA was demonstrated, thus showing that this codon belongs to the sRNA seed region needed for this interaction (Figure 2.2.4A). This is in line with previous observations showing that often highly conserved sRNA parts harbor the seed region (63,75). The *S. meliloti* Trp codons were also predicted to base pair with *trpD* mRNA (Figure 2.1.5A) (156). However, it was not tested whether these codons belong to the sRNA seed region.

Ec-rnTrpL is a homolog of the attenuator sRNA rnTrpL in *Rhizobaiceae* and *Bradyrhizobiaceae* (151,156). In *S. meliloti*, rnTrpL is constitutively transcribed during growth, and its termination is regulated by attenuation (150). The primary function of the rhizobial sRNA seems to be the coordination of the expression of separate *trp* operons. In *E. coli* having the *trp* genes in a single operon, this function is not needed and consequently, overproduction of Ec-rnTrpL has no effect on the expression of *trp* genes (156). Despite these differences, Ec-rnTrpL obviously adopted functions in *trans* during evolution and was integrated into the cellular regulatory networks of *E. coli*. This was probably favored by its Rho-independent terminator, which can serve as an Hfq-binding site, thus making the attenuation-liberated Ec-rnTrpL sRNA a suitable candidate for a riboregulator (173). Indeed, *hfq* was needed for downregulation of both *dnaA* and *rsuA* mRNA upon Ec-rnTrpL overproduction (Figure 2.2.9A), supporting the view that rnTrpL is a Hfq-dependent sRNA. In *E. coli*, RNase E as a single-strand dependent endoribonuclease is responsible for about 60 % of the mRNA decay in the whole transcriptome (15,16), and RNase III as double-strand dependent endoribonuclease participates in about 12 % of mRNA decay (20). This work shows that RNase E but not RNase III is necessary for downregulation *dnaA* by Ec-rnTrpL (Figure 2.2.9B and Figure 2.2.9C). However, neither RNase E nor RNase III were found to be necessary for downregulation of *rsuA* mRNA by Ec-rnTrpL, suggesting that a novel mechanism operates in this antibiotic-dependent regulation.

The pseudouridine synthase RsuA serves to exert the pseudouridylation of 16S rRNA at position 516 (158,159) during 16S rRNA assembly of 30S ribosomal subunits (158). An *rsuA* mutation causes a defect in pseudouridylation at position 516 of the 16S rRNA, and a D102N or D102T mutation at a conserved aspartate was shown to cause a defect in catalytic activity (159). An *rsuA* mutant does not exhibit any obvious growth defect (159). According to the results presented here, the sRNA Ec-rnTrpL regulates *rsuA* mRNA at the posttranscriptional

level, and this regulation probably leads to ribosomes without this pseudouridylation and without an obvious growth defect under standard growth conditions. Since this sRNA regulation is antibiotic-dependent, in future it will be interesting to test whether the absence of this pseudourydilation has an effect on *E. coli* resistance to Tc.

Interestingly, *bcr* is co-transcribed with *rsuA* and encodes a Bcr protein which is a multidrug efflux pump. When the major efflux pump permease AcrB is lacking and *bcr* is present in multiple copies in a K-12 strain (174), a medium resistance to tetracycline, fosfomycin, kanamycin and acriflavine is shown, but the resistance to other types of antibiotics and toxic compounds was not influenced (175). According to this work, downregulation of *rsuAbcr* by Ec-rnTrpL is Tc-dependent (Figure 2.2.6 Figure 2.2.7). However, it is difficult to understand why *bcr* is downregulated by Ec-rnTrpL in the presence of Tc, which is expected to be pumped out by the Bcr multidrug efflux pump if AcrB does not work. One hypothesis to explain this contradiction is that *rsuAbcr* downregulation by Ec-rnTrpL under Tc exposure takes place only if the major efflux pump permease AcrB exist in the cell. In another words, when AcrB is present in the cell, Bcr multidrug efflux pump will not be activated to pump out Tc, and therefore under such conditions Tc contributes to *rsuAbcr* downregulation by the sRNA. Here two strategies or models during downregulation should be considered. The first one is that *rsuAbcr* co-transcript mRNA first interacts with Tc and the complex is detected by the sRNA Ec-rnTrpL for degradation. The second one, based on the sRNA Ec-rnTrpL half-life results (Figure 2.2.2), is that sRNA Ec-rnTrpL maybe first interacts with Tc and then acts to degrade the *rsuAbcr* co-transcript mRNA. This hypothesis should be tested by *in vitro* experiments in the furture.

It is known that overproduction of DnaA stimulates initiation of chromosome replication, but leads to decreased replication speed, and therefore the total DNA amount in the cell is not increased (176). Additionally, it was reported that that up to four-fold overproduction of DnaA increases the origins per mass ratio up to 1.8 –fold (177). The here observed increase in the *oriC* level of approximately 1.5-fold in the *ΔtrpL* deletion mutant supports the view that the posttranscriptional regulation of *dnaA* by sRNA Ec-rnTrpL affects the cellular level of the DnaA protein (Figure 2.2.8E).

As explained in the introduction, the production of Ec-rnTrpL is regulated at the transcriptional and posttranscriptional level by repression and attenuation, respectively (133). Since the transcription initiation of Ec-rnTrpL depends on the cellular Trp level, while its termination and thus the liberation as sRNA on the amount of charged $tRNA^{Trp}$ (132), Ec-rnTrpL may link important cellular processes in response to tryptophan availability. Such a link is plausible, because production of Trp is of very high metabolic energy costs (133). Thus, the cellular level of Trp may serve as a measure of "prosperity" and be used to regulate (via Ec-rnTrpL) *dnaA* expression under different nutritional conditions. In rich medium with high Trp supply, transcription of the sRNA is mostly repressed by the Trp-binding repressor. The results of this work support the view that high Trp concentration in rich medium leads to accumulation of *dnaA* mRNA, higher DnaA production and more frequent initiation of chromosome replication, which is needed for faster growth under these conditions. In minimal medium, however, Ec-rnTrpL transcription is derepressed. Since relieve of transcription

attenuation (co-transcription of *trpLEGDCFBA*) takes place only under severe Trp insufficiency conditions (157), in prototrophic *E. coli* in minimal medium Ec-rnTrpL transcription is regularly terminated and the sRNA accumulates. The increased Ec-rnTrpL production in minimal medium leads to downregulation of *dnaA* expression, which helps to adjust the levels of the DnaA protein to the slower growth rate. In the last consequece, this model suggests that Trp is a signal for regulation of chromosome initiation in *E. coli*. As mentioned above, in rich Trp condition, the Trp-binding repressor will prevent transcription of sRNA Ec-rnTrpL, thus *dnaA* mRNA level and *oriC/terC* ratio will increase. Indeed, Figure 2.2.8F shows that only in the wild type but not in the Δ*trpL* mutant, addition of Trp minimal medium cultures led to increase of the *oriC* level (as normalized to *terC*).

Due to the transcription attenuation (132), in minimal medium oscillation in the Ec-rnTrpL production is expected. On the one hand, since the Trp biosynthesis ensures Trp supply, transcription of the structural genes is mostly attenuated and the Ec-rnTrpL sRNA is liberated. On the other hand, during cellular growth, when the intracellular Trp becomes scarce, attenuation is relieved and Ec-rnTrpL production decreased (*trpL* is cotranscribed with the structural genes). This is counterintuitive in the light of *dnaA* regulation, since it implies an increase in the level of *dnaA* mRNA and thus accumulation of DnaA under conditions of Trp insufficiency. Whether such an oscillation plays a role in DnaA homeostasis in minimal medium (for example, via a negative feedback-loop together with unknown factors (173,178,179), remains to be analyzed. However, since the attenuator regulates the *trp* operon expression 5- to 8-fold, while the transcription repression is capable to regulate it over a 100-fold range (132,157), the production of Ec-rnTrpL is regulated mainly at the transcriptional level, in response to the cellular Trp concentration. Thus, the sRNA Ec-rnTrpL is well suited to regulate *dnaA* expression according to the nutrient availability.

Recently, RNA-based regulation of *dnaA* was described in Alphaproteobacteria. In *S. meliloti*, *dnaA* mRNA is destabilized by the sRNA EspR1, which is induced in a stress- and growth-stage dependent manner (154). In *Caulobacter crescentus*, regulation of translation initiation in response to nutrient availability was shown (180). Furthermore, sRNAs were predicted to regulate *dnaA* in in *C. crescentus* (181). INterestingly, *trans*-translation was described to affect *dnaA* expression in *C. crescentus* and *E. coli* (182). Thus, the here described regulation of *dnaA* by the sRNA Ec-rnTrpL may be only a part of the posttranscriptional mechanisms ensuring the DnaA homeostasis in *E. coli*.

If defined as a sRNA liberated by transcription attenuation upstream of structural Trp biosynthesis genes, rnTrpL homologs are present in a wide range of Gram-negative and Gram-positive bacteria (133,134). This suggests tat rnTrpL could belong to the most conserved base-pairing sRNAs in bacteria. However, due to the different attenuation mechanisms of *trp* operons, which are typically detected in Gram-positive (183,184) and Gram-negative (132,133) bacteria, their attenuator sRNAs candidates differ markedly. Those of Gram-negative bacteria harbor a *trpL* ORF and arise due to ribosome-dependent attenuation. Therefore, they are potential dual-function sRNAs, which in addition to being candidates for base-pairing riboregulators, can also act as small mRNAs (185,186). Indeed, as mentioned above, the *trpL*-encoded leader peptide peTrpL has an independent role in

multiresistance of *S. meliloti* and related Alphaproteobacteria (156). Now, after providing evidence for an own function of Ec-rnTrpL as a riboregulator in this work, it is tempting to speculate that the corresponding Ec-peTrpL peptide is also functional.

In summary, this work expands the limited knowledge on *trans*-acting sRNAs derived from 5′-UTRs in bacteria. The data suggests that in *S. meliloti*, the sRNA rnTrpL, the cellular level of which is related to tryptophan availability, contributes to degradation of *trpDC* mRNA by base-pairing, and also downregulates *rplUrpmA* and *rpoE1*mRNAs by different mechanisms under different conditions. Furthermore, this work identified the amino acids necessary for functionality of the peptide peTrpL, which is encoded by the sRNA rnTrpL, in downregulation of *rplUrpmA* and *smeR* upon antibiotic exposure. Finally, this work demonstrates that in *E. coli*, the sRNA Ec-rnTrpL accumulates in minimal medium, acts in *trans* at the posttranscriptional level, and has antibiotic-dependent and independent targets similarly to its *S. meliloti* homolog. The existence of Tc-dependent target of Ec-rnTrpl is in line with the presented finding that Tc stress accelerates it degradation, provided the sRNA and the mRNA are co-degraded. The presented data suggest that upon Tc exposure, 16S rRNA pseudourydilation could be decreased, since Ec-rnTrpL decreases the level of *rsuA* mRNA in a Tc-dependent manner. Furthermore, the results show that by responding to Trp availability, the sRNA Ec-rnTrpL contributes to the regulation of chromosome initiation via posttranscriptional regulation of *dnaA*. These results imply that Trp is a signal for regulation of chromosome initiation in *E. coli*, and the data of this work support this suggestion.

4 Methods

4.1 Cultivation of Bacteria

E. coli strains were cultivated in LB or M9 minimal medium supplemented with appropriate antibiotics: Tetracycline (Tc, 20 µg/ml), gentamycin (Gm, 10 µg/ml), ampicillin (200 µg/ml). Liquid cultures of *E. coli* strains were cultivated in 10 ml medium in a 50 ml or 100 ml Erlenmayer flask with shaking at 180 rpm at 37°C from an OD_{600nm} of 0.02 to an OD_{600nm} of 0.3~0.5, and then processed further. TY was used as growth medium for prototrophic *S. meliloti* strains (151). Auxotrophic *S. meliloti* 2011*ΔtrpC* strains were grown in minimal GMX medium (187) supplemented with L-tryptophan (Trp). Liquid cultures of *S. meliloti* strains were cultivated semiaerobically (30 ml medium in a 50 ml Erlenmayer flask with shaking at 140 rpm.) at 32°C to an OD_{600nm} of 0.5, and then processed further. Antibiotics in selective plates or liquid media for Alphaproteobacteria were used at the following concentrations, unless stated otherwise: Tetracycline (20 µg/ml), gentamycin (10 µg/ml in liquid cultures and 20 µg/ml in plates), streptomycin (250 µg/ml), spectinomycin (100 µg/ml). Unless stated otherwise, to both *E. coli* and *S. meliloti* strains IPTG was added to a final concentration of 1 mM. For *S. meliloti* growth experiments in 96-well microtiter plates, 300 µl culture (diluted to an OD_{600nm} of 0.1) per well was used. Plates were incubated on the shaker (140 rpm) at 30 °C for 60 h (till the cultures entered the stationary phase). For *E. coli* growth experiments, cultures in 100 ml medium were incubated in a 500 ml Erlenmayer flasks, diluted to an OD_{600nm} of 0.02 and incubated on the shaker (180 rpm.) at 37 °C from the exponential phase to the stationary phase).

The following subinhibitory concentrations of antibiotics and flavonoids were used: 1.5 µg/ml Tc, 27 µg/ml Em, 9 µg/ml Cl, 45 µg/ml Km, 90 µg/ml Gs, and 45 µg/ml Lt. Other concentrations used are given in the figures and their legends. The time of exposure to antibiotics and flavonoids is indicated in the legends(155).

4.2 Plasmid Construction and Conjugation for *S. meliloti*

Cloning procedures were performed essentially as described (156,188). FastDigest Restriction Endonucleases and Phusion polymerase (Thermo Fischer Scientific) were used routinely for cloning in *E. coli* JM109 or *E. coli* DH5α. When pJet1.2/blunt (CloneJet PCR Cloning Kit, Thermo Fischer Scientific) was used for cloning, the inserts were subcloned into the conjugative plasmids pRK4352, pSRKGm, pSRKTc, or pK18mobsacB. Insert sequences were analyzed by Sanger sequencing with plasmid-specific primers (sequencing service by Microsynth Seqlab, Göttingen, Germany) prior to conjugation into *S. meliloti*. All used plasmids for conjugation in *S. meliloti* are listed in Table 5.5 Strains and Plasmids and all oligonucleotides in Table 5.6 Oligonucleotide. The oligonucleotides were synthesized by Eurofins Genomics, Ebersberg (Germany) and Microsynth, Balgach (Switzerland).

Plasmids pSRKTc-rnTrpL and pSRKGm-rnTrpL for IPTG-inducible transcription of lacZ′-rnTrpL were constructed as follows. Primers RcsR1_ ATG_NdeI_fw and RcsR1_SpeI were used to amplify the rnTrpL-sequence. The PCR products were cleaved with NdeI and SpeI, and cloned into pSRKTc or pSRKGm cleaved with the same enzymes, resulting in an

in-frame insertion of the *trpL* sORF to the ATG of NdeI. To construct pSRKTc-rnTrpL-CG40,41GC and pSRKTc-rnTrpL-GG46,47CC, mutated rnTrpL-sequences were amplified with primers RcsR1_ ATG_NdeI_fw and RcsR1_SpeI using as template pDrive-rnTrpL-CG40,42GC and pDrive-RcsR1-GG46,47CC, respectively. The PCR products were cloned into pSRKTc cleaved with NdeI and SpeI.

To construct pSUP-PasRegfp, approximately 200 bp upstream of the putative transcription start site (TSS) of the antisense RNA as-s*meR* was amplified using primers EcoRI-asP-smeR-f and asP-smeR-sSD-rev. The first two nucleotides downstream of the putative TSS were included in the reverse primer, which in addition contained the sequence of a typical bacterial ribosome binding site and the 5′-sequence of *gfp*. The *gfp* sequence of plasmid pLK64 was amplified with primers sSD-egfp-f and PstI-egfp-rev, and the two PCR products were used for overlapping PCR with primers EcoRI-asP-smeR-f and PstI-egfp-rev. The resulting PCR product was cloned into plasmid pSUP202pol4-exoP, which contains 300 nt of the 3′ exoP region as a suitable chromosomal integration site, and was cut with EcoRI and PstI (189). The resulting plasmid pSUP-PasRegfp was used to analyze the antibiotic-induced transcription from a putative antisense promoter located downstream of *smeR*, using the *egfp* mRNA as reporter. Since pSUP-PasRegfp confers Tc resistance, it was necessary to incubate *S. meliloti* strains with chromosomally integrated pSUP-PasRegfp overnight without Tc (essentially all cells retained the plasmid, as revealed by qPCR analysis), before adding Tc again to test for induced promoter activity by qRT-PCR analysis of the reporter *egfp* mRNA.

To construct pSRKGm-trpDC′-egfp, the *trpDC′* sequence was amplified with primers NdeI-trpD-fwd and 5′-egfp-trpC-rev. In parallel, *egfp* was amplified using pLK64 (37) as template and primers trpC-egfp-fwd and XbaI-egfp-rev. The two PCR products were mixed and used for overlap-PCR with the primers NdeI-trpD-fwd and XbaI-egfp-rev. The resulting amplicon was ligated with pJet1.2/blunt, resulting in pJet-trpDC′-egfp. The insert was subcloned into pSRKGm using NdeI and XbaI. The resulting plasmid pSRKGm-trpDC′-egfp allows for IPTG-inducible transcription of a bicistronic *trpDC′::egfp* mRNA encoding TrpD and the fusion protein TrpC′-EGFP. The fusion construct contains the first 16 *trpC* codons fused in frame to the third codon of *egfp*. To introduce compensatory mutations into the *trpDC′::egfp* reporter, pJet-trpDC′-egfp was subjected to site-directed mutagenesis. Primers trpD-CG985GC-FW and trpD-CG985GC-RV were used for the compensatory mutation that restores the interaction with rnTrpL-CG40,41GC. Similarly, primers trpD-CC978GG-FW and trpD-CC978GG-RV were used to restore the interaction with rnTrpL-GG46,47CC. The mutated inserts were subcloned into pSRKGm using NdeI and XbaI, resulting in pSRKGm-trpD-CG985,986GC-trpC′-egfp and pSRKGm-trpD-CC977,978GG-trpC′-egfp. Transconjugants containing one of the pSRK-plasmids were stored at -80°C. Double transconjugants (containing pSRK-plasmids with different antibiotic resistance genes) were used directly after the transfer of the second plasmid to *S. meliloti*.

To construct plasmid pK18mobsacB-ΔtrpL for marker-less deletion of the rnTrpL-sequence in the chromosome of *S. meliloti*, a region located upstream of *trpL* in the chromosome was amplified with primers del_RcsR1_up_Fw and del_RcsR1_up_Rv. In parallel, a region downstream of the rnTrpL transcription terminator was amplified with

primers del_RcsR1_dw_Fw and del_RcsR1_dw_Rv. The two PCR products were mixed and overlapping PCR was performed with primers del_RcsR1_up_Fw and del_RcsR1_dw_Rv. The resulting amplicon was cloned into pK18mobsacB, which was cleaved with EcoRI and PstI. Plasmid pK18mobsacB-ΔtrpL was used to delete the chromosomal sequence ranging from the third nucleotide after the rnTrpL transcription start site to the last T in the TTTT stretch of the rnTrpL transcription terminator. Similarly, plasmid pK18mobsacB-ΔtrpC for marker-less in-frame deletion in gene *trpC* was constructed. A region starting upstream of *trpC* was amplified with primers del_trpC_up_Fw and del_trpC_up_Rv. In parallel, the a region downstream of *trpC* was amplified with primers del_trpC_dw_Fw and del_trpC_dw_Rv. The two PCR products were mixed and overlapping PCR was performed with primers del_trpC_up_Fw and del_trpC_dw_Rv. The resulting amplicon was cleaved with EcoRI and PstI and cloned into pK18mobsacB (36). Also, plasmid pK18mobsacB-ΔsinRI for marker-less *sinRI* deletion was constructed. A region starting upstream of *sinRI* was amplified with primers del_tsinRI_up_Fw and del_sinRI_up_Rv. In parallel, a region downstream of *sinRI* was amplified with primers del_sinRI_dw_Fw and del_sinRI_dw_Rv. The two PCR products were mixed and overlapping PCR was performed with primers del_sinRI_up_Fw and del_sinRI_dw_Rv. Plasmid pK18mobsacB-ΔsmeR for marker-less in-frame deletion in gene *smeR* was also constructed. A region starting upstream of *smeR* was amplified with primers del_smeR_up_Fw and del_smeR_up_Rv. In parallel, the a region downstream of *smeR* was amplified with primers del_smeR_dw_Fw and del_smeR_dw_Rv. The two PCR products were mixed and overlapping PCR was performed with primers del_smeR_up_Fw and del_smeR_dw_Rv. The resulting amplicon was cleaved with EcoRI and PstI and cloned into pK18mobsacB. Plasmid pK18mobsacB-ΔexpR for marker-less in-frame deletion in gene *expR* was also constructed. A region starting upstream of *expR* was amplified with primers del_expR_up_Fw and del_expR_up_Rv. In parallel, a region downstream of *smeR* was amplified with primers del_expR_dw_Fw and del_expR_dw_Rv. The two PCR products were mixed and overlapping PCR was performed with primers del_expR_up_Fw and del_expR_dw_Rv. The resulting amplicon was cleaved with EcoRI and PstI and cloned into pK18mobsacB.

Plasmids constructs were transferred to *S. meliloti* by diparental conjugation with *E. coli* S17-1 as the donor. Bacteria were mixed, washed in saline and spotted onto a sterile membrane filter, which was placed onto a TY plate without antibiotics. After incubation for at least 4 h at 30 °C, serial dilutions were plated on TY agar with selective antibiotics.

4.3 Plasmid Construction for Analysis of Ec-rnTrpL in *E. coli* MG1655

Plasmids pRS-P_{trp}-egfp and pRS-P_{trp}rnTrpL-egfp were constructed as follows. First pRS1 plasmid was used to clone a promoterless *egfp* between the XbaI and EcoRI restriction sites. A Shine-Dalgarno (SD) sequence was included in the forward primer(by Robina Scheuer). Then, the *trp* promoter region with the three operators (position – 61 to + 10; +1 is the transcription start site) was amplified and the PCR product was cloned between the NdeI and XbaI restriction sites upstream of SD-*egfp*, resulting in pRS-P_{trp}-egfp. Similarly, the region from position -61 to position + 140, which includes the *trp* promoter and the Ec-rnTrpL

sequence corresponding to the *trp* transcription attenuator, was amplified and cloned upstream of SD-*egfp*, resulting in pRS-P_{trp}rnTrpL-egfp.

Plasmids pSRKTc(Gm)-Ec-rnTrpL for IPTG-inducible transcription of lacZ′-Ec-rnTrpL contain the Ec-rnTrpL sequence from position + 27 to + 140 (+1 is the transcription start site; position +27 correspond to A of the ATG start codon of the *trpL* ORF). The Ec-rnTrpL sequence, which was cloned in plasmid pJet-Ec-rnTrpL, was cleaved out with NdeI and XbaI and inserted into pSRKGm or pSRKTc, which was cleaved by the same restriction endonucleases. To introduce mutations Mutant-1 and Muntant-2 in Ec-rnTrpL, site directed mutagenesis of pJet-Ec-rnTrpL was performed, and the mutated sRNA sequence was re-cloned in pSRKTc.

To construct pSRKGm-dnaA′-egfp, first the *egfp* sequence of plasmid pLK64 was amplified from the third to the stop codon. The forward primer contained a BamHI restriction site and codons for a GGGS linker in frame with EGFP, while the reverse primer contained a Hind III restriction site. The PCR product was cloned between the BamHI and HindIII restriction sites of pSRKGm, resulting in pSRKGm-GGGSegfp. Then the *dnaA* sequence from the first to the 32th codon was amplified with primers containing the NdeI (forward primer) and BamHI (reverse primer) restriction sites and cloned in pJet1.2, resulting in plasmid pJet-dnaA′. The insert was cleaved out using NdeI and BamHI and cloned in frame with *egfp* between the NdeI and BamHI restriction sites of pSRKGm-GGGSegfp. The resulting plasmid pSRKGm-dnaA′-egfp allows for IPTG-inducible transcription of *dnaA′::egfp* mRNA. To introduce compensatory mutation Ec-rnTrpL-Mutant-1, pJet-dnaA′ was subjected to site-directed mutagenesis, and the mutated *dnaA′Mut* sequence was re-cloned in pSRKGm-GGGSegfp, resulting in pSRKGm-dnaA′Mut-egfp. Similarly, pSRKGm-rsuAbcr′-egfp and pSRKGm-rsuA′Mut-egfp were constructed.

4.4 Construction of *S. meliloti* 2011 Deletion Mutants

Clone *trpL*, *sinRI*, *trpC*, *smeR* or *expR* DNA fragment containing the desired deletion into plasmid pK18mobsacB, which cannot be replicated in strain *S. meliloti* 2011. Introduce the pK18mobsacB-Δ*trpL*, -Δ*sinRI*, -Δ*trpC*, -Δ*smeR* plasmids into strain *S. meliloti* 2011 by conjugation. Pick up the transconjugants which are Km resistant. These single crossover clones are restreaked on the TY-Agar (+ 20µg/ml tryptophan for *ΔtrpC*) plate which contains Sm and Km antibiotics. Pick up single colony, resuspend into 100 µl and 1 000 µl 0.9% NaCl solution, and plate each 100 µl solution on 10% sucrose TY-plates (+tryptophan for *ΔtrpC*) which only contain Sm antibiotic. Culture the cells for 2-3 days. The growing colonies are double crossover clones selected for surose resistance (clones that have lost the plasmid). Pick up a double crossover colony and resuspend into 50 µl 0.9% NaCl solution. Drop 2 µl of the suspension on the TY-plates (+tryptophan for *ΔtrpC*) with Sm antibiotic, and in parallel on TY-plates (+tryptophan for *ΔtrpC*) with Sm and Km antibiotics. Clones that have lost the plasmid (double cross over strains) can only can gowth on plates with Sm antibiotic but whithout Km. Such clones are either deletion mutant or wild type strains. Perform colony PCR to distinguish deletion mutants from wild type clones.

4.5 Preparation and Transformation of $CaCl_2$-Competent *E. coli* MG1655 Cells for Plasmid Transformation

Dilute overnight culture 1:100 (inoculate 10 ml LB with 100 µl of overnight culture). Incubation and shaking at 180 rpm and 37°C for 90 min. Culture was filled into a tube and pelleted by centrifugation at 6 000 g at 4 °C for 2 min. Resuspend cell pellet in 2 ml ice-cold 0.1 M $CaCl_2$ and incubation on ice for 30 min. Centrifugation at 13 000 rpm and 4°C for 1 min. Resuspend in 600 µl 0.1 M $CaCl_2$ and incubate on ice for 2 h. Add 100 µl of competent cells to 10-100 ng DNA. Incubate on ice for 30 min. Subject to a heat shock at 42°C for 1 min. Put on ice for 1 min. Add 1 ml LB (pre-warmed). Culture cells at 37°C for 1 h. Spread 100 µl or the complete sample on selective medium.

4.6 Construction of *E. coli* MG1655 Deletion Mutants

Use standard primers to amplify resistance cassette for knockout. The PCR product is transformed in lambda-red competent cells and integrates in the chromosmome by homologous recombination. For this, add chromosome homology sequences to your primers (at the 5′ end). The homology region should be at least 40 bp. It remains in the final construct, everything in between gets deleted or replaced by the *scar* sequence, depending on the chosen method.

Preparation of Lambda-red Competent Cells for Electroporation of a PCR Product

Grow overnight culture of the receiving strain containing the pSim-5-tet plasmid at 30℃ in LB with Tc (6 µg/ml) for selection. Dilute overnight culture 1:100 in 20 ml fresh LB (100 ml flask) with Tc (6µg/ml) for selection, and grow at 180 rpm and 30 ℃ till OD_{600nm} 0.4. Start shaking water bath at 42 ℃. Switch culture to 42 ℃ at 180 rpm for 15 min. Cool immediately in ice-slurry. Rotate the flask so the whole culture is cooled down quickly. Spin down 4 200 rpm at 4℃ for 10min. Pour off supernatant. Wash 3x times with 20ml ice cold 10% glycerol. Keep cells on ice/ at 4℃, use pre-cooled piptettes etc if possible. Resuspend cells in 400 µl ice cold 10% glycerol. Mix cells and PCR product and electroporate; 40 µl cells are used with 250-500 ng PCR product (deletion construct with antibiotic cassette); max 3 µl PCR product should be used. Electroporate with standard settings for *E. coli* (Ec2: 2.5 kv 4 msec). Immeditately add 1ml of pre-warmed LB and let cells recover for 1.5 hours at 30℃ in electroporation cuvettes. Transfer cell suspension to Eppenddorf tube and centrifuge at 10 000 rpm at room temperature for 2 min. Pour off supernatant and resuspend pellet in remaining LB (about 100 µl). Plate everything on selective plates and 50 µl electrocompentent cells as negative control also on selective plates (LB + 12.5 µg/ml Cm). Incubate plates over night at 30 ℃. Restreak colonies on selective plates (LB + Cm) and incubate overnight at 30℃. Screen colonies with PCR. Restreak selected colonies 2-times on selective plates (LB + Cm) and incubate overnight at 42 ℃ to lose pSim5 –tet plasmid present in the used strain. Re-streak again on new plate and Tc plate to check for pSim5-tet loss.

PCR Mixture

HF Buffer	10 µl
dNTP(10mM)	1 µl
KOprimers(1µM)	2.5 µl

sYFP2-cat template	2 µl
Phusion DNA Polymerase	0.5 µl
H_2O	31.5 µl

PCR program

1. 98℃ (30 s)
2. 98℃ (10 s)
3. 53℃ (10 s)
4. 72℃ (2 min)
5. repeat 2-4 steps for 34 cycles
6. 72℃ (10 min)

Removal of Cm Selection Marker

Pre-culture a Cm-deletion mutation strain in 10 ml LB +10 µl Cm（15 µg/ml）at 30 ℃ overnight. Transform the cells with 709-FLPe plasmid: Dilute the pre-culture to OD 0.04 in fresh 10 ml LB medium , then shake at 180 rpm and 30℃ for 150 min to OD 0.5. Transfer cells to 50 ml tubes. Incubate for 10 min on ice. Centrifuge at 3 000 rpm and 4℃ for 15 min. Resuspend in 3 ml CCMB) (cold) medium (provided by Susanne Barth-Weber) to prepare chemically competent cells. Incubate for 10 min on ice immediately. Transfer to 2ml Eppis (1.5 ml suspension per Eppi), centrifuge at 3 000 rpm and 4℃ for 15 min. Resuspend and pool in 800 µl CCMB (cold). Transfer 150 µl competent cells to a new tube and add 150 ng/µl 709-FLPe plasmid 2 µl. Incubate for 10 min on ice. Perform heat shock at 42℃ for 1 min and immediately put on ice 2 min. Add 1ml LB medium. Incubate at 180 rpm and 30℃ for 100 min. Plate on LB agar plate with 50 µg/ml Amp. Incubate at 30℃ overnight. Pick 3 colonies into 5 ml LB medium. Incubate at 180 rpm and 30℃ for 2.5 hours. Change to 37℃ condition incubation at180 rpm for 2.5 hours until OD=3. Dilute the culture to 10^{-6} and 10^{-7} and plate 100 µl on only LB agar plate (without antibiotics). Incubate at 37℃ overnight. Re-streak 36 colonies each on only LB plates and LB-Amp-Cm (15 µg/ml) plates. Incubate at 37℃ overnight. Only Cm sensitive clonies can grow on LB only plates but not on plates with Cm. Screen candicate colonies by PCR test.

The procedure describe above was applied to construct the *E. coli* MG1655 *ΔtrpL* mutant. The *E. coli* MG1655 *Δhfq* mutant used in this work was constructed by Daniel Edelman. In this mutant, the *hfq* gene was replaced by the chloramphenicol cassette. Furthermore, *E. coli rnc* and *rne* mutants were used. The mutants and their respective parental strains were described previously (190).

4.7 Isolation of Total DNA

1.5 ml *S. melililoti* culture in stationary phase was filled into tubes and cells were harvested by centrifugation at 6 000 g and 4 °C for 10 min. The pellet was resuspended in 350 µl TEN-buffer and then centrifugation was conducted at 6 000rpm and 4℃ for 10 min. The following steps were performed: Discard supernatant. Resuspend pellet in 350 µl TENS-buffer. Add 35 µl 10% SDS, 20 µl proteinase K (20 µg/ul , -20℃) and incubate in 37℃ for 2-4 hours. Add 500 ul phenol/chloroform/isoamylalkohol (25:24:1) (volume 1:1). Vortex 30s or shake sufficiently, centrifuge at 13 000 rpm and room temperature for 10 min. Transfer upper

phase to a new Eppi tube. Repeat phenol/chloroform/isoamylalkohol purification steps again. Add chloroform/ isoamylalkohol(24:1) (volume 1:1). Vortex 30 s or shake sufficiently. Centrifuge at 13 000 rpm and room temperature for 5 min. Transfer upper phase to a new Eppi tube. Add 0.1 fold volume 3M sodium acetate pH 5.2, and 2.5 fold volume 96% Ethanol which was kept at -20℃. Shake until DNA precipitate appears. Centrifuge at 13000 and room temperature for 5 min. Discard supernantant. Wash pellet in 1ml 75% Ethanol kept at -20℃. Centrifuge at 13 000 rpm and room temperature for 5min. Discard supernatant. Dry the pellet under the hood. Dissolve the DNA in 100 µl TE buffer. DNA store at 4℃ for long time. DNA concentration and purity was analyzed by measuring absorbance at 260 nm and 280 nm. 1% argrose gels were used to control the integrity of the isolated DNA.

4.8 Plasmid Isolation by Mini-prep

1.5 ml *E. coli* DH5α or JM109 culture in stationary phase was filled into tubes and cells were harvested by centrifugation at 6 000 g and room temperature for 5 min. The pellet was resuspended in 250 µl Solution P1. Add 250 µI Solution P2. Slowly shake tubes 3 times by hand. Incubate at room temperature for 5 min. Add 250 µl solution P3. Mix well by hand. Centrifuge at 13000 rpm and room temperature for 15 min. Transfer supernantant to a new Eppi tube. Centrifuge once again 13 000 rpm at room temperature for 10 min. Transfer supernantant into a new tube with 400 µl isopropanol. Vortex 30s or shake sufficiently. Centrifuge at 13 000 rpm and room temperature for 15 min. Discard supernantant, wash pellet in 1 ml 70% Ethanol at room temperature. Centrifugation at 13 000 rpm and room temperature for 1min. Discard supernatant. Dry the pellet under the hood, dissolve the plamsid DNA in 30 µl ultrapure water. Plasmid DNA is stored at -20℃. Plasmid DNA concentration and purity was analyzed by measuring absorbance at 260 nm and 280 nm. 1% argrose gels were used to control the integrity of the isolated plasmid DNA.

4.9 RNA Purification

15 ml *S. melililoti* culture (OD_{600} = 0.5) or 10 ml *E. coli* MG1655(OD_{600} = 0.3) culture was filled into tubes with ice rocks (corresponding to a volume of 15 ml) and pelleted by centrifugation at 6 000 g for 10 min at 4 ℃. The pellet was resuspended in 500 µl TRIzol, only for *E. coli* MG1655 M9 culture, 1 µl (1 ng/ µl) spike in RNA [*in vitro* transcript provided by Robina Scheuer] of *S. solfatraicus* gene *rrp41* was added to the sample at this step. And incubated at 65 ℃ for 10 min. Then additional 500 µl TRIzol were added to the samples and folowing steps were performed: Mix by vortexing.Stand still and incubate for 15 min at room temperature. Centrifugation the glass beads down at 13 000 rpm and room temperature for 5 sec. Transfer the supernatant (pink) into a tube with 200 µl chloroform. Mix the supernatant and the chloroform thoroughly about 2 min. Incubate the mixture for 3 min at room temperature. Centrifuge at 10 000 rpm and 4℃ for 20 min to separate the organic (pink) and water (RNA-containing) fraction. Put the probes back on ice. Transfer the upper (clear) phase to a tube with 500 µl isopropanol. Mix by vortexing. Centrifuge at 10 000 rpm and 4℃ for at least 30 min. Discard the supernatant; RNA is distributed at the tube wall. Wash the RNA with 1 ml 75% Ethanol (cold, -20℃). Centrifuge at 10 000 rpm andt 4℃ for 5 min. Remove and discard the ethanol. Dry shortly the pellet under the hood, dissolve the RNA in 200 µl cold, RNase-rree water. Work fast and keep the samples cold. To remove residual

RNases, add 200 µl hot-phenol, incubate at 65 ℃ for 3-5 min, vortex for 30s or shake sufficiently 3 times. Centrifuge at 10 000 rpm and room temperature for 10 min. Transfer the upper phase to a new tube with 200 µl phenol:chloroform:isoamylalcohol (25:24:1). Mix by vortexing. Centrifuge at 10 000 rpm and room temperature for 10 min. Transfer the upper phase to 200 µl 24:1 chloroform:isoamylalcohol. Centrifuge at 10 000 rpm and room temperature for 10 min. Transfer the upper phase to 2.5 fold volume of 96 % ethanol (cold, -20℃) and 0.1 fold volume 3M sodium acetate to precipitate RNA. Incubate at -20 ℃ overnight. Centrifuge at 10 000 rpm and 4℃ for 20 min. Discard the supernatant. RNA is distributed at the tube wall; wash the RNA with 1 ml 75% ethanol (cold, -20℃). Centrifuge at 10 000 rpm and 4℃ for 5 min. Discard the ethanol. Dry the pellet under the hood, elute the RNA in 30 µl RNase-free water. RNA is stored at -20℃

RNA concentration and purity was analyzed by measuring absorbance at 260 nm and 280 nm. 10% polyacrylamide-urea gels and staining with ethidium bromide were used to control the integrity of the isolated RNA. For qRT-PCR RNA, 10 µg samples were digested with 1 µl TURBO-DNase for 30 minutes to remove remaining DNA. PCR with *rpoB*-specific primers was performed for each sample, to check for residual DNA. The DNA-free RNA was then diluted to a concentration of 20 ng/µl for the qRT-PCR analysis.

4.10 Digestion of Puirfied Insert PCR Product or Plasmid DNA with Two Restriction Enzymes

Double digestion was performed according to the Thermofisher Fastdigest Restriction Enzyme kit protocol for plasmid and PCR product. 1% argrose gels were used to control the integrity of the two enzymes digestion of plasmid DNA, however, digested PCR product can not be check by gel test.

4.11 Purification and Ligation of Double Digested Insert PCR Product and Plasmid

E.Z.N.A. DNA Probe Purification Kit and E.Z.N.A. Gel Extraction Kit were used to purifiy the digested PCR product and plasmid. The following steps were performed: Mix 200 ng vector and 100 ng insert DNA with ddH_2O to a final volime of 30 µl. To each mixture, and 3.5 µl ligase buffer (10x) and 1.5 µl T4 DNA ligase.Incubate at 16 ℃ for overnight or at room temperature for 2 h.

4.12 Northern Blot Hybridization

Total RNA (10 µg) was denatured in urea-formamide containing loading buffer at 65 °C. Samples were placed on ice and loaded on 1 mm thick, 20 x 20 cm, 10% polyacrylamide-urea gel. Separation by electrophoresis in TBE buffer was performed at 300 V for 4 h. The RNA was transferred to a positively charged nylon membrane for 2 h at 100 mA using a Semi-Dry Blotter. RNA was crosslinking the to the membrane by UV light. The membrane was pre-hybridized for 2 h at 56 °C with a buffer containing 6× SSC, 2.5× Denhardts solution, 1% SDS and 10 µg/ml Salmon Sperm DNA. Hybridization was performed with radioactively labeled oligonucleotides (see Table 5.5 Oligonucleotides) in a solution containing 6× SSC, 1% SDS, 10 µg/ml salmon sperm DNA for at least 6 h at 56 °C. The membranes were washed twice for 2 to 5 min in 0.01% SDS, 5× SSC at room temperature. Signal detection was performed with a BioRad molecular imager and the Quantity One (BioRad) software. For

quantification, the intensity of the sRNA bands was normalized to the intensity of the 5S rRNA. For re-hybridization, membranes were stripped for 20 min at 96 °C in 0.1% SDS.

4.13 Radioactive Labeling of Oligonucleotide Probes

5′-labeling of 10 pmol oligonucleotide was performed with 5 U T4 polynucleotide kinase (PNK) and 15 µCi [γ-^{32}P]-ATP in a 10 µl reaction mixture containing buffer A provided by the manufacturer. The reaction mixture was incubated for 60 min at 37 °C. 30 µl water was added. Unincorporated nucleotides were removed using MicroSpin G-25 columns.

4.14 Quantitative RT-PCR (qRT-PCR)

For analysis of relative steady state levels of RNAs by one step real time RT-PCR (qRT-PCR) or Strand specific qRT-PCR, the Brilliant III Ultra Fast SYBR® Green QRT-PCR Mastermix (Agilent) was used. Each 10 µl reaction mixture contained 5 µl Master Mix (supplied), 0.1 µl DTT (100 mM; supplied), 0.5 µl RT/RNase Block solution (supplied), 0.4 µl water, 1 µl of each primer (10 pmol/µl)(Table Oligonucleotide), and 2 µl RNA (20 ng/µl). Rountly ,first only the primer needed for cDNA synthesis was added to the reaction mixture. After cDNA synthesis and incubation for 10 min at 96 °C to inactivate the reverse transcriptase, the probes were cooled to 4 °C, the second primer was added, and PCR was performed starting with 5 min incubation at 96 °C. For one-step qRT-PCR, both primers were added simultaneously, before the cDNA synthesis step. Used primer pairs and their efficiencies (as determined by PCR using serial two-fold dilutions of RNA) are listed in Table Oligonucleotide. The qRT-PCR reaction was performed in a spectrofluorometric thermal cycler (Biorad). The quantification cycle (Cq), was set to a cycle at which the curvature of the amplification is maximal. As a reference gene for determination of steady-state mRNA levels, *rpoB* (encodes the β subunit of RNA polymerase) was used (Baumgardt et al., 2016). Cq-values of genes of interest and the reference gene were used in the Pfaffl-formula to calculate fold changes of mRNA amounts by Pfaffl method.

Two-step qRT-PCR Mixture

RNase free water	0.4 µl
MasterMix	4 µl
First primer	1 µl
DTT	0.1 µl
RNase block	0.5 µl
RNA	2 µl(20 ng/µl)

Two-step qRT-PCR Protocol

Incubate the above mixture at 50℃ (10 min). Inactivate the reverse transcriptase at 95℃(3 min). Add the second primer (1 µl) and perform the following PCR program:

1. 94℃ (3 s)
2. 56℃ (5 s)
3. 60℃ (5 s)
4. repeat steps 4-6 for 39 cycles

5. 95℃ (10 s)
6. Melt Curve 65℃ to 95℃, increment 0.5℃ + Plate Read

One-step qRT-PCR Mixture

RNase free water	0.4 µl
MasterMix	4 µl
Forward primer	1 µl
Reverse primer	1 µl
DTT	0.1 µl
RNase block	0.5 µl
RNA	2 µl (20 ng/µl)

One-step qRT-PCR Program

1. 50℃ (10 min)
2. 95℃ (3 min)
3. 94℃ (3 s)
4. 56℃ (5 s)
5. 60℃ (5 s)
6. repeat steps 3-5 for 39 cycles
7. 95℃ (10 s)
8. Melt Curve 65℃ to 95℃, increment 0.5℃ + Plate Read

4.15 qPCR

To determine plasmid-DNA levels, qPCR with plasmid-specific primers (Table Oligonucleotide) and Power SYBR® PCR Mastermix were performed. The provided PCR master mix included all components necessary for performing real-time PCR except primers, template, and water, which were added as described for qRT-PCR. The qPCR reaction and quantification were performed like described for qRT-PCR analysis of total RNA.

qPCR Mixture

RNase free water	0.4 µl
MasterMix	4 µl
Forward primer	1 µl
Reverse primer	1 µl
DTT	0.1 µl
RNase block	0.5 µl
DNA	2 µl(20 ng/µl)

qPCR Program

1. 95℃(3 min)
2. 94℃ (3 s)
3. 56℃ (5 s)
4. 60℃ (5 s),
5. repeat 3-5 steps 39 cycles

6. 95℃ (10 s)
7. Melt Curve 65℃ to 95℃, increment 0.5℃ + Plate Read

4.16 eGFP Fluorescence Measurement in *S. meliloti*

S. meliloti 2011*ΔtrpL* strains containing two plasmids (pSRKGm- and pSRKTc-constructs for IPTG-induced expression of eGFP reporter fusions and the sRNA, respectively) were used. Cultures were grown in TY with Gm and Tc to an OD_{600nm} of 0.5. ODs were measured on the spectrometer. The production of an eGFP fusion protein and the regulatory sRNA was induced simultaneously with 1 mM IPTG for 20 min. 300 µl of the cultures were transferred to a 96-well microtiter plate. eGFP fluorescence was measured on a Tecan Infinite M200 reader. OD vaues measured on the Tecan were used for normalization.

4.17 eGFP Fluorescence Measurement in *E. coli*

E. coli MG1655 strains containing plasmids pRS-PtrpL-sSD-egfp or pRS-PtrpL-rnTrpL-sSD-egfp were used. Strains were cultured in M9 medium to OD_{600nm} 0.5 or stationary phase (OD_{600nm} 1.7). ODs were measured on the spectrometer. Tryptophan was added at the indicated concentrations. 300 µl of the cultures were transferred to a 96-well microtiter plate. eGFP fluorescence was measured on a Tecan Infinite M200 reader, OD measured on the Tecan was used for normalization.

4.18 Analysis of Reporter *egfp* mRNA in *S. meliloti*

S. meliloti 2011*ΔtrpL* (pSUP-PassmeR-egfp) was used. Antibiotics were added. 10 ml of the cultures were transferred to 50 ml with ice rocks, and pelleted by centrifugation at 6,000 g for 10 min at 4 °C. RNA was isolated by TRIzol protocol. *egfp* mRNA level before and after addition of an antibiotic was measured by qRT-PCR.

4.19 Analysis of Reporter *egfp* mRNA in *E. coli*

E. coli MG1655 strains containing pSRKGm- and pSRKTc-constructs for IPTG-induced expression of *egfp* mRNA reporter fusions and the sRNA, respectively), were used. Starins were cultured in LB medium with Gm and Tc to OD_{600nm} 0.5. The production of the *egfp* fusion reporter mRNA and the regulatory sRNA was induced simultaneously with 1 mM IPTG for 3 min. 10 ml of the cultures were transferred to 50 ml tubes filled with ice rocks, and pelleted by centrifugation at 6,000 g for 10 min at 4 °C. RNA was isolated using TRIzol. *egfp* mRNA level was measured by qRT-PCR.

4.20 Determination of the Half-life of sRNA Ec-rnTrpL in *E. coli* MG1655

E. coli MG1655 strain was pre-cultivated in M9 minimal medium at 37℃ overnight. Culture was diluted to $OD_{600\ nm}$ 0.02 and grown to $OD_{600\ nm}$ 0.3 at 37℃, using 100 ml M9 minimal medium in 500 ml Erlenmayer flask. The culture were separated in 10 ml-portions into 50 ml Erlenmayer flasks as fast as possible. To each 10 ml culture 10 µl Tc was added to a final concentration of 1 µg/ml or same volume 70% alcohol was added as a negative control. After 3 min, rifampicin (50 µg/ml) was immediately added to stop transcription. Samples for RNA isolation were withdrawn after incubation at 180 rpm and 37 ℃ for a series of timepoints (0 min, 0.5 min, 1 min, 1.5 min, 2 min, 2.5 min, 3 min, 5 min, 10 min). RNA was isolated as described above. The sRNA level was analyzed by Northern blot hybridization.

sRNA signals were quantified and normalized to internal control signals (5S rRNA). Linear-log graphs were used for half-life calculation.

5 Materials

5.1 Antibiotics

Antibiotics	Concentration (mg/ml)	Dissolved in	*E.coli* (µg/ml)	*E.coli* (ml/ml)	*S.mel* (µg/ml)
Tc	10	75% EtOH	20	0.2	20
Km	10	ddH_2O	25	0.25	200!
Amp	100	ddH_2O	100-200	0.1-0.2	200
Gm	4	ddH_2O	10	0.25	10!!
Sm	100	ddH_2O	100-250	0.1-0.25	250
Sp	10	ddH_2O	10	0.1-1	100
Nm	100	ddH_2O	120	0.12	120
Cap	17	75% EtOH	34	0.2	500
Nal	40	0.2M NaOH	20	0.05	10
Rif	30	MeOH/NaOH	200	0.2	500

! 10 µg/ml in liquid medium, 20 µg/ml in plate

Antibiotics dissolved in ddH_2O were sterilized using 0.22 µm filter.

Antibiotics dissolved in 75% EtOH were not sterilized.

Km,Sp: 300 mg (10 mg/ml*30), in 30 ml ddH_2O

Ap,Sm,Nm: 3 g(100 mg/ml*30), in 30 ml ddH_2O

Gm: 120 mg(4 mg/ml*30), in 30 ml ddH_2O

Tc: 300 mg(10 mg/ml*30), in 30 ml 75% EtOH

Cap: 510 mg(17 mg/ml*30), in 30 ml 75%EtOH

Nal: 1.2 g(40 mg/ml*30), in 30 ml ddH_2O

5.2 For 1 Liter TY Medium and TY Soild Medium:

BactoTrypton	5 g
Heteextract	3 g
$CaCl_2$	0.3 g
Fill up with water to 1 L	
for TY solid medium, add 6 g Bacto-Agar to 400 ml TY medium	
Autoclave for 15 min at 121 ℃	

5.3 For 1 Liter LB medium and LB Soild Medium:

Peptone	10 g
YEASTextract	5 g
NaCl	10 g
Water diltuted to 1 L	
for LB solid medium add 6 g LB-Agar to 400 ml LB-medium	

Autoclave for 15 min at 121 ℃

5.4 For 1 liter M9 mineral medium:

100 ml	M9 salt solution (10X)	Na_2HPO_4	33.7 mM
		KH_2PO_4	22.0 mM
		NaCl	8.55 mM
		NH_4Cl	9.35 mM
20 ml	20% glucose	glucose	0.4 %
1 ml	1 M $MgSO_4$	$MgSO_4$	1 mM
0.3 ml	1 M $CaCl_2$	$CaCl_2$	0.3 mM
1 ml	biotin (1 mg/ml)	biotin	1 µg
1 ml	thiamin (1 mg/ml)	thiamin	1 µg
10 ml	trace elements solution (100X)	trace elements	1X
add to 867 ml sterile water			

Stock Solutions:

M9 salt solution (10X)	Na_2HPO_4-$2H_2O$	75.2 g/L
	KH_2PO_4	30 g/L
	NaCl	5 g/L
	NH_4Cl	5 g/L
For 500 ml stock solution add 100 g glucose to 440 ml water. Autoclave for 15 min at 121°C.		

1 M $MgSO_4$	1 M $MgSO_4$-$7H_2O$	24.65 g/100 ml
For 100 ml stock solution dissolve 24.65 g MgSO4-7H2O in 87 ml water. Autoclave for 15 min at 121°C.		

1 M $CaCl_2$	1 M $CaCl_2$-$2H_2O$	14.70 g/100 ml
For 100 ml stock solution dissolve 14,70 g $CaCl_2$-$2H_2O$ in 94.5 ml water. Autoclave for 15 min at 121°C.		

Biotin (1 mg/ml)	biotin (1mg/ml)	50 mg/50 ml
For 50 ml stock solution dissolve 50 mg biotin in 45 ml water. Add small aliquots of 1N NaOH until the biotin has dissolved. Add water to a final volume of 50 ml. Sterilize the solution over a 0.22-µM filter. Prepare 1 ml aliquots and store at -20°C.		

Thiamin (1 mg/ml)	thiamin-HCl (1mg/ml)	50 mg/50 ml
For 50 ml stock solution dissolve 50 mg thiamin-HCl in 45 ml water. Add water to a final volume of 50 ml. Sterilize the solution over a 0.22-µm filter. Prepare 1 ml aliquots and store at -20°C.		

100X trace elements solution	EDTA	5 g /L	13.4 mM
	$FeCl_3$-$6H_2O$	0.83 g/L	3.1 mM
	$ZnCl_2$	84 mg/L	0.62 mM
	$CuCl_2$-$2H_2O$	13 mg/L	76 μM
	$CoCl_2$-$2H_2O$	10 mg/L	42 μM
	H_3BO_3	10 mg/L	162 μM
	$MnCl_2$-$4H_2O$	1.6 mg/L	8.1 μM
Dissolve 5 g EDTA in 800 ml water and adjust the pH to 7.5 with NaOH. Then add the other components in the quantities mentioned above and add water to a final volume of 1 L. Sterilize the solution over a 0.22-μm filter.			

5.5 Strains and Plasmids

Plasmids present in strains of *E. coli* DH5α or JM109	**Resistance**
pSRKTc	Tc^r
pSRKGm	Gm^r
pk18mobsacB	Km^r
pSUP202poL4-ExoP	Tc^r
pRS1-sSD-egfp	Gm^r
pRK4352	Tc^r
pSRKTc-rnTrpL	Tc^r
pSRKTc-sinRI-rnTrpL	Tc^r
pSRKTc-Ec-rnTrpL	Tc^r
pSRKTc-rnTrpL-CG40,41GC	Tc^r
pSRKTc-rnTrpL-GG46,47CC	Tc^r
pSRKTc-EcrnTrpL-Mutant-1	Tc^r
pSRKTc-EcrnTrpL-Mutant-2	Tc^r
pSRKGm-rnTrpL	Gm^r
pSRKGm-sinRI-rnTrpL	Gm^r
pSRKGm-peTrpL	Gm^r
pSRKGm-EcrnTrpL	Gm^r
pSRKGm-trpDC′-egfp	Gm^r
pSRKGm-trpD-CG985,986GC-trpC′-egfp	Gm^r
pSRKGm-trpD-CC977,978GG-trpC′-egfp	Gm^r
pSRKGm-dnaA′-egfp	Gm^r
pSRKGm-dnaAMUT-egfp	Gm^r
pSRKGm-rsuA′-egfp	Gm^r
pSRKGm-rsuAMUT-egfp	Gm^r
pSRKGm-peTrpL-N3A	Gm^r
pSRKGm-peTrpL-T4A	Gm^r
pSRKGm-peTrpL-Q5A	Gm^r
pSRKGm-peTrpL-N6A	Gm^r
pSRKGm-peTrpL-I7A	Gm^r
pSRKGm-peTrpL-S8A	Gm^r
pSRKGm-peTrpL-I9A	Gm^r
pSRKGm-peTrpL-W10A	Gm^r
pSRKGm-peTrpL-W11A	Gm^r
pSRKGm-peTrpL-W12A	Gm^r
pSRKGm-peTrpL-R14A	Gm^r

pk18mobsacBΔtrpL	Km^r
pk18mobsacBΔtrpC	Km^r
pk18mobsacBΔsmeR	Km^r
pk18mobsacBΔsinR-I	Km^r
pSUP202poL4-PasR-egfp	Tc^r
pBAD-tm-Ec-peTrpL	Amp^r
pRS1-PtrpL-sSD-egfp	Gm^r
pRS1-PtrpL-EctrpL-sSD-egfp	Gm^r
Plasmids present in strains of *E. coli* S17-1	**Resistance**
pSRKTc	Tc^r
pSRKGm	Gm^r
pRK4352	Tc^r
pSRKTc-rnTrpL	Tc^r
pSRKTc-sinRI-rnTrpL	Tc^r
pSRKTc-rnTrpL-CG40,41GC	Tc^r
pSRKTc-rnTrpL-GG46,47CC	Tc^r
pSRKGm-rnTrpL	Gm^r
pSRKGm-sinRI-rnTrpL	Gm^r
pSRKGm-peTrpL	Gm^r
pSRKGm-trpDC′-egfp	Gm^r
pSRKGm-trpD-CG985,986GC-trpC′-egfp	Gm^r
pSRKGm-trpD-CC977,978GG-trpC′-egfp	Gm^r
pSRKGm-peTrpL-N3A	Gm^r
pSRKGm-peTrpL-T4A	Gm^r
pSRKGm-peTrpL-Q5A	Gm^r
pSRKGm-peTrpL-N6A	Gm^r
pSRKGm-peTrpL-I7A	Gm^r
pSRKGm-peTrpL-S8A	Gm^r
pSRKGm-peTrpL-I9A	Gm^r
pSRKGm-peTrpL-W10A	Gm^r
pSRKGm-peTrpL-W11A	Gm^r
pSRKGm-peTrpL-W12A	Gm^r
pSRKGm-peTrpL-R14A	Gm^r
pk18mobsacBΔtrpL	Km^r
pk18mobsacBΔtrpC	Km^r
pk18mobsacBΔsmeR	Km^r
pk18mobsacBΔsinR-I	Km^r
pSUP202poL4-PasR-egfp	Tc^r
***S. meliloti* strains**	**Resistance**
S. meliloti 2011	Sm^r
S. meliloti 2011ΔtrpL	Sm^r
S. meliloti 2011 ΔtrpC	Sm^r
S. meliloti 2011 ΔsmeR	Sm^r
S. meliloti 2011 ΔsinRI	Sm^r
S. meliloti 2011ΔtrpL ΔtrpC	Sm^r
S. meliloti 2011ΔtrpL ΔsmeR	Sm^r
S. meliloti 2011ΔtrpL ΔsinRI	Sm^r
S. meliloti 2011 (pSRKTc-rnTrpL)	Sm^r, Tc^r

S. meliloti 2011 pSRKGm-rnTrpL	Sm^r, Gm^r
S. meliloti 2011ΔtrpL pSRKTc-rnTrpL	Sm^r, Tc^r
S. meliloti 2011ΔtrpL pSRKGm-rnTrpL	Sm^r, Gm^r
S. meliloti 2011ΔtrpL pSRKGm-peTrpL	Sm^r, Gm^r
S. meliloti 2011ΔtrpL pRK4352 pSRKGm-peTrpL	Sm, ^{r} Tc^r,Gm^r
S. meliloti 2011ΔtrpL pRK4352 pSRKGm	Sm^r, Tc^r, Gm^r
S. meliloti 2011 pRK4352 pSRKGm-peTrpL-N3A	Sm^r, Tc^r, Gm^r
S. meliloti 2011 pRK4352 pSRKGm-peTrpL-T4A	Sm^r, Tc^r, Gm^r
S. meliloti 2011 pRK4352 pSRKGm-peTrpL-Q5A	Sm^r, Tc^r, Gm^r
S. meliloti 2011 pRK4352 pSRKGm-peTrpL-N6A	Sm^r, Tc^r, Gm^r
S. meliloti 2011 pRK4352 pSRKGm-peTrpL-I7A	Sm^r, Tc^r, Gm^r
S. meliloti 2011 pRK4352 pSRKGm-peTrpL-S8A	Sm^r, Tc^r, Gm^r
S. meliloti 2011 pRK4352 pSRKGm-peTrpL-I9A	Sm^r, Tc^r, Gm^r
S. meliloti 2011 pRK4352 pSRKGm-peTrpL-W10A	Sm^r, Tc^r, Gm^r
S. meliloti 2011 pRK4352 pSRKGm-peTrpL-W11A	Sm^r, Tc^r, Gm^r
S. meliloti 2011 pRK4352 pSRKGm-peTrpL-W12A	Sm^r, Tc^r, Gm^r
S. meliloti 2011 pRK4352 pSRKGm-peTrpL-R14A	Sm^r, Tc^r, Gm^r
S. meliloti 2011 pSRKGm-peTrpL pSUP202poL4-PasR-egfp	Sm^r, Tc^r, Gm^r
S. meliloti 2011ΔtrpL pSRKTc pSRKGm-trpDC′-egfp	Sm^r, Tc^r, Gm^r
S. meliloti 2011ΔtrpL pSRKTc pSRKGm-trpD-CG985,986GC-trpC′-egfp	Sm^r, Tc^r, Gm^r
S. meliloti 2011ΔtrpL pSRKTc pSRKGm-trpD-CC977,978GG-trpC′-egfp	Sm^r, Tc^r, Gm^r
S. meliloti 2011ΔtrpL pSRKTc-rnTrpL pSRKGm-trpDC′-egfp	Sm^r, Tc^r, Gm^r
S. meliloti 2011ΔtrpL pSRKTc-rnTrpL pSRKGm-trpD-CG985,986GC-trpC′-egfp	Sm^r, Tc^r, Gm^r
S. meliloti 2011ΔtrpL pSRKTc-rnTrpL pSRKGm-trpD-CC977,978GG-trpC′-egfp	Sm^r, Tc^r, Gm^r
S. meliloti 2011ΔtrpL pSRKTc-rnTrpL-CG40,41GC pSRKGm-trpDC′-egfp	Sm^r, Tc^r, Gm^r
S. meliloti 2011ΔtrpL pSRKTc-rnTrpL-CG40,41GC pSRKGm-trpD-CG985,986GC-trpC′-egfp	Sm^r, Tc^r, Gm^r
S. meliloti 2011ΔtrpL pSRKTc-rnTrpL-CG40,41GC pSRKGm-trpD-CC977,978GG-trpC′-egfp	Sm^r, Tc^r, Gm^r
S. meliloti 2011ΔtrpL pSRKTc-rnTrpL-GG46,47CC pSRKGm-trpDC′-egfp	Sm^r, Tc^r, Gm^r
S. meliloti 2011ΔtrpL pSRKTc-rnTrpL-GG46,47CC pSRKGm-trpD-CG985,986GC-trpC′-egfp	Sm^r, Tc^r, Gm^r
S. meliloti 2011ΔtrpL pSRKTc-rnTrpL-GG46,47CC pSRKGm-trpD-CC977,978GG-trpC′-egfp	Sm^r, Tc^r, Gm^r
S. meliloti 2011 ΔtrpL ΔtrpC pSRKGm-rnTrpL	Sm^r, Gm^r
S. meliloti 2011ΔtrpL ΔsinRI pSRKGm-sinRI-rnTrpL	Sm^r, Gm^r
***E. coli* strains**	**Resistance**
E. coli MG1655	None

E. coli MG1655 *ΔtrpL*	None
E. coli MG1655 pSRKTc-Ec-rnTrpL	Tc^r
E. coli MG1655 pSRKGm-Ec-rnTrpL	Gm^r
E. coli MG1655 pSRKTc-Ec-rnTrpL-Mutant-1	Tc^r
E. coli MG1655 pSRKTc-Ec-rnTrpL-Mutant-2	Tc^r
E. coli MG1655 pSRKTc	Tc^r
E. coli MG1655 pSRKTc pSRKGm-dnaA′-egfp	Tc^r
E. coli MG1655 pSRKTc pSRKGm-dnaAMUT′-egfp	Tc^r, Gm^r
E. coli MG1655 pSRKTc-Ec-rnTrpL pSRKGm-dnaA′-egfp	Tc^r, Gm^r
E. coli MG1655 pSRKTc-Ec-rnTrpL pSRKGm-dnaAMUT′-egfp	Tc^r, Gm^r
E. coli MG1655 pSRKTc-Ec-rnTrpL-Mutant-1 pSRKGm-dnaA′-egfp	Tc^r, Gm^r
E. coli MG1655 pSRKTc-Ec-rnTrpL-Mutant-1 pSRKGm-dnaAMUT′-egfp	Tc^r, Gm^r
E. coli MG1655 pSRKTc-Ec-rnTrpL-Mutant-2 pSRKGm-dnaA′-egfp	Tc^r, Gm^r
E. coli MG1655 pSRKTc-Ec-Mutant-2 pSRKGm-dnaAMUT′-egfp	Tc^r, Gm^r
E. coli MG1655 pSRKTc pSRKGm-rsuA′-egfp	Tc^r, Gm^r
E. coli MG1655 pSRKTc pSRKGm-rsuAMUT′-egfp	Tc^r, Gm^r
E. coli MG1655 pSRKTc-Ec-rnTrpL pSRKGm-rsuA′-egfp	Tc^r, Gm^r
E. coli MG1655 pSRKTc-Ec-rnTrpL pSRKGm-rsuAMUT′-egfp	Tc^r, Gm^r
E. coli MG1655 pSRKTc-Ec-rnTrpL-Mutant-1 pSRKGm-rsuA′-egfp	Tc^r, Gm^r
E. coli MG1655 pSRKTc-Ec-rnTrpL-Mutant-1 pSRKGm-rsuAMUT′-egfp	Tc^r, Gm^r
E. coli MG1655 pSRKTc-Ec-rnTrpL-Mutant-2 pSRKGm-rsuA′-egfp	Tc^r, Gm^r
E. coli MG1655 pSRKTc-Ec-Mutant-2 pSRKGm-rsuAMUT′-egfp	Tc^r, Gm^r
E. coli MG1655 pBAD-tm-Ec-peTrpL	Amp^r
E. coli MG1655 pRS1- sSD-egfp	Gm^r
E. coli MG1655 pRS1-PtrpL-sSD-egfp	Gm^r
E. coli MG1655 pRS1-PtrpL-EctrpL-sSD-egfp	Gm^r
E. coli BL322 RNase III^+ pSRKTc-Ec-rnTrpL	Sm^r, Tc^r
E. coli BL321 RNase III^- pSRKTc-Ec-rnTrpL	Sm^r, Tc^r
E. coli N3433 RNase E^+ pSRKTc-Ec-rnTrpL	Tc^r
E. coli N3431 RNase E^- pSRKTc-Ec-rnTrpL	Tc^r
E. coli MG1655 Hfq^+ pSRKTc-Ec-rnTrpL	Tc^r
E. coli MG1655 Hfq^- pSRKTc-Ec-rnTrpL	Tc^r

5.6 Oligonucleotides

Name	Sequence
For work with *S. meliloti* 2011	
RcsR1_ ATG_NdeI_fw	CGCACATATGGCAAACACGCAGAACATTTCG
RcsR1_SpeI	CGCACTAGTAAAAAAGCCGCCTCGAAATCTC
RcsR1-CG40GC-fw2	GTGGGCTGCCTGAGGCGGCCTTGACCAG
RcsR1-CG40GC-re2	GCCTCAGGCAGCCCACCACCAGATCGAA
RcsR1-GG46CC-fwd	GGCTCGCTGACCCGGCCTTGACCAGTCATGCG
RcsR1-GG46CC-rev	GTCAAGGCCGGGTCAGCGAGCCCACCACCAGAT C
Fw_SinR_NdeI	CGCACATATGGCTAATCAACAGGCTGTC
Rv_5′rcsR1_SinI_TSS	CGAAATGTTCTGCGTGTTTGCCATGTAGCGATGC TGTCAGGCTC
Fw_ SinI _ TSS _5′rcsR1	GAGCCTGACAGCATCGCTACATGGCAAACACGC AGAACATTTCG
RcsR1_SpeI_rev	CGCACTAGTAAAAAAGCCGCCTCGAAATCTC
Sm-trpLORF-seNde	TATGGCGAACACCCAGAACATCAGCATTTGGTG GTGGGCCCGGTAGT
Sm-trpLORF-asXba	CTAGACTACCGGGCCCACCACCAAATGCTGATGT TCTGGGTGTTCGCCA
del_RcsR1_up_Fw	AAAGAATTCTCGTGGATATGACCGGGTG
del_RcsR1_up_Rv	GCCGTCGACGGATCCGAGGCAATGGGCGGAAGT GTTAGCGC
del_RcsR1_dw_Fw	TGCCTCGGATCCGTCGACGGCCGCGTGGAAAGA CCGGCTT
del_RcsR1_dw_Rv	AAACTGCAGCAGCGCCAGCAGCACTTCGC
Sm_delta_rcsR1_mut_checkFW	TCCGGCAGAAAGAGAACCAT
Sm_delta_rcsR1_mut_checkRV	GACGCAACGCTTCTGATCAT
delsinRI-up-Fw-Eco	AAAGAATTCGGAATATGGAGGTTGCGCAG
delsinRI-up-Rv	GCCGTCGACGGATCCGAGGCACGACATGTTTG
delsinRI-dw-Fw	TGCCTCGGATCCGTCGACGGCTTCTTTCCCCA
delsinRI-dw-Rv-Pst	AAACTGCAGCTTCTTCTCGCTGCCAATGG
Sm-trpLORF-seNde	TATGGCGAACACCCAGAACATCAGCATTTGGTG GTGGGCCCGGTAGT
Sm-trpLORF-asXba	CTAGACTACCGGGCCCACCACCAAATGCTGATGT TCTGGGTGTTCGCCA
del_trpC_up_Fw	AAAGAATTCGGCACGATCACCAACTTCG
del_trpC_up_Rv	GCCGTCGACGGATCCGAGCAGGCTTCGATGCGG CGCAG
del_trpC_dw_Fw	TGCCTCGGATCCGTCGACGGCGGCTCGGCAAGC ATCATG
del_trpC_dw_Rv	AAACTGCAGCTTCGCCATTGCCTCGACG
Sm_delta_trpC_mut_checkFW	CATCTTCAATCTGCTCGGCC
Sm_delta_trpC_mut_checkRV	CAGTCAACGCCTCCATTTCG
del_smeR_up_Fw	AAAGAATTCATGAGAGCTGGTCCATTCCG
del_smeR_up_Rv	GCCGTCGACGGATCCGAGGCACTCGGCGTCGGC CTTGGT
del_smeR_dw_Fw	TGCCTCGGATCCGTCGACGGCGCACTCCAGTCTC

	TCTTTGC
del_smeR_dw_Rv	AAACTGCAGCCTCAACCGGAAAGCAAGAG
Cheak-ΔsmeR-Fw	ATCCTGATGACCTCGCTCG
Cheak-ΔsmeR-Rv	CCAATTCAACACGATCCGCT
XbaI-egfp-rev	TGCTCTAGATTACTTGTACAGCTCGTCCA
NdeI-trpD-fwd	CGCACATATGAGTGATTTGAAGCCGTTC
5′-egfp-trpC-rev	ACAGCTCCTCGCCCTTGCTGATCTCCTCTCGCTTATAGG
trpC-egfp-fwd	CCTATAAGCGAGAGGAGATCAGCAAGGGCGAGGAGCTGT
trpD-CG-985-GC-FW	CTTGCAGGCGTTGATCACCGTCTCGAAC
trpD-CG-985-GC-RV	GATCAACGCCTGCAAGGCGACCTTGGCG
trpD-CC-978-GG-FW:	AAGGTCGGGTTGCAGCGGTTGATCACCG
trpD-CC-978-GG-RV:	GCTGCAACCCGACCTTGGCGCCGCCGCT
TrpL-N3A-fw	TATGGCGGCCACCCAGAACATCAGCATTTGGTGGTGGGCCCGGTAGT
TrpL-N3A-rv	CTAGACTACCGGGCCCACCACCAAATGCTGATGTTCTGGGTGGCCGCCA
TrpL-T4A-fw	TATGGCGAACGCCCAGAACATCAGCATTTGGTGGTGGGCCCGGTAGT
TrpL-T4A-rv	CTAGACTACCGGGCCCACCACCAAATGCTGATGTTCTGGGCGTTCGCCA
TrpL-Q5A-fw	TATGGCGAACACCGCGAACATCAGCATTTGGTGGTGGGCCCGGTAGT
TrpL-Q5A-rv	CTAGACTACCGGGCCCACCACCAAATGCTGATGTTCGCGGTGTTCGCCA
TrpL-N6A-fw	TATGGCGAACACCCAGGCCATCAGCATTTGGTGGTGGGCCCGGTAGT
TrpL-N6A-rv	CTAGACTACCGGGCCCACCACCAAATGCTGATGGCCTGGGTGTTCGCCA
TrpL-I7A-fw	TATGGCGAACACCCAGAACGCCAGCATTTGGTGGTGGGCCCGGTAGT
TrpL-I7A-rv	CTAGACTACCGGGCCCACCACCAAATGCTGGCGGTTCTGGGTGTTCGCCA
TrpL-S8A-fw	TATGGCGAACACCCAGAACATCGCCATTTGGTGGTGGGCCCGGTAGT
TrpL-S8A-rv	CTAGACTACCGGGCCCACCACCAAATGGCGATGTTCTGGGTGTTCGCCA
TrpL-I9A-fw	TATGGCGAACACCCAGAACATCAGCGCCTGGTGGTGGGCCCGGTAGT
TrpL-I9A-rv	CTAGACTACCGGGCCCACCACCAGGCGCTGATGTTCTGGGTGTTCGCCA
TrpL-W10A-fw	TATGGCGAACACCCAGAACATCAGCATTGCGTGGTGGGCCCGGTAGT
TrpL-W10A-rv	CTAGACTACCGGGCCCACCACGCAATGCTGATGTTCTGGGTGTTCGCCA
TrpL-W11A-fw	TATGGCGAACACCCAGAACATCAGCATTTGGGCGTGGGCCCGGTAGT
TrpL-W11A-rv	CTAGACTACCGGGCCCACGCCCAAATGCTGATGT

	TCTGGGTGTTCGCCA
TrpL-W12A-fw	TATGGCGAACACCCAGAACATCAGCATTTGGTG GGCGGCCCGGTAGT
TrpL-W12A-rv	CTAGACTACCGGGCCGCCCACCAAATGCTGATGT TCTGGGTGTTCGCCA
TrpL-R14A-fw	TATGGCGAACACCCAGAACATCAGCATTTGGTG GTGGGCCGCGTAGT
TrpL-R14A-rv	CTAGACTACGCGGCCCACCACCAAATGCTGATGT TCTGGGTGTTCGCCA
EcoRI-asP-smeR-fw	CGGAATTCGCTCCTGGGCTGCATCTTCTG
asP-smeR-SSD-rev	CTCCTCTTTAATTCCCGCCTCGGCCCTAACTGA
RcsR1-RT-PCR-f	ATGGCAAACACGCAGAACAT
RcsR1-RT-PCR-r	AAAGCCGCCTCGAAATCTCC
sinI -F-qrt	TCAGGATAGTGAACGGAAA
sinI -R-qrt	GTATCGTCCAGCATATTCG
motE -F-qrt	GCGAAATCGAAAAGTTCTG
motE -R-qrt	GCTTAAGCCAGTCCTCGTAT
phoR -F-qrt	GATCGTCAAGCATATCCTCA
phoR -R-qrt	CCGATGGCTACAGCTTTTAT
flgA -F-qrt	TGAGCAAGAACCTGAGGTAA
flgA -R-qrt	CGGGATAGATCGTCTGCT
trpC -F-qrt	CGTCCTCGTCGAAGTACAC
trpC -R-qrt	GGTAATCCCGCTCTTCTCTA
gntR-F-qrt	ACGTTGACCTATTCCCAGAT
gntR-R-qrt	GGAACCGTAGAGATTGTCCT
mcpU-F-qrt	CCGTCTATATCGACAGTCTCC
mcpU-R-qrt	CGACATAGGTGGAGATGAAT
rpmA-F-qrt	ATGGCACACAAGAAAGCTG
rpmA-R-qrt	GTAAGCGCAAAAATCGTATG
smeR-F-qrt	GTAAAGGGCGAGGAAAAGAT
smeR-R-qrt	GAGCGGATGTTCTACAAGAA
trpE-F-qrt	ATGCTTTCGAGGAAGAGGTC
trpE-R-qrt	TTGGTCATGATGGTGAAGGC
rpoB -F-qrt	ATCCTCGACACCTTCTACAC
rpoB -R-qrt	GATAGTTGCCGTAGAGATCG
SmeBR-RT-PCRf	GATCTTCTTCGTCCCGGTCT
SmeBR-RT-PCRr	ATCATGTCTTCGTGGGGCA
pSUP_fwd	TCCTTGAAGCTGTCCCTGAT
pSUP_rev	GAGAAGCAGGCCATTATCGC
pSRK_fwd	CTCTTCGCTATTACGGCAGC
pSRK_rev	GGGCTGCAGGAATTCGATATC
SmelRcsR1-NB	GCTCCATCTCTCAATCACGCATG
5S-rRNA_Smel-NB	GTTCGGAATGGGAACGGGTGCAG
For work with *E. coli* MG1655	
Ec-rnTrpL-fw_NdeI	CGCACATATGAAAGCAATTTTCGTACTGAA
Ec-rnTrpL-fw_XbaI	TGCTCTAGAAAAAAAAGCCCGCTCATTAGGC
Ec-trpL-KO-Fw	GTTAACTAGTACGCAAGTTCACGTAAAAAGGGT ATCGACAGCCTTTGAGTGAGCTGATAC

Ec-trpL-KO-rv	GTTTTTGTGTTTGCATTGTTATTCTCTAATTTTGT TCGCTCATATGAATATCCTCCTTAG
EcTpL-mutant1-Fw	AAAGGTTCCTGGCGCACTTCCTGAAACG
EcTpL-mutant1-Rv	TGCGCCAGGAACCTTTCAGTACGAAAAT
EcTpL-mutant2-Fw	TCGTACTCTTAGGTTGGTGGCGCACTTC
EcTpL-mutant2-Rv	CCAACCTAAGAGTACGAAAATTGCTTTC
Ec-trpLp-NheI-Fw	CGCTAGCTGGCAAATATTCGTAAATG
Ec-trpLp-XbaI-Rv	CTCTAGAACGTGAACTTGCGTACTAG
Ec-p-trpL-XbaI-Rv	CTCTAGAAAAAAAAAGCCCGCTCATTAGG
EcRsu-IGR-AAGfw	CTAACTTAAGAATGACTTTCAGGAGCCC
EcRsu-IGR-AAGrv	AGTCATTCTTAAGTTAGACGACGCTGGCA
EcDnaA-CC62-63GGf	TGAGTTAGGAGCCACAGAATTCAGTATG
EcDnaA-CC62-63GGr	TGTGGCTCCTAACTCATCCTGCAATCGG
Ec-RsuA-qRT-Fw	CACCCAACGGTGCTCTATTT
Ec-RsuA-qRT-Rv	CTGCCGTATCGTCAGCTACA
Ec-Bcr-qRT-Fw	TTCGGCAATGATTTTCTTCC
Ec-Bcr-qRT-Rv	CGGCGCTTAAGAATGAGAAC
Ec-SanA-qRT-Fw	TTAGTCCTGATCGGCTTGCT
Ec-SanA-qRT-Rv	GGCATTAATCGCTCCTTGAA
Ec-Ycao-qRT-Fw	CAGCGAGTGGGAAAAAGAAG
Ec-Ycao-qRT-Rv	AGACCAGAGCCTGTTCCAGA
Ec-DnaA-qRT-Fw	ATCATTCTCACCTCGGATCG
Ec-DnaA-qRT-Rv	AGACGTTGGCGATAAAGAA
Ec-MhpC -qRT-Fw	ACGCTGCGCATCCATTTTAA
Ec-MhpC -qRT-Rv	CCACGCTTTTCAGGATTCGT
Sso41-qRT-Fw	GCATCCAAGGCACCTATCTC
Sso41-qRT-Rv	GGAGGCGGCCATTAATGAAA
RT-rsuA-bcr-Fw	AATTGCCAGCGTCGTCTAAC
RT-rsuA-bcr-Rv	CTGAGGGTCATCTGCGTACT
Ec_rntrpL_NB_oligo	GGCTGGGTATCTGATTGCTTTACG
Ec_5S_NB_oligo	CATCGGCGCTACGGCGTTTCACTT

5.7 Enzymes

Name	**Company**
TURBO-DNase	Invitrogen
T4-DNA-ligase	Thermofisher Scientific
T4-polynucleotidkinase	Thermofisher Scientific
Taq-polymerase	Qiagen
FastDigest-RestrictionEnzymes	Thermofisher Scientific
Phusion Polymerase	Thermofisher Scientific

5.8 Kits

E.Z.N.A. Gel Extraction Kit	OMEGA
E.Z.N.A. DNA Probe Purification Kit	OMEGA
Brilliant III Ultra-Fast SYBR®Green QRT-PCR Master Mix	Agilent Technologies

5.9 Special Tubes and 96-well Plates

0.2ml Low Profile Thin-walled 8 Tube Strips	Thermofisher Scientific
Optically clear flat 8 Cap Strips	Thermofisher Scientific
MICROPLATE 96WELL PS F-BOTTOM CLEAR MICROLON	Greiner bio-one

6 References

1. Rauhut, R. and Klug, G. (1999) mRNA degradation in bacteria. *FEMS Microbiol Rev*, **23**, 353-370.
2. Deutscher, M.P. (2006) Degradation of RNA in bacteria: comparison of mRNA and stable RNA. *Nucleic Acids Res*, **34**, 659-666.
3. Apirion, D. (1973) Degradation of RNA in Escherichia coli. A hypothesis. *Mol Gen Genet*, **122**, 313-322.
4. Carpousis, A.J. (2007) The RNA degradosome of Escherichia coli: an mRNA-degrading machine assembled on RNase E. *Annu Rev Microbiol*, **61**, 71-87.
5. Carpousis, A.J., Van Houwe, G., Ehretsmann, C. and Krisch, H.M. (1994) Copurification of E. coli RNAase E and PNPase: evidence for a specific association between two enzymes important in RNA processing and degradation. *Cell*, **76**, 889-900.
6. Py, B., Higgins, C.F., Krisch, H.M. and Carpousis, A.J. (1996) A DEAD-box RNA helicase in the Escherichia coli RNA degradosome. *Nature*, **381**, 169-172.
7. Vanzo, N.F., Li, Y.S., Py, B., Blum, E., Higgins, C.F., Raynal, L.C., Krisch, H.M. and Carpousis, A.J. (1998) Ribonuclease E organizes the protein interactions in the Escherichia coli RNA degradosome. *Genes Dev*, **12**, 2770-2781.
8. Ikeda, Y., Yagi, M., Morita, T. and Aiba, H. (2011) Hfq binding at RhlB-recognition region of RNase E is crucial for the rapid degradation of target mRNAs mediated by sRNAs in Escherichia coli. *Mol Microbiol*, **79**, 419-432.
9. Apirion, D. and Lassar, A.B. (1978) A conditional lethal mutant of Escherichia coli which affects the processing of ribosomal RNA. *J Biol Chem*, **253**, 1738-1742.
10. McDowall, K.J. and Cohen, S.N. (1996) The N-terminal domain of the rne gene product has RNase E activity and is non-overlapping with the arginine-rich RNA-binding site. *J Mol Biol*, **255**, 349-355.
11. Li, Z. and Deutscher, M.P. (2002) RNase E plays an essential role in the maturation of Escherichia coli tRNA precursors. *RNA*, **8**, 97-109.
12. Ow, M.C. and Kushner, S.R. (2002) Initiation of tRNA maturation by RNase E is essential for cell viability in E. coli. *Genes Dev*, **16**, 1102-1115.
13. Lalaouna, D., Simoneau-Roy, M., Lafontaine, D. and Masse, E. (2013) Regulatory RNAs and target mRNA decay in prokaryotes. *Biochim Biophys Acta*, **1829**, 742-747.
14. Hammarlof, D.L., Bergman, J.M., Garmendia, E. and Hughes, D. (2015) Turnover of mRNAs is one of the essential functions of RNase E. *Mol Microbiol*, **98**, 34-45.
15. Bernstein, J.A., Khodursky, A.B., Lin, P.H., Lin-Chao, S. and Cohen, S.N. (2002) Global analysis of mRNA decay and abundance in Escherichia coli at single-gene resolution using two-color fluorescent DNA microarrays. *Proc Natl Acad Sci U S A*, **99**, 9697-9702.
16. Stead, M.B., Marshburn, S., Mohanty, B.K., Mitra, J., Pena Castillo, L., Ray, D., van Bakel, H., Hughes, T.R. and Kushner, S.R. (2011) Analysis of Escherichia coli RNase E and RNase III activity in vivo using tiling microarrays. *Nucleic Acids Res*, **39**, 3188-3203.
17. Feng, Y., Vickers, T.A. and Cohen, S.N. (2002) The catalytic domain of RNase E shows inherent 3' to 5' directionality in cleavage site selection. *Proc Natl Acad Sci U S A*, **99**, 14746-14751.
18. Ghunberg-Manago, M. (1963), *Progress in Nucleic Acid Research and Molecular Biology*. Elsevier, Vol. 1, pp. 93-133.

19. Umitsuki, G., Wachi, M., Takada, A., Hikichi, T. and Nagai, K. (2001) Involvement of RNase G in in vivo mRNA metabolism in Escherichia coli. *Genes Cells*, **6**, 403-410.
20. Robertson, H.D., Webster, R.E. and Zinder, N.D. (1967) A nuclease specific for double-stranded RNA. *Virology*, **32**, 718-719.
21. Lim, B., Sim, S.H., Sim, M., Kim, K., Jeon, C.O., Lee, Y., Ha, N.C. and Lee, K. (2012) RNase III controls the degradation of corA mRNA in Escherichia coli. *J Bacteriol*, **194**, 2214-2220.
22. Vogel, J., Argaman, L., Wagner, E.G. and Altuvia, S. (2004) The small RNA IstR inhibits synthesis of an SOS-induced toxic peptide. *Curr Biol*, **14**, 2271-2276.
23. Braun, F., Le Derout, J. and Regnier, P. (1998) Ribosomes inhibit an RNase E cleavage which induces the decay of the rpsO mRNA of Escherichia coli. *EMBO J*, **17**, 4790-4797.
24. Condon, C. (2003) RNA processing and degradation in Bacillus subtilis. *Microbiol Mol Biol Rev*, **67**, 157-174, table of contents.
25. Chevrier-Miller, M., Jacques, N., Raibaud, O. and Dreyfus, M. (1990) Transcription of single-copy hybrid lacZ genes by T7 RNA polymerase in Escherichia coli: mRNA synthesis and degradation can be uncoupled from translation. *Nucleic Acids Res*, **18**, 5787-5792.
26. Joyce, S.A. and Dreyfus, M. (1998) In the absence of translation, RNase E can bypass 5' mRNA stabilizers in Escherichia coli. *J Mol Biol*, **282**, 241-254.
27. Sharp, J.S. and Bechhofer, D.H. (2005) Effect of 5'-proximal elements on decay of a model mRNA in Bacillus subtilis. *Mol Microbiol*, **57**, 484-495.
28. Bouvet, P. and Belasco, J.G. (1992) Control of RNase E-mediated RNA degradation by 5'-terminal base pairing in E. coli. *Nature*, **360**, 488-491.
29. Jarrige, A.C., Mathy, N. and Portier, C. (2001) PNPase autocontrols its expression by degrading a double-stranded structure in the pnp mRNA leader. *EMBO J*, **20**, 6845-6855.
30. Schuck, A., Diwa, A. and Belasco, J.G. (2009) RNase E autoregulates its synthesis in Escherichia coli by binding directly to a stem-loop in the rne 5' untranslated region. *Mol Microbiol*, **72**, 470-478.
31. Hambraeus, G., Karhumaa, K. and Rutberg, B. (2002) A 5' stem-loop and ribosome binding but not translation are important for the stability of Bacillus subtilis aprE leader mRNA. *Microbiology*, **148**, 1795-1803.
32. Mohanty, B.K. and Kushner, S.R. (1999) Analysis of the function of Escherichia coli poly(A) polymerase I in RNA metabolism. *Mol Microbiol*, **34**, 1094-1108.
33. Mohanty, B.K. and Kushner, S.R. (2006) The majority of Escherichia coli mRNAs undergo post-transcriptional modification in exponentially growing cells. *Nucleic Acids Res*, **34**, 5695-5704.
34. Campos-Guillen, J., Bralley, P., Jones, G.H., Bechhofer, D.H. and Olmedo-Alvarez, G. (2005) Addition of poly(A) and heteropolymeric 3' ends in Bacillus subtilis wild-type and polynucleotide phosphorylase-deficient strains. *J Bacteriol*, **187**, 4698-4706.
35. Selinger, D.W., Saxena, R.M., Cheung, K.J., Church, G.M. and Rosenow, C. (2003) Global RNA half-life analysis in Escherichia coli reveals positional patterns of transcript degradation. *Genome Res*, **13**, 216-223.
36. Osada, Y., Saito, R. and Tomita, M. (1999) Analysis of base-pairing potentials between 16S rRNA and 5' UTR for translation initiation in various prokaryotes. *Bioinformatics*, **15**, 578-581.
37. Nie, L., Wu, G. and Zhang, W. (2006) Correlation of mRNA expression and protein abundance affected by multiple sequence features related to translational efficiency in Desulfovibrio vulgaris: a quantitative analysis. *Genetics*, **174**, 2229-2243.

38. van de Guchte, M., van der Lende, T., Kok, J. and Venema, G. (1991) A possible contribution of mRNA secondary structure to translation initiation efficiency in Lactococcus lactis. *FEMS Microbiol Lett*, **65**, 201-208.
39. Rocha, E.P., Danchin, A. and Viari, A. (1999) Translation in Bacillus subtilis: roles and trends of initiation and termination, insights from a genome analysis. *Nucleic Acids Res*, **27**, 3567-3576.
40. Akashi, H. and Gojobori, T. (2002) Metabolic efficiency and amino acid composition in the proteomes of Escherichia coli and Bacillus subtilis. *Proc Natl Acad Sci U S A*, **99**, 3695-3700.
41. Mitarai, N., Sneppen, K. and Pedersen, S. (2008) Ribosome collisions and translation efficiency: optimization by codon usage and mRNA destabilization. *J Mol Biol*, **382**, 236-245.
42. Vitreschak, A.G., Rodionov, D.A., Mironov, A.A. and Gelfand, M.S. (2004) Riboswitches: the oldest mechanism for the regulation of gene expression? *Trends Genet*, **20**, 44-50.
43. Coppins, R.L., Hall, K.B. and Groisman, E.A. (2007) The intricate world of riboswitches. *Curr Opin Microbiol*, **10**, 176-181.
44. Brantl, S. (2007) Regulatory mechanisms employed by cis-encoded antisense RNAs. *Curr Opin Microbiol*, **10**, 102-109.
45. Kaberdin, V.R. and Blasi, U. (2006) Translation initiation and the fate of bacterial mRNAs. *FEMS Microbiol Rev*, **30**, 967-979.
46. Dennis, P.P., Ehrenberg, M. and Bremer, H. (2004) Control of rRNA synthesis in Escherichia coli: a systems biology approach. *Microbiol Mol Biol Rev*, **68**, 639-668.
47. Van Assche, E., Van Puyvelde, S., Vanderleyden, J. and Steenackers, H.P. (2015) RNA-binding proteins involved in post-transcriptional regulation in bacteria. *Front Microbiol*, **6**, 141.
48. Babitzke, P. (2004) Regulation of transcription attenuation and translation initiation by allosteric control of an RNA-binding protein: the Bacillus subtilis TRAP protein. *Curr Opin Microbiol*, **7**, 132-139.
49. Zhang, A., Wassarman, K.M., Rosenow, C., Tjaden, B.C., Storz, G. and Gottesman, S. (2003) Global analysis of small RNA and mRNA targets of Hfq. *Mol Microbiol*, **50**, 1111-1124.
50. Gottesman, S. (2004) The small RNA regulators of Escherichia coli: roles and mechanisms*. *Annu Rev Microbiol*, **58**, 303-328.
51. Udekwu, K.I., Darfeuille, F., Vogel, J., Reimegard, J., Holmqvist, E. and Wagner, E.G. (2005) Hfq-dependent regulation of OmpA synthesis is mediated by an antisense RNA. *Genes Dev*, **19**, 2355-2366.
52. Clarke, J.E., Kime, L., Romero, A.D. and McDowall, K.J. (2014) Direct entry by RNase E is a major pathway for the degradation and processing of RNA in Escherichia coli. *Nucleic Acids Res*, **42**, 11733-11751.
53. Edri, S. and Tuller, T. (2014) Quantifying the effect of ribosomal density on mRNA stability. *PLoS One*, **9**, e102308.
54. Kuzj, A.E., Medberry, P.S. and Schottel, J.L. (1998) Stationary phase, amino acid limitation and recovery from stationary phase modulate the stability and translation of chloramphenicol acetyltransferase mRNA and total mRNA in Escherichia coli. *Microbiology*, **144 (Pt 3)**, 739-750.
55. Redon, E., Loubiere, P. and Cocaign-Bousquet, M. (2005) Role of mRNA stability during genome-wide adaptation of Lactococcus lactis to carbon starvation. *J Biol Chem*, **280**, 36380-36385.

56. Shalem, O., Dahan, O., Levo, M., Martinez, M.R., Furman, I., Segal, E. and Pilpel, Y. (2008) Transient transcriptional responses to stress are generated by opposing effects of mRNA production and degradation. *Mol Syst Biol*, **4**, 223.
57. El-Sharoud, W.M. and Graumann, P.L. (2007) Cold shock proteins aid coupling of transcription and translation in bacteria. *Sci Prog*, **90**, 15-27.
58. Wassarman, K.M. (2002) Small RNAs in bacteria: diverse regulators of gene expression in response to environmental changes. *Cell*, **109**, 141-144.
59. Shimoni, Y., Friedlander, G., Hetzroni, G., Niv, G., Altuvia, S., Biham, O. and Margalit, H. (2007) Regulation of gene expression by small non-coding RNAs: a quantitative view. *Mol Syst Biol*, **3**, 138.
60. Sharma, C.M. and Vogel, J. (2009) Experimental approaches for the discovery and characterization of regulatory small RNA. *Curr Opin Microbiol*, **12**, 536-546.
61. Waters, L.S. and Storz, G. (2009) Regulatory RNAs in bacteria. *Cell*, **136**, 615-628.
62. Diel, B., Dequivre, M., Wisniewski-Dye, F., Vial, L. and Hommais, F. (2019) A novel plasmid-transcribed regulatory sRNA, QfsR, controls chromosomal polycistronic gene expression in Agrobacterium fabrum. *Environ Microbiol*, **21**, 3063-3075.
63. Sharma, C.M., Darfeuille, F., Plantinga, T.H. and Vogel, J. (2007) A small RNA regulates multiple ABC transporter mRNAs by targeting C/A-rich elements inside and upstream of ribosome-binding sites. *Genes Dev*, **21**, 2804-2817.
64. Vecerek, B., Moll, I. and Blasi, U. (2007) Control of Fur synthesis by the non-coding RNA RyhB and iron-responsive decoding. *EMBO J*, **26**, 965-975.
65. Hammer, B.K. and Bassler, B.L. (2007) Regulatory small RNAs circumvent the conventional quorum sensing pathway in pandemic Vibrio cholerae. *Proc Natl Acad Sci U S A*, **104**, 11145-11149.
66. Prevost, K., Salvail, H., Desnoyers, G., Jacques, J.F., Phaneuf, E. and Masse, E. (2007) The small RNA RyhB activates the translation of shiA mRNA encoding a permease of shikimate, a compound involved in siderophore synthesis. *Mol Microbiol*, **64**, 1260-1273.
67. Gottesman, S. (2005) Micros for microbes: non-coding regulatory RNAs in bacteria. *Trends Genet*, **21**, 399-404.
68. Urban, J.H. and Vogel, J. (2008) Two seemingly homologous noncoding RNAs act hierarchically to activate glmS mRNA translation. *PLoS Biol*, **6**, e64.
69. Sedlyarova, N., Shamovsky, I., Bharati, B.K., Epshtein, V., Chen, J., Gottesman, S., Schroeder, R. and Nudler, E. (2016) sRNA-Mediated Control of Transcription Termination in E. coli. *Cell*, **167**, 111-121 e113.
70. De Lay, N. and Gottesman, S. (2009) The Crp-activated small noncoding regulatory RNA CyaR (RyeE) links nutritional status to group behavior. *J Bacteriol*, **191**, 461-476.
71. Urbanowski, M.L., Stauffer, L.T. and Stauffer, G.V. (2000) The gcvB gene encodes a small untranslated RNA involved in expression of the dipeptide and oligopeptide transport systems in Escherichia coli. *Mol Microbiol*, **37**, 856-868.
72. Gorke, B. and Vogel, J. (2008) Noncoding RNA control of the making and breaking of sugars. *Genes Dev*, **22**, 2914-2925.
73. Torres-Quesada, O., Millán, V., Nisa-Martínez, R., Bardou, F., Crespi, M., Toro, N. and Jiménez-Zurdo, J.I. (2013) Independent activity of the homologous small regulatory RNAs AbcR1 and AbcR2 in the legume symbiont Sinorhizobium meliloti. *PLoS One*, **8**, e68147.

74. Robledo, M., Peregrina, A., Millán, V., García‐Tomsig, N.I., Torres‐Quesada, O., Mateos, P.F., Becker, A. and Jiménez‐Zurdo, J.I. (2017) A conserved α‐proteobacterial small RNA contributes to osmoadaptation and symbiotic efficiency of rhizobia on legume roots. *Environmental microbiology*, **19**, 2661-2680.
75. Peer, A. and Margalit, H. (2011) Accessibility and evolutionary conservation mark bacterial small-rna target-binding regions. *J Bacteriol*, **193**, 1690-1701.
76. Bartel, D.P. (2009) MicroRNAs: target recognition and regulatory functions. *Cell*, **136**, 215-233.
77. Balbontin, R., Fiorini, F., Figueroa-Bossi, N., Casadesus, J. and Bossi, L. (2010) Recognition of heptameric seed sequence underlies multi-target regulation by RybB small RNA in Salmonella enterica. *Mol Microbiol*, **78**, 380-394.
78. Kawamoto, H., Koide, Y., Morita, T. and Aiba, H. (2006) Base-pairing requirement for RNA silencing by a bacterial small RNA and acceleration of duplex formation by Hfq. *Mol Microbiol*, **61**, 1013-1022.
79. Papenfort, K., Bouvier, M., Mika, F., Sharma, C.M. and Vogel, J. (2010) Evidence for an autonomous 5' target recognition domain in an Hfq-associated small RNA. *Proc Natl Acad Sci U S A*, **107**, 20435-20440.
80. Guillier, M. and Gottesman, S. (2008) The 5' end of two redundant sRNAs is involved in the regulation of multiple targets, including their own regulator. *Nucleic Acids Res*, **36**, 6781-6794.
81. Caron, M.P., Lafontaine, D.A. and Masse, E. (2010) Small RNA-mediated regulation at the level of transcript stability. *RNA Biol*, **7**, 140-144.
82. Opdyke, J.A., Fozo, E.M., Hemm, M.R. and Storz, G. (2011) RNase III participates in GadY-dependent cleavage of the gadX-gadW mRNA. *J Mol Biol*, **406**, 29-43.
83. Masse, E., Escorcia, F.E. and Gottesman, S. (2003) Coupled degradation of a small regulatory RNA and its mRNA targets in Escherichia coli. *Genes Dev*, **17**, 2374-2383.
84. Huntzinger, E., Boisset, S., Saveanu, C., Benito, Y., Geissmann, T., Namane, A., Lina, G., Etienne, J., Ehresmann, B., Ehresmann, C. *et al.* (2005) Staphylococcus aureus RNAIII and the endoribonuclease III coordinately regulate spa gene expression. *EMBO J*, **24**, 824-835.
85. Vogel, J. and Luisi, B.F. (2011) Hfq and its constellation of RNA. *Nat Rev Microbiol*, **9**, 578-589.
86. Fender, A., Elf, J., Hampel, K., Zimmermann, B. and Wagner, E.G. (2010) RNAs actively cycle on the Sm-like protein Hfq. *Genes Dev*, **24**, 2621-2626.
87. Hopkins, J.F., Panja, S. and Woodson, S.A. (2011) Rapid binding and release of Hfq from ternary complexes during RNA annealing. *Nucleic Acids Res*, **39**, 5193-5202.
88. Hwang, W., Arluison, V. and Hohng, S. (2011) Dynamic competition of DsrA and rpoS fragments for the proximal binding site of Hfq as a means for efficient annealing. *Nucleic Acids Res*, **39**, 5131-5139.
89. Soper, T., Mandin, P., Majdalani, N., Gottesman, S. and Woodson, S.A. (2010) Positive regulation by small RNAs and the role of Hfq. *Proc Natl Acad Sci U S A*, **107**, 9602-9607.
90. Maki, K., Morita, T., Otaka, H. and Aiba, H. (2010) A minimal base-pairing region of a bacterial small RNA SgrS required for translational repression of ptsG mRNA. *Mol Microbiol*, **76**, 782-792.
91. Otaka, H., Ishikawa, H., Morita, T. and Aiba, H. (2011) PolyU tail of rho-independent terminator of bacterial small RNAs is essential for Hfq action. *Proc Natl Acad Sci U S A*, **108**, 13059-13064.

92. Sauer, E. and Weichenrieder, O. (2011) Structural basis for RNA 3'-end recognition by Hfq. *Proc Natl Acad Sci U S A*, **108**, 13065-13070.
93. Lybecker, M.C., Abel, C.A., Feig, A.L. and Samuels, D.S. (2010) Identification and function of the RNA chaperone Hfq in the Lyme disease spirochete Borrelia burgdorferi. *Mol Microbiol*, **78**, 622-635.
94. Nielsen, J.S., Lei, L.K., Ebersbach, T., Olsen, A.S., Klitgaard, J.K., Valentin-Hansen, P. and Kallipolitis, B.H. (2010) Defining a role for Hfq in Gram-positive bacteria: evidence for Hfq-dependent antisense regulation in Listeria monocytogenes. *Nucleic Acids Res*, **38**, 907-919.
95. Iosub, I.A., van Nues, R.W., McKellar, S.W., Nieken, K.J., Marchioretto, M., Sy, B., Tree, J.J., Viero, G. and Granneman, S. (2020) Hfq CLASH uncovers sRNA-target interaction networks linked to nutrient availability adaptation. *Elife*, **9**.
96. Ramos, C.G., Sousa, S.A., Grilo, A.M., Feliciano, J.R. and Leitao, J.H. (2011) The second RNA chaperone, Hfq2, is also required for survival under stress and full virulence of Burkholderia cenocepacia J2315. *J Bacteriol*, **193**, 1515-1526.
97. Smirnov, A., Forstner, K.U., Holmqvist, E., Otto, A., Gunster, R., Becher, D., Reinhardt, R. and Vogel, J. (2016) Grad-seq guides the discovery of ProQ as a major small RNA-binding protein. *Proc Natl Acad Sci U S A*, **113**, 11591-11596.
98. Melamed, S., Adams, P.P., Zhang, A., Zhang, H. and Storz, G. (2020) RNA-RNA Interactomes of ProQ and Hfq Reveal Overlapping and Competing Roles. *Mol Cell*, **77**, 411-425 e417.
99. Chaulk, S.G., Smith Frieday, M.N., Arthur, D.C., Culham, D.E., Edwards, R.A., Soo, P., Frost, L.S., Keates, R.A., Glover, J.N. and Wood, J.M. (2011) ProQ is an RNA chaperone that controls ProP levels in Escherichia coli. *Biochemistry*, **50**, 3095-3106.
100. Pandey, S.P., Minesinger, B.K., Kumar, J. and Walker, G.C. (2011) A highly conserved protein of unknown function in Sinorhizobium meliloti affects sRNA regulation similar to Hfq. *Nucleic Acids Res*, **39**, 4691-4708.
101. Licatalosi, D.D. and Darnell, R.B. (2010) RNA processing and its regulation: global insights into biological networks. *Nat Rev Genet*, **11**, 75-87.
102. Babitzke, P. and Romeo, T. (2007) CsrB sRNA family: sequestration of RNA-binding regulatory proteins. *Curr Opin Microbiol*, **10**, 156-163.
103. Sonnleitner, E. and Haas, D. (2011) Small RNAs as regulators of primary and secondary metabolism in Pseudomonas species. *Appl Microbiol Biotechnol*, **91**, 63-79.
104. Wassarman, K.M. (2007) 6S RNA: a regulator of transcription. *Mol Microbiol*, **65**, 1425-1431.
105. Thomason, M.K. and Storz, G. (2010) Bacterial antisense RNAs: how many are there, and what are they doing? *Annu Rev Genet*, **44**, 167-188.
106. Chant, E.L. and Summers, D.K. (2007) Indole signalling contributes to the stable maintenance of Escherichia coli multicopy plasmids. *Mol Microbiol*, **63**, 35-43.
107. Storz, G., Vogel, J. and Wassarman, K.M. (2011) Regulation by small RNAs in bacteria: expanding frontiers. *Mol Cell*, **43**, 880-891.
108. Landt, S.G., Lesley, J.A., Britos, L. and Shapiro, L. (2010) CrfA, a small noncoding RNA regulator of adaptation to carbon starvation in Caulobacter crescentus. *J Bacteriol*, **192**, 4763-4775.
109. Salvail, H., Lanthier-Bourbonnais, P., Sobota, J.M., Caza, M., Benjamin, J.A., Mendieta, M.E., Lepine, F., Dozois, C.M., Imlay, J. and Masse, E. (2010) A small RNA promotes siderophore

production through transcriptional and metabolic remodeling. *Proc Natl Acad Sci U S A*, **107**, 15223-15228.

110. Masse, E., Vanderpool, C.K. and Gottesman, S. (2005) Effect of RyhB small RNA on global iron use in Escherichia coli. *J Bacteriol*, **187**, 6962-6971.
111. Sharma, C.M., Papenfort, K., Pernitzsch, S.R., Mollenkopf, H.J., Hinton, J.C. and Vogel, J. (2011) Pervasive post-transcriptional control of genes involved in amino acid metabolism by the Hfq-dependent GcvB small RNA. *Mol Microbiol*, **81**, 1144-1165.
112. Backofen, R. and Hess, W.R. (2010) Computational prediction of sRNAs and their targets in bacteria. *RNA Biol*, **7**, 33-42.
113. Beisel, C.L. and Storz, G. (2011) The base-pairing RNA spot 42 participates in a multioutput feedforward loop to help enact catabolite repression in Escherichia coli. *Mol Cell*, **41**, 286-297.
114. Levine, E., Zhang, Z., Kuhlman, T. and Hwa, T. (2007) Quantitative characteristics of gene regulation by small RNA. *PLoS Biol*, **5**, e229.
115. Sharma, C.M., Hoffmann, S., Darfeuille, F., Reignier, J., Findeiss, S., Sittka, A., Chabas, S., Reiche, K., Hackermuller, J., Reinhardt, R. *et al.* (2010) The primary transcriptome of the major human pathogen Helicobacter pylori. *Nature*, **464**, 250-255.
116. Mitschke, J., Georg, J., Scholz, I., Sharma, C.M., Dienst, D., Bantscheff, J., Voss, B., Steglich, C., Wilde, A., Vogel, J. *et al.* (2011) An experimentally anchored map of transcriptional start sites in the model cyanobacterium Synechocystis sp. PCC6803. *Proc Natl Acad Sci U S A*, **108**, 2124-2129.
117. Lalaouna, D. and Masse, E. (2015) Identification of sRNA interacting with a transcript of interest using MS2-affinity purification coupled with RNA sequencing (MAPS) technology. *Genom Data*, **5**, 136-138.
118. Hobbs, E.C., Astarita, J.L. and Storz, G. (2010) Small RNAs and small proteins involved in resistance to cell envelope stress and acid shock in Escherichia coli: analysis of a bar-coded mutant collection. *J Bacteriol*, **192**, 59-67.
119. Mandin, P. and Gottesman, S. (2010) Integrating anaerobic/aerobic sensing and the general stress response through the ArcZ small RNA. *EMBO J*, **29**, 3094-3107.
120. Papenfort, K., Pfeiffer, V., Lucchini, S., Sonawane, A., Hinton, J.C. and Vogel, J. (2008) Systematic deletion of Salmonella small RNA genes identifies CyaR, a conserved CRP-dependent riboregulator of OmpX synthesis. *Mol Microbiol*, **68**, 890-906.
121. Blanco, P., Hernando-Amado, S., Reales-Calderon, J.A., Corona, F., Lira, F., Alcalde-Rico, M., Bernardini, A., Sanchez, M.B. and Martinez, J.L. (2016) Bacterial Multidrug Efflux Pumps: Much More Than Antibiotic Resistance Determinants. *Microorganisms*, **4**.
122. Paulsen, I.T., Chen, J., Nelson, K.E. and Saier, M.H., Jr. (2001) Comparative genomics of microbial drug efflux systems. *J Mol Microbiol Biotechnol*, **3**, 145-150.
123. Poole, K. (2001) Multidrug resistance in Gram-negative bacteria. *Curr Opin Microbiol*, **4**, 500-508.
124. Poole, K. (2002) Outer membranes and efflux: the path to multidrug resistance in Gram-negative bacteria. *Curr Pharm Biotechnol*, **3**, 77-98.
125. Putman, M., van Veen, H.W. and Konings, W.N. (2000) Molecular properties of bacterial multidrug transporters. *Microbiol Mol Biol Rev*, **64**, 672-693.

126. Lubelski, J., Konings, W.N. and Driessen, A.J. (2007) Distribution and physiology of ABC-type transporters contributing to multidrug resistance in bacteria. *Microbiol Mol Biol Rev*, **71**, 463-476.
127. Eda, S., Mitsui, H. and Minamisawa, K. (2011) Involvement of the smeAB multidrug efflux pump in resistance to plant antimicrobials and contribution to nodulation competitiveness in Sinorhizobium meliloti. *Appl Environ Microbiol*, **77**, 2855-2862.
128. Slonczewski, L., Foster, W. and Gillen, M. (2009) Microbiology An Evolving Science ‖ WW Norton Company. *Inc., New York*.
129. Hansen, F.G. and Atlung, T. (2018) The DnaA Tale. *Front Microbiol*, **9**, 319.
130. Speck, C., Weigel, C. and Messer, W. (1999) ATP- and ADP-dnaA protein, a molecular switch in gene regulation. *EMBO J*, **18**, 6169-6176.
131. Bertrand, K., Korn, L., Lee, F., Platt, T., Squires, C.L., Squires, C. and Yanofsky, C. (1975) New features of the regulation of the tryptophan operon. *Science*, **189**, 22-26.
132. Yanofsky, C. (1981) Attenuation in the control of expression of bacterial operons. *Nature*, **289**, 751-758.
133. Merino, E., Jensen, R.A. and Yanofsky, C. (2008) Evolution of bacterial trp operons and their regulation. *Curr Opin Microbiol*, **11**, 78-86.
134. Vitreschak, A.G., Lyubetskaya, E.V., Shirshin, M.A., Gelfand, M.S. and Lyubetsky, V.A. (2004) Attenuation regulation of amino acid biosynthetic operons in proteobacteria: comparative genomics analysis. *FEMS Microbiol Lett*, **234**, 357-370.
135. Dar, D., Shamir, M., Mellin, J.R., Koutero, M., Stern-Ginossar, N., Cossart, P. and Sorek, R. (2016) Term-seq reveals abundant ribo-regulation of antibiotics resistance in bacteria. *Science*, **352**, aad9822.
136. Storz, G., Wolf, Y.I. and Ramamurthi, K.S. (2014) Small proteins can no longer be ignored. *Annu Rev Biochem*, **83**, 753-777.
137. Gaballa, A., Antelmann, H., Aguilar, C., Khakh, S.K., Song, K.B., Smaldone, G.T. and Helmann, J.D. (2008) The Bacillus subtilis iron-sparing response is mediated by a Fur-regulated small RNA and three small, basic proteins. *Proc Natl Acad Sci U S A*, **105**, 11927-11932.
138. Yin, X., Wu Orr, M., Wang, H., Hobbs, E.C., Shabalina, S.A. and Storz, G. (2019) The small protein MgtS and small RNA MgrR modulate the PitA phosphate symporter to boost intracellular magnesium levels. *Mol Microbiol*, **111**, 131-144.
139. Tenaillon, O., Skurnik, D., Picard, B. and Denamur, E. (2010) The population genetics of commensal Escherichia coli. *Nat Rev Microbiol*, **8**, 207-217.
140. Bentley, R. and Meganathan, R. (1982) Biosynthesis of vitamin K (menaquinone) in bacteria. *Microbiol Rev*, **46**, 241-280.
141. Hudault, S., Guignot, J. and Servin, A.L. (2001) Escherichia coli strains colonising the gastrointestinal tract protect germfree mice against Salmonella typhimurium infection. *Gut*, **49**, 47-55.
142. Reid, G., Howard, J. and Gan, B.S. (2001) Can bacterial interference prevent infection? *Trends Microbiol*, **9**, 424-428.
143. Russell, J.B. and Jarvis, G.N. (2001) Practical mechanisms for interrupting the oral-fecal lifecycle of Escherichia coli. *J Mol Microbiol Biotechnol*, **3**, 265-272.
144. Biondi, E.G., Pilli, E., Giuntini, E., Roumiantseva, M.L., Andronov, E.E., Onichtchouk, O.P., Kurchak, O.N., Simarov, B.V., Dzyubenko, N.I., Mengoni, A. *et al.* (2003) Genetic relationship

of Sinorhizobium meliloti and Sinorhizobium medicae strains isolated from Caucasian region. *FEMS Microbiol Lett*, **220**, 207-213.

145. Gage, D.J. (2004) Infection and invasion of roots by symbiotic, nitrogen-fixing rhizobia during nodulation of temperate legumes. *Microbiol Mol Biol Rev*, **68**, 280-300.
146. Galibert, F., Finan, T.M., Long, S.R., Puhler, A., Abola, P., Ampe, F., Barloy-Hubler, F., Barnett, M.J., Becker, A., Boistard, P. *et al.* (2001) The composite genome of the legume symbiont Sinorhizobium meliloti. *Science*, **293**, 668-672.
147. Barnett, M.J., Fisher, R.F., Jones, T., Komp, C., Abola, A.P., Barloy-Hubler, F., Bowser, L., Capela, D., Galibert, F., Gouzy, J. *et al.* (2001) Nucleotide sequence and predicted functions of the entire Sinorhizobium meliloti pSymA megaplasmid. *Proc Natl Acad Sci U S A*, **98**, 9883-9888.
148. Finan, T.M., Weidner, S., Wong, K., Buhrmester, J., Chain, P., Vorholter, F.J., Hernandez-Lucas, I., Becker, A., Cowie, A., Gouzy, J. *et al.* (2001) The complete sequence of the 1,683-kb pSymB megaplasmid from the N2-fixing endosymbiont Sinorhizobium meliloti. *Proc Natl Acad Sci U S A*, **98**, 9889-9894.
149. Zurawski, G., Elseviers, D., Stauffer, G.V. and Yanofsky, C. (1978) Translational control of transcription termination at the attenuator of the Escherichia coli tryptophan operon. *Proc Natl Acad Sci U S A*, **75**, 5988-5992.
150. Bae, Y.M. and Crawford, I.P. (1990) The Rhizobium meliloti trpE(G) gene is regulated by attenuation, and its product, anthranilate synthase, is regulated by feedback inhibition. *J Bacteriol*, **172**, 3318-3327.
151. Baumgardt, K., Smidova, K., Rahn, H., Lochnit, G., Robledo, M. and Evguenieva-Hackenberg, E. (2016) The stress-related, rhizobial small RNA RcsR1 destabilizes the autoinducer synthase encoding mRNA sinI in Sinorhizobium meliloti. *RNA Biol*, **13**, 486-499.
152. Santiago-Frangos, A. and Woodson, S.A. (2018) Hfq chaperone brings speed dating to bacterial sRNA. *Wiley Interdiscip Rev RNA*, **9**, e1475.
153. Becker, A., Overloper, A., Schluter, J.P., Reinkensmeier, J., Robledo, M., Giegerich, R., Narberhaus, F. and Evguenieva-Hackenberg, E. (2014) Riboregulation in plant-associated alpha-proteobacteria. *RNA Biol*, **11**, 550-562.
154. Robledo, M., Frage, B., Wright, P.R. and Becker, A. (2015) A stress-induced small RNA modulates alpha-rhizobial cell cycle progression. *PLoS Genet*, **11**, e1005153.
155. Melior, H., Maass, S., Li, S., Forstner, K.U., Azarderakhsh, S., Varadarajan, A.R., Stotzel, M., Elhossary, M., Barth-Weber, S., Ahrens, C.H. *et al.* (2020) The Leader Peptide peTrpL Forms Antibiotic-Containing Ribonucleoprotein Complexes for Posttranscriptional Regulation of Multiresistance Genes. *mBio*, **11**.
156. Melior, H., Li, S., Madhugiri, R., Stotzel, M., Azarderakhsh, S., Barth-Weber, S., Baumgardt, K., Ziebuhr, J. and Evguenieva-Hackenberg, E. (2019) Transcription attenuation-derived small RNA rnTrpL regulates tryptophan biosynthesis gene expression in trans. *Nucleic Acids Res*, **47**, 6396-6410.
157. Yanofsky, C. and Horn, V. (1994) Role of regulatory features of the trp operon of Escherichia coli in mediating a response to a nutritional shift. *J Bacteriol*, **176**, 6245-6254.
158. Wrzesinski, J., Bakin, A., Nurse, K., Lane, B.G. and Ofengand, J. (1995) Purification, cloning, and properties of the 16S RNA pseudouridine 516 synthase from Escherichia coli. *Biochemistry*, **34**, 8904-8913.

159. Conrad, J., Niu, L., Rudd, K., Lane, B.G. and Ofengand, J. (1999) 16S ribosomal RNA pseudouridine synthase RsuA of Escherichia coli: deletion, mutation of the conserved Asp102 residue, and sequence comparison among all other pseudouridine synthases. *RNA*, **5**, 751-763.
160. Haugan, M.S., Charbon, G., Frimodt-Moller, N. and Lobner-Olesen, A. (2018) Chromosome replication as a measure of bacterial growth rate during Escherichia coli infection in the mouse peritonitis model. *Sci Rep*, **8**, 14961.
161. Melior, H., Maaß, S., Stötzel, M., Li, S., Förstner, K.U., Schütz, R., Azarderakhsh, S., Shevkoplias, A., Barth-Weber, S. and Varadarajan, A.R. (2019) The bacterial leader peptide peTrpL has a conserved function in antibiotic-dependent posttranscriptional regulation of ribosomal genes. *bioRxiv*, 606483.
162. Smirnov, A., Wang, C., Drewry, L.L. and Vogel, J. (2017) Molecular mechanism of mRNA repression in trans by a ProQ-dependent small RNA. *EMBO J*, **36**, 1029-1045.
163. Aaboud, M., Aad, G., Abbott, B., Abdallah, J., Abdinov, O., Abeloos, B., Aben, R., AbouZeid, O.S., Abraham, N.L., Abramowicz, H. *et al.* (2016) Measurement of the Inelastic Proton-Proton Cross Section at √s=13 TeV with the ATLAS Detector at the LHC. *Phys Rev Lett*, **117**, 182002.
164. Maguire, B.A., Beniaminov, A.D., Ramu, H., Mankin, A.S. and Zimmermann, R.A. (2005) A protein component at the heart of an RNA machine: the importance of protein l27 for the function of the bacterial ribosome. *Mol Cell*, **20**, 427-435.
165. Lau, C.H., Fraud, S., Jones, M., Peterson, S.N. and Poole, K. (2012) Reduced expression of the rplU-rpmA ribosomal protein operon in mexXY-expressing pan-aminoglycoside-resistant mutants of pseudomonas aeruginosa. *Antimicrob Agents Chemother*, **56**, 5171-5179.
166. Searles, L.L., Wessler, S.R. and Calvo, J.M. (1983) Transcription attenuation is the major mechanism by which the leu operon of Salmonella typhimurium is controlled. *J Mol Biol*, **163**, 377-394.
167. Raivio, T.L. and Silhavy, T.J. (2001) Periplasmic stress and ECF sigma factors. *Annu Rev Microbiol*, **55**, 591-624.
168. Missiakas, D. and Raina, S. (1998) The extracytoplasmic function sigma factors: role and regulation. *Mol Microbiol*, **28**, 1059-1066.
169. Nies, D.H. (2004) Incidence and function of sigma factors in Ralstonia metallidurans and other bacteria. *Arch Microbiol*, **181**, 255-268.
170. Bastiat, B., Sauviac, L. and Bruand, C. (2010) Dual control of Sinorhizobium meliloti RpoE2 sigma factor activity by two PhyR-type two-component response regulators. *J Bacteriol*, **192**, 2255-2265.
171. Flechard, M., Fontenelle, C., Trautwetter, A., Ermel, G. and Blanco, C. (2009) Sinorhizobium meliloti rpoE2 is necessary for H(2)O(2) stress resistance during the stationary growth phase. *FEMS Microbiol Lett*, **290**, 25-31.
172. Flechard, M., Fontenelle, C., Blanco, C., Goude, R., Ermel, G. and Trautwetter, A. (2010) RpoE2 of Sinorhizobium meliloti is necessary for trehalose synthesis and growth in hyperosmotic media. *Microbiology*, **156**, 1708-1718.
173. Hor, J., Matera, G., Vogel, J., Gottesman, S. and Storz, G. (2020) Trans-Acting Small RNAs and Their Effects on Gene Expression in Escherichia coli and Salmonella enterica. *EcoSal Plus*, **9**.

174. Hirakawa, H., Takumi-Kobayashi, A., Theisen, U., Hirata, T., Nishino, K. and Yamaguchi, A. (2008) AcrS/EnvR represses expression of the acrAB multidrug efflux genes in Escherichia coli. *J Bacteriol*, **190**, 6276-6279.
175. Nishino, K. and Yamaguchi, A. (2001) Analysis of a complete library of putative drug transporter genes in Escherichia coli. *J Bacteriol*, **183**, 5803-5812.
176. Atlung, T., Lobner-Olesen, A. and Hansen, F.G. (1987) Overproduction of DnaA protein stimulates initiation of chromosome and minichromosome replication in Escherichia coli. *Mol Gen Genet*, **206**, 51-59.
177. Atlung, T. and Hansen, F.G. (1993) Three distinct chromosome replication states are induced by increasing concentrations of DnaA protein in Escherichia coli. *J Bacteriol*, **175**, 6537-6545.
178. Mank, N.N., Berghoff, B.A. and Klug, G. (2013) A mixed incoherent feed-forward loop contributes to the regulation of bacterial photosynthesis genes. *RNA Biol*, **10**, 347-352.
179. Nitzan, M., Rehani, R. and Margalit, H. (2017) Integration of Bacterial Small RNAs in Regulatory Networks. *Annu Rev Biophys*, **46**, 131-148.
180. Leslie, D.J., Heinen, C., Schramm, F.D., Thuring, M., Aakre, C.D., Murray, S.M., Laub, M.T. and Jonas, K. (2015) Nutritional Control of DNA Replication Initiation through the Proteolysis and Regulated Translation of DnaA. *PLoS Genet*, **11**, e1005342.
181. Beroual, W., Brilli, M. and Biondi, E.G. (2018) Non-coding RNAs Potentially Controlling Cell Cycle in the Model Caulobacter crescentus: A Bioinformatic Approach. *Front Genet*, **9**, 164.
182. Wurihan, W., Wunier, W., Li, H., Fan, L.F. and Morigen, M. (2016) Trans-translation ensures timely initiation of DNA replication and DnaA synthesis in Escherichia coli. *Genet Mol Res*, **15**.
183. Gollnick, P., Babitzke, P., Antson, A. and Yanofsky, C. (2005) Complexity in regulation of tryptophan biosynthesis in Bacillus subtilis. *Annu Rev Genet*, **39**, 47-68.
184. Babitzke, P., Lai, Y.J., Renda, A.J. and Romeo, T. (2019) Posttranscription Initiation Control of Gene Expression Mediated by Bacterial RNA-Binding Proteins. *Annu Rev Microbiol*, **73**, 43-67.
185. Vanderpool, C.K., Balasubramanian, D. and Lloyd, C.R. (2011) Dual-function RNA regulators in bacteria. *Biochimie*, **93**, 1943-1949.
186. Gimpel, M. and Brantl, S. (2017) Dual-function small regulatory RNAs in bacteria. *Mol Microbiol*, **103**, 387-397.
187. Schluter, J.P., Reinkensmeier, J., Daschkey, S., Evguenieva-Hackenberg, E., Janssen, S., Janicke, S., Becker, J.D., Giegerich, R. and Becker, A. (2010) A genome-wide survey of sRNAs in the symbiotic nitrogen-fixing alpha-proteobacterium Sinorhizobium meliloti. *BMC Genomics*, **11**, 245.
188. Sambrook, J., Fritsch, E.F. and Maniatis, T. (1989) *Molecular cloning: a laboratory manual*. Cold spring harbor laboratory press.
189. Schluter, J.P., Czuppon, P., Schauer, O., Pfaffelhuber, P., McIntosh, M. and Becker, A. (2015) Classification of phenotypic subpopulations in isogenic bacterial cultures by triple promoter probing at single cell level. *J Biotechnol*, **198**, 3-14.
190. Basineni, S.R., Madhugiri, R., Kolmsee, T., Hengge, R. and Klug, G. (2009) The influence of Hfq and ribonucleases on the stability of the small non-coding RNA OxyS and its target rpoS in E. coli is growth phase dependent. *RNA Biol*, **6**, 584-594.

7 Publications

7.1 In Peer-reviewed Journals

1. Melior H, **Li S**, Madhugiri R, et al. Transcription attenuation-derived small RNA rnTrpL regulates tryptophan biosynthesis gene expression in trans[J]. Nucleic acids research, 2019, 47(12): 6396-6410.
2. Melior H, Maaß S, **Li S**, et al. The Leader Peptide peTrpL Forms Antibiotic-Containing Ribonucleoprotein Complexes for Posttranscriptional Regulation of Multiresistance Genes[J]. Mbio, 2020, 11(3):e01027-20.
3. Bioinformatic prediction reveals posttranscriptional regulation of the chromosomal replication initiator gene dnaA by the attenuator sRNA rnTrpL in *Escherichia coli*. (As First Author Submitted to RNA Biology)
4. Posttranscriptional regulation of ribosomal genes by an antibiotic-dependent complex of the attenuator sRNA rnTrpL and the leader peptide peTrpL. (As second author, submitted)

7.2 Contributions to Congresses

Sensory and Regulatory RNAs in Prokaryotes, Poster Show, 2018, Giessen, Germany

Sensory and Regulatory RNAs in Prokaryotes, Poster Show, 2019, Freiburg, Germany

Vereinigung für Allgemeine und Angewandte Mikrobiologie (VAAM), Poster Show, 2019, Mains, Germany

8 Acknowledgements

First of all, I would like to thank Apl. Prof. Elena Evguenieva-Hackenberg for providing the research topic, funding for research and laboratory space for conducting this work. Big thanks for her teaching and support during the whole process, especially for her encouragement in times of hardship.

Special thanks go to Prof. Kai Thormann for being my second Reviewer at Justus Liebig University Giessen.

I also want to thank Deutsche Forschungsgemeinschaft (DFG) for providing the funding for travels and symposiums allowing me to improve presenting skills and scientific thinking, and China Scholarship Council (CSC) for supporting me to study and live here.

I express my great thanks also to my colleagues and friends Hendrik Melior, Saina Azarderakhsh, Robina Scheuer, Maximilian Stötzel, and Susanne Barth-Weber for sharing their experimental experiences with me. I thank Daniel Edelmann and Bork Berghoff as well for for initial discussions about *E. coli* part project and valuable help with the experiments..

Additionally, I want to thank Jens Georg for the bioinformatic prediction of Ec-rnTrpL targets. Big thanks to Prof. Gabriele Klug and Prof. Kai Thormann for allowing me to use their equipment and reagents.

Also, I want to thank my Chinese friends Qingfeng Li, Xin Nie and Zhiping Zhao for their kindness and valuable help. And special thanks to all the chinese basketball friends for accompanying me through summer weekends and let me keep good health for science. In addtion, I sincerly thank to Hendrik Melior who is my first friend in Germany for his selflessly help, no matter what and when to ask him about science or life trivia, he always trys his best to help me, makes me feelling comfortable like an old brother. And I believe our friendship will be forever.

I am forever and ever indebted to my parents for their understanding and support. Special thanks to Pan Hu for being a conscientious wife and a faithful partner, her unconditional love makes me brave.